




1995

The Expression of Early Insulin Signaling Components in an Animal Model of Insulin-Resistant Diabetes Mellitus

James A. Bonini
Loyola University Chicago

Follow this and additional works at: https://ecommons.luc.edu/luc_theses

 Part of the [Molecular Biology Commons](#)

Recommended Citation

Bonini, James A., "The Expression of Early Insulin Signaling Components in an Animal Model of Insulin-Resistant Diabetes Mellitus" (1995). *Master's Theses*. 4032.
https://ecommons.luc.edu/luc_theses/4032

This Thesis is brought to you for free and open access by the Theses and Dissertations at Loyola eCommons. It has been accepted for inclusion in Master's Theses by an authorized administrator of Loyola eCommons. For more information, please contact ecommons@luc.edu.



This work is licensed under a [Creative Commons Attribution-Noncommercial-No Derivative Works 3.0 License](#).
Copyright © 1995 James A. Bonini

LOYOLA UNIVERSITY CHICAGO

THE EXPRESSION OF EARLY INSULIN SIGNALING COMPONENTS IN AN
ANIMAL MODEL OF INSULIN-RESISTANT DIABETES MELLITUS

A DISSERTATION SUBMITTED TO
THE FACULTY OF THE GRADUATE SCHOOL IN PARTIAL
FULFILLMENT OF THE REQUIREMENTS FOR THE DEGREE OF
DOCTOR OF PHILOSOPHY
DEPARTMENT OF MOLECULAR AND CELLULAR BIOCHEMISTRY

BY

JAMES A. BONINI

CHICAGO, ILLINOIS

MAY, 1995

Copyright by James A. Bonini, 1995
All rights reserved.

ACKNOWLEDGMENTS

I would like to acknowledge the great support and guidance of Dr. Cecilia Hofmann, and the comments and suggestions of Drs. Allen Frankfater, William Simmons, James Filkins, Leon Plataniias, and Jerry Colca. I would also like to thank Dr. Colca and the Upjohn company for supplying the animal tissue used in this work.

TABLE OF CONTENTS

ACKNOWLEDGMENTS	iii
LIST OF ILLUSTRATIONS	vi
LIST OF TABLES	viii
 Chapter	
I. INTRODUCTION	1
II. REVIEW OF RELATED LITERATURE	4
Overview	4
Insulin Dependent Diabetes Mellitus	4
Non-Insulin Dependent Diabetes Mellitus	9
Signal Transduction	14
Hypothesis and Specific Aims	31
Significance	35
III. MATERIALS AND METHODS	37
Materials	37
Experimental Models and Design	44
RNA Preparation	51
Protein Preparation	59
Image Analysis	64
Statistics	65
IV. RESULTS	67
Glycemic State and Insulin Levels of KKA ^y Mice	67
Expression of Insulin Signaling Components in Animal NIDDM	68
Function of the Insulin Receptor and IRS-1 in Animal NIDDM	79
The Effects of Insulin and Glucose on Signal Transduction Components	87
V. DISCUSSION	115
Proteins with Altered Expression or Function in KKA ^y Mice or STZ-treated Rats	117
Proteins Elevated in KKA ^y Mice	139

Significance of Alterations in Signaling Components	150
Pioglitazone as an Antihyperglycemic Agent	153
Caveats of this Study	154
Summary and Conclusions	156
REFERENCES	159
VITA	181

LIST OF ILLUSTRATIONS

Figure	Page
1. Early Steps in Insulin Signal Transduction	24
2. Protein Levels of IR, IRS-1, and PI3K p85 α in Animal NIDDM	71
3. Protein levels of GRB2, Nck, and Syp in Animal NIDDM	73
4. IR mRNA Levels in Animal NIDDM	76
5. IRS-1 mRNA Levels in Animal NIDDM	77
6. PI3K p85 α mRNA levels in Animal NIDDM	78
7. Anti-phosphotyrosine Western Blot of Isolated Adipocytes	81
8. Tyrosine Phosphorylation of IR in Animal NIDDM	82
9. IR Phosphorylation per Receptor in Animal NIDDM	83
10. IRS-1 Phosphorylation in Animal NIDDM	84
11. PI3K Association with IRS-1 in Animal NIDDM - Western Blot	89
12. PI3K Association with IRS-1 in Animal NIDDM - Graphed Results	90
13. Effect of Insulin and Glucose Pre-incubation on Glucose transport in 3T3-L1 Adipocytes	91
14. IR Expression in 3T3-L1 Adipocytes	93
15. Insulin Receptor Tyrosine Phosphorylation in 3T3-L1 Adipocytes	95

16.	Time Course for Insulin-stimulated Tyrosine phosphorylation of IR and IRS-1 . . .	96
17.	IRS-1 Expression in 3T3-L1 Adipocytes	98
18.	IRS-1 Tyrosine Phosphorylation in 3T3-L1 Adipocytes	99
19.	PI3K p85 α Expression in 3T3-L1 Adipocytes . .	100
20.	Expression of GRB2, Nck, and Syp in 3T3-L1 Adipocytes	102
21.	IR Expression in Liver in Animal IDDM	104
22.	IR Expression in Fat in Animal IDDM	106
23.	IRS-1 Expression in Fat in Animal IDDM	107
24.	IRS-1 mRNA Levels in Liver in Animal IDDM.	108
25.	PI3K p85 α Expression in Fat in Animal IDDM	110
26.	PI3K p85 α Expression in Liver in Animal IDDM	111
27.	Expression of GRB2, Nck, and Syp in Fat in Animal IDDM	112
28.	Expression of GRB2, Nck, and Syp in Liver in Animal IDDM	113

LIST OF TABLES

Table	Page
1. Observed Protein and Transcript Sizes of Signaling Components	69

CHAPTER I

INTRODUCTION

Glucose homeostasis is normally maintained by a balance between hepatic glucose production and glucose utilization by peripheral tissues (fat, muscle, and brain) (1). Insulin and glucagon, which are both secreted from the pancreatic islets, help to maintain this balance by their actions on peripheral tissues (primarily muscle, liver, and fat). Failure of the body to regulate blood glucose levels properly can lead to a variety of disorders, the most common of which is diabetes mellitus.

Diabetes mellitus is a heterogeneous disease that is characterized by hyperglycemia with insulin resistance of peripheral tissues and a deficiency of adequate insulin levels to lower blood glucose in the presence of a glucose challenge (2,3). There are two main categories of diabetes which fall under this definition. The first is Type I or Insulin-Dependent Diabetes Mellitus (IDDM), a condition wherein destruction of the pancreatic β cells leads to loss of insulin production and consequent loss of glycemic control. The result is hypoinsulinemia with hyperglycemia (2). The other category is Type II or Non-Insulin-Dependent

Diabetes Mellitus (NIDDM), in which patients display hyperglycemia, insulin resistance of peripheral tissues, and, in the earlier stages of the disease, hyperinsulinemia (1,3-9).

In both disorders, peripheral tissues display a resistance to insulin, although this resistance is particularly pronounced in NIDDM (2,6). Insulin initiates cellular actions by binding to a cell surface receptor, and recent studies have begun to clarify the first stages of insulin signaling (10). Insulin resistance in NIDDM is thought to result in many cases from a post-receptor defect in insulin signaling (1,4,8,9,11,12). We therefore evaluated in an animal model of NIDDM the expression and function of proteins involved in the early signaling events following insulin binding to its receptor. We further examined these parameters following treatment of such insulin resistant diabetic animals with an anti-hyperglycemic agent of the thiazolidinedione class known to lower blood glucose levels by sensitizing cells to insulin (13-20). In addition, an animal model of IDDM was similarly studied to determine if early insulin signaling events are altered by hyperglycemia in the absence of hyperinsulinemia. The goal of these studies was to gain a better understanding of the cause of cellular insulin resistance, as well as to further understand the corrective action mechanism of a novel class of compounds with great potential for the

treatment of non-insulin-dependent diabetes mellitus.

CHAPTER II

REVIEW OF RELATED LITERATURE

Overview

The focus of this project was to study alterations in early steps of the insulin signaling pathway in insulin resistant diabetes, and to compare these alterations with possible defects in insulin deficient diabetes. Therefore, both diabetic syndromes will be discussed, followed by an overview of insulin signal transduction.

Insulin Dependent Diabetes Mellitus (IDDM)

Suspected Causes of IDDM

Five percent of the population of the United States is afflicted with diabetes mellitus. Of these individuals, about 80-85% have NIDDM, and 15-20% have IDDM (21). IDDM, like NIDDM, apparently results from a mixture of genetic and environmental factors (21). The main defect in IDDM is a destruction of the pancreatic β cells, resulting in a loss of the ability to produce and secrete insulin (2). This insulin deficit causes two problems. First, ingested glucose is not utilized or disposed of by tissues

efficiently. Secondly, insulin deficiency stimulates glucagon secretion, which stimulates glucose release from the liver. Consequently, this results in hyperglycemia, dehydration, and glycosuria (2).

Although the etiology of IDDM is much more clear than the cause of NIDDM, there is some controversy concerning the primary origin of the disease. This is probably due to the fact that although there is a genetic predisposition to IDDM, environmental factors play a substantial role (22,23). In fact, although the incidence of IDDM is greater in relatives of IDDM patients (5-6%) than in the general population (0.3-0.5%), the concordance rate between identical twins is only about 34% (22). The one point that is agreed upon is that the cause of islet cell destruction is an autoimmune response targeted at the β cells (22,24).

Genetic Factors Leading to IDDM

One of the strongest genetic indicators of IDDM is found in the Human Leukocyte Antigen (HLA) system of the Major Histocompatibility Complex (MHC) class II proteins. These are the proteins expressed on the surface of cells, in this case pancreatic β cells, which are responsible for recognition of "self" by the immune system (22,23). There are two main HLA markers which are associated with a predisposition to susceptibility to IDDM. The first is that DR3/DR4 heterozygotes have a 46-fold increased risk of

developing IDDM (22,23). The second is that a mutated DQ β chain with an amino acid other than aspartate at position 57 has an even stronger link with the incidence of IDDM (22,23). Although there is no direct association between the function of these proteins and the cause of IDDM, these genotypes have been found to be more susceptible to infection with Coxsackie B virus (23). Also, these MHC proteins may be involved in autoimmunity caused by early exposure to milk proteins, which is discussed below.

Another genetic cause of type I diabetes involves antibodies to islet cell-specific antigens. Among the proteins found to cross-react with islet cell antibodies found in IDDM patients are glutamic acid decarboxylase (GAD), insulin, proinsulin, heat shock protein 65, carboxypeptidase H (an enzyme involved in the conversion of proinsulin to insulin), and glucose transporter GLUT-2 (23,25-27). Antibodies to GAD have been found in 80% of recent onset type I diabetics (26).

Environmental Factors Leading to IDDM

Because the concordance rate of IDDM in monozygotic twins is only about 34%, environmental influences may also play a role in the development of IDDM. Environmental factors involved in the development of type I diabetes are stress, nitrosamines from smoked meat, seasonal variation, high nitrates, coffee, sugar, high latitude, low average

temperature, exposure to certain insecticides, and exposure to solid foods before three months of age (24,28). However, the two most likely environmental influences are viral infection and early exposure to cow's milk (23,24,28-30).

Viral influences. Evidence for the involvement of viruses in IDDM centers on the presence of Coxsackie B virus in newly diagnosed IDDM patients, a strong correlation of maternal rubella infection during pregnancy and IDDM of the offspring, and the fact that Coxsackie B3, Coxsackie B4, and retrovirus type 3 viruses can all infect human β cells in culture (29,30). In addition, SJL/J mice infected with Coxsackie B virus, Mengovirus, and Encephalomyocarditis (EMC) virus all developed IDDM (29). There is also a strong correlation between the Cytomegalovirus (CMV) genome and islet cell antibodies found in IDDM patients (23). It is not known whether the viruses necessarily infect the β cells themselves or if the viral-induced destruction of these cells are a result of antibodies directed against viral antigens cross-reacting with islet antigens.

Milk proteins. Recent studies have shown that early exposure to cow's milk could contribute to the development of IDDM, and that breast-feeding of infants could have protective properties against this disorder (23,24,30).

In newly diagnosed diabetic children and in spontaneously diabetic rats fed cow's milk, antibodies to bovine serum albumin (BSA) and β -lactoglobulin were found in high levels (30). Anti-BSA antibodies have been found to recognize an islet-specific plasma membrane protein of M_r 69,000, known as islet cell antibody 69 (ICA69) (24,30). Also, BSA shares a region of homology with the MHC class II proteins Ia, DQ, and DR (30). Interestingly, the region of homology between BSA and DQ β includes the position 57 amino acid discussed above. Further, the difference between human and bovine serum albumin is that the human serum albumin has an aspartate in the region of homology with DQ β corresponding to amino acid number 57, while BSA has an alanine. Therefore, this could partially explain an increased incidence of IDDM in patients with an amino acid other than aspartate at position 57 of the DQ β MHC protein (30).

There is much controversy concerning all of these possible causes, mainly because individuals with any of these predisposing factors do not necessarily develop IDDM (24). Because of this, IDDM is thought to be a multifactorial disease of heterogeneous origin.

Treatment of IDDM

The most widely used treatment for type I diabetes is the administration of exogenous insulin and tight dietary control (2).

Non-Insulin-Dependent Diabetes Mellitus (NIDDM)

The Cause and Progression of NIDDM

Insulin resistant or non-insulin dependent diabetes mellitus is a condition of unknown etiology which is associated with insulin resistance of peripheral tissues, hepatic glucose overproduction, and impaired β cell function (1,3-6,8,9,31-34). The result of these anomalies is hyperglycemia, hyperlipidemia and hyperinsulinemia in the earlier stages, followed by hypoinsulinemia in the later stages when overt NIDDM ensues (1,3,4,34).

This condition is precipitated by both genetic and environmental factors (1,6-9,33,34). Unknown genetic factors initiate the development of diabetes, resulting in altered expression of diabetes-related genes. These alterations are exacerbated by diet and obesity to bring about insulin resistance and eventually overt diabetes (1,6,33,34).

Although there is some controversy as to whether insulin resistance or pancreatic β cell dysfunction is the primary genetic defect causing diabetes, there is considerable evidence suggesting that insulin resistance occurs before β cell dysfunction (1,6). One of the best arguments for insulin resistance preceding a β cell defect is that in the early stages of NIDDM, patients exhibit hyperinsulinemia and resistance to exogenously supplied

insulin or endogenously secreted insulin (1,6). One of the earliest detectable defects in first-degree relatives of NIDDM patients is impaired insulin action in muscle and adipose tissues (21). In studies where individuals with a family history of NIDDM were followed longitudinally, insulin resistance appeared to be present for many years before the clinical onset of the disease (1). However, given the probable polygenic inheritance of the disease, it is possible that either a defect in β cell function alone or both insulin resistance and β cell defects are contributing factors in some cases (6).

In addition to these genetic factors, other contributing factors are obesity and dietary conditions. In particular, increased abdominal obesity is associated with insulin resistance and increases the risk of developing NIDDM (1). Also, in offspring of diabetic parents, insulin resistance was found to increase as body weight increased (35). Thirdly, KK mice, which show glucose intolerance and insulin resistance but not hyperglycemia when fed laboratory chow, developed hyperglycemia and glycosuria when fed a diet that induced obesity (36).

KKA^y Mice as a Model of NIDDM

The Upjohn colony of KKA^y mice was originally obtained from Takeda Chemical Industries in Osaka, Japan. The KKA^y mouse strain was established as a model of obese type II

diabetes for the purpose of screening antihyperglycemic compounds (37). The colony is maintained by crossing obese insulin-resistant yellow KKA^y males with glucose intolerant KK females (37). KKA^y mice originally were the result of a cross between albino KK mice and yellow obese mice (A^y) (36). KK mice are an inbred strain with a diabetic phenotype consisting of impaired glucose tolerance, moderate hyperglycemia, insulin resistance of peripheral tissue, and hyperinsulinemia (36). The A^y gene causes mice to become obese and also causes a yellow coat pigmentation of the animals carrying this gene (36). The offspring from the KK x A^y cross consisted of four groups: yellow KK mice or KKA^y mice ($A^y a$, BB, Cc); albino KKA^y mice ($A^y a$, BB, cc); black KK mice (aa, BB, Cc); and albino KK mice (aa, BB, cc) (36). Therefore, the yellow offspring from the KK x A^y cross possess the diabetic features of the KK mice as well as the obesity trait of the A^y parent (36).

KKA^y mice have significantly higher body weight, fat pad size, blood glucose and plasma insulin levels than nondiabetic C57Bl/6 control mice (37). In contrast to the elevated plasma insulin levels, KKA^y mice have only a very small amount of pancreatic insulin as compared to C57 mice, suggesting that the islet cells are under considerable stress to secrete more insulin to meet the demand of the insulin-resistant tissues (37). KKA^y mice also have a higher basal glucose uptake than C57 mice and are insulin-

resistant as assayed by insulin-stimulated glucose transport into isolated adipocyte cells (18). Because of these observed phenotypic similarities with NIDDM, KKA^y mice are considered an attractive model for studying obesity-linked type II diabetes (37).

The only drawback to the KKA^y model of insulin-resistant diabetes is that since both parental strains possess diabetes-related characteristics, there is no genetically-related control mouse strain. C57Bl/6J mice have been used as controls in past studies with KKA^y mice because in comparison with KKA^y mice, C57Bl/6J mice display normal glucose, insulin, and triglyceride levels, and are insulin-sensitive (18,19,37).

Treatments for NIDDM

Past Treatments

Regardless of the precipitating cause of NIDDM, the end result in overt diabetes is hyperglycemia and inadequate insulin secretion. To correct this condition, treatments for NIDDM patients have focused on increasing insulin output from the pancreas by oral administration of insulin secretagogues (11), and also by increasing exercise and by altering diet for desired weight loss to reverse insulin resistance (4,11,34).

Future Treatments

A recent development in the treatment of NIDDM has been the discovery of a new class of compounds that acts to sensitize tissues to insulin rather than increasing the secretion of insulin. These compounds, the thiazolidinediones, increase insulin sensitivity in Wistar fatty rats as well as obese insulin resistant KKA^y mice (13-15,17,18,20). In addition, triglyceride levels, nonesterified fatty acids, and cholesterol levels were also lowered in the treated animals (15,38). The mechanism of action of thiazolidinediones is unknown, but several studies have shown that they work by increasing glucose uptake (18,20), altering gene expression (17-19,39-41), and enhancing insulin receptor kinase activity (16,42-44) without increasing insulin binding. Incubation of Rat-1 fibroblasts with the thiazolidinedione troglitazone (CS045) reversed the inhibitory effect of high glucose on insulin-stimulated tyrosine phosphorylation of the insulin receptor and the insulin receptor substrate-1 (IRS-1) (42). Also, epididymal fat pads from diabetic ob/ob mice pretreated with the thiazolidinedione ciglitazone showed an increase in insulin-stimulated glucose oxidation and lipogenesis as compared to untreated diabetic mice (45). The thiazolidinediones are presently in clinical trials (46). One compound of this class, pioglitazone, was used in our study in order to determine if it elicited its effects at

the level of insulin signal transduction. Two recent studies by Sizer, *et al.* (47) and Zhang, *et al.* (48) suggest that pioglitazone may act by directly augmenting early steps of signal transduction, specifically activation of phosphatidylinositol 3'-kinase.

Signal Transduction

Upon reaching its target cells (primarily muscle, liver, and adipose), insulin transmits its signal to the cell interior by binding to its receptor on the plasma membrane. The binding of insulin initiates an intracellular signaling cascade which distributes insulin's signal to the rest of the cell, activating insulin-dependent processes such as glucose uptake, glycolysis, glycogen synthesis, amino acid uptake, and DNA synthesis. Insulin resistance of peripheral tissues is due to an attenuation of insulin's signaling system or a defect in one or more of the processes of glucose metabolism. Due to the recent elucidation of the first steps of insulin action, it is the beginning of the signaling cascade which has been the focus of this study. Therefore, the components involved in the first stage of insulin signaling will be discussed.

The Insulin Receptor

Structure

The insulin receptor is a heterotetrameric structure composed of two α and two β subunits linked by disulfide bonds to yield an $\alpha_2\beta_2$ receptor (49-53). The two α subunits are extracellular glycoproteins, each of MW 135,000, and are responsible for the binding of insulin (4,54). The two β subunits are 95,000 MW transmembrane glycoproteins which contain ATP binding sites and the tyrosine kinase activity of the receptor (49-51,53-55). Each $\alpha\beta$ dimer is encoded by a gene of 22 exons located on human chromosome 19. The proreceptor, translated from a single mRNA, is either a 1343 or 1355 amino acid protein depending on alternative splicing of exon 11, plus an additional 27 amino acid signal peptide at the NH_2 -terminal end (56). The two forms of the insulin receptor generated by alternative splicing of exon 11 (in the α subunit) are believed to have different properties. The A form, without exon 11, has a higher affinity for insulin (57). The B form, with exon 11, has a lower affinity for insulin (higher K_m), but has an 8-fold higher V_{max} and shows a two-fold higher insulin-stimulation of phosphotyrosine in the insulin receptor β subunit and a synthetic substrate (57,58). In addition to the splicing of exon 11 in the mRNA from which the protein is translated, alternate poly-A site selection results in two different-

sized transcripts, 9.5 and 7.5 kb. This poly-A site selection does not have a known role in the expression of the insulin receptor (59).

As the receptor protein is processed, the signal peptide is cleaved and the proreceptor is glycosylated. Two of these proreceptors are then joined by disulfide bonds within the regions corresponding to the α subunits, and then another cleavage event cuts each proreceptor into α and β subunits. The α and β subunits are also joined by disulfide bonds, and thus the mature insulin receptor is an $\alpha_2\beta_2$ heterotetramer held together by disulfide bonds (56).

Receptor Activation

Once insulin binds to the α subunit, the receptor undergoes a conformational change that results in a series of intramolecular tyrosine autophosphorylation events and subsequent activation of the β subunit tyrosine kinase activity toward exogenous substrates (49,51,54,56). Autophosphorylation experiments carried out at 0°C suggest that tyrosine 1146 is the first residue to be phosphorylated in the β subunit, followed by phosphorylation of tyrosine 1150 or 1151. This region is considered a regulatory region of the β subunit, since all three of these tyrosines must be phosphorylated in order to fully stimulate the phosphotransferase activity of the insulin receptor toward its exogenous cellular substrates (51). All of these

tyrosine phosphorylation events seem to require lysine at position 1018, which is positioned in a potential ATP binding site. Mutation of this residue to alanine, arginine, or methionine inactivated the receptor kinase activity (56,60).

Once the β subunit is tris-phosphorylated in this region, it is further phosphorylated at tyrosine residues 1316 and 1322. Phosphorylation of tyrosines 1316 and 1322 does not seem to be required for activation of the β subunit phosphotransferase (61), although this carboxy-terminal region may play a role in regulating insulin's growth-promoting effects (62). Studies by Kaliman, *et al.* and Pang, *et al.* have shown that this C-terminal domain of the receptor may be involved in negatively regulating the insulin receptor kinase (63,64); however, other work has shown that deletion of the C-terminus of the β subunit actually caused a decrease in insulin-stimulated receptor autophosphorylation and receptor internalization without changing insulin-stimulated IRS-1 phosphorylation, phosphatidylinositol 3'-kinase activity, glucose uptake, or DNA synthesis (65). In contrast to this study, Smith *et al.* found that the C-terminus of the receptor was not important in receptor internalization (66).

Another important region of the insulin receptor β subunit is the juxtamembrane domain. Mutation of tyrosine 960 to phenylalanine impaired the insulin-stimulated

phosphorylation of the main insulin receptor substrate, IRS-1, as well as the activation of phosphatidylinositol 3'-kinase and microtubule-associated protein kinase (MAPK) (67). Mutation of aspartate 938 to valine caused the tyrosine kinase of the receptor to be activated in the absence of insulin (68). The amino acids between positions 954 and 965 in this region of the receptor are also involved in insulin-stimulated receptor internalization (67).

Other important functional domains of the receptor include serine/threonine phosphorylation sites and glycosylation sites. The insulin receptor is known to be phosphorylated on serine and threonine residues after insulin stimulation (69-73), and there is some evidence for this phosphorylation inhibiting the insulin receptor kinase (69,70). Several studies involving mutation of serines 967, 974, 976 and threonine 1336 showed that these sites are not important in insulin receptor function (72,73). In addition, elimination of serine phosphorylation of the juxtamembrane domain had no effect on insulin receptor autophosphorylation (71). Unlike the serine/threonine phosphorylation, glycosylation of the receptor is very important in receptor function. Mutation of the glycosylation sites of the α subunit caused the insulin receptor to be retained in the endoplasmic reticulum in the proreceptor form, while the β subunit glycosylation sites were found to be required for signal transduction (74).

Insulin Receptor Defects

Alternative splicing of exon 11. Recent evidence suggests that alternative splicing of exon 11 of the insulin receptor may play a role in the development of NIDDM, although this has been controversial. Some data has shown that there is a higher ratio of the B form of the receptor (with exon 11), which has a lower affinity for insulin, in NIDDM patients as compared to nondiabetic controls (57,75-77). However, there are also reports of equal ratios of A and B forms between control and NIDDM patients (78,79), and also some reports of a higher ratio of the A form in NIDDM as compared to nondiabetic controls (80,81). It is difficult to rationalize the differences between these studies, but one explanation may be that different NIDDM groups have different ratios, or possibly that there is not an absolute correlation between splicing products of the insulin receptor and NIDDM.

Other mutations. There are several documented mutations of the insulin receptor leading to insulin resistance, and such mutations reportedly affect the insulin receptor at different points in its synthesis, processing, binding, function, and internalization (82). The most severe forms of NIDDM, such as Rabson-Mendenhall syndrome and leprechaunism, were associated with mutations in the α

and β subunits of the insulin receptor (83). However, these collective mutations only account for the insulin resistance of 1-10% of all NIDDM patients, and thus there are probably some other defects which cause insulin resistance in the majority of NIDDM patients (3,12,82,83). These other defects are likely to occur in intermediate steps of the insulin signaling pathway.

The Insulin Receptor Substrate-1 (IRS-1)

Structure of IRS-1

As mentioned above, insulin binding to its receptor activates the tyrosine kinase activity of the receptor toward intracellular substrates. The main protein identified to be tyrosine phosphorylated upon insulin stimulation migrates between 160 and 185 kDa on SDS-polyacrylamide gel electrophoresis (84-87). This protein has been cloned and sequenced by two separate groups from Fao hepatoma cells and 3T3-L1 adipocytes, and has been named insulin receptor substrate-1 (IRS-1) (85-88). Although IRS-1 migrates as a larger protein on SDS-PAGE, it is a 131,000 MW hydrophilic protein, translated from a 9.5 kb mRNA. The difference in mobility and molecular weight is thought to be due to the high basal serine phosphorylation and high β -sheet content of IRS-1 causing the protein to migrate as a larger protein (85,89). Although it contains a putative ATP

binding site (gly¹³⁷-val-gly-glu-ala-gly-...-lys¹⁵⁶-X-ile), it lacks the asp-phe-gly or ala-pro-glu sequences diagnostic of a protein kinase (85).

Before insulin stimulation, IRS-1 exists as a phosphoprotein containing phosphoserine and some phosphothreonine but no phosphotyrosine. IRS-1 contains 35 serine/threonine phosphorylation sites, and at least 20 potential tyrosine phosphorylation sites (85,90). There is some evidence for an increase in serine/threonine phosphorylation on insulin stimulation (89,90), which could inhibit tyrosine phosphorylation of IRS-1 or inhibit the docking of other proteins to the activated IRS-1 (89,90). However, the majority of insulin stimulated phosphorylation of IRS-1 occurs on tyrosine residues, and this has been shown to activate it as a multisite docking protein (10,91).

Tyrosine Phosphorylation and Function of IRS-1

There are several lines of evidence which indicate that IRS-1 is involved in insulin signaling. First, aside from the IR β subunit, IRS-1 is the major protein phosphorylated on tyrosine residues after insulin stimulation (55,84,86,92,93). Second, phosphorylation of IRS-1 occurs within the same time frame and with similar insulin concentrations as phosphorylation of the insulin receptor β subunit (55,92). In fact, maximal phosphorylation of IRS-1 in response to insulin occurs within 30 seconds, which

directly correlates with phosphorylation of the insulin receptor. This implicates IRS-1 as a direct substrate of the insulin receptor tyrosine kinase, since no other phosphorylated products are seen earlier. Third, an insulin receptor mutated at tyrosine 960 of the juxtamembrane region and transfected into CHO cells was unable to phosphorylate IRS-1 in response to insulin stimulation, nor was this receptor capable of mediating normal cellular responses to insulin such as stimulation of glycogen synthase, amino acid uptake, or thymidine uptake into DNA, even though this receptor was still able to phosphorylate itself and other exogenous substrates (50). Likewise, mutation of the ATP binding site lysine-1018 prevented insulin receptor autophosphorylation and IRS-1 phosphorylation in the presence of insulin (60). Also, cells expressing receptors with a mutation of tyr-1146 to phenylalanine had impaired β subunit autophosphorylation as well as impaired IRS-1 phosphorylation (94).

IRS-1 function has been linked to both the metabolic (95-102) and mitogenic (90,97,103-107) actions of insulin. An example of the mitogenic involvement of IRS-1 in insulin signaling is shown in studies with Chinese hamster ovary (CHO) cells. Expression of IRS-1 in CHO cells doubles the maximal amount of thymidine incorporation into DNA stimulated by insulin, and expression of IRS-1 antisense RNA in CHO cells reduced the mitogenic response to insulin

(89,108). Similarly, *Xenopus* oocytes, which have very little or no IRS-1 and which normally do not mature in response to insulin or IGF-1, were found to mature in response to insulin and IGF-1 when IRS-1 was transfected into these cells (106). Other data showed that disruption of IRS-1 gene expression in transgenic mice caused a decrease in intrauterine and postnatal growth by more than 50% (90,109,110). The strongest evidence supporting a role for IRS-1 in the metabolic effects of insulin comes from the association of IRS-1 with phosphatidylinositol 3'-kinase. IRS-1 has been shown to associate with and activate phosphatidylinositol 3'-kinase on insulin stimulation (111-115). The catalytic activity of phosphatidylinositol 3'-kinase can be specifically inhibited by a fungal toxin, wortmannin, and this action results in inhibition of insulin-stimulated glucose uptake (95,96,99,102), thus linking IRS-1 and PI3K with a well-known metabolic response to insulin.

As mentioned above, once IRS-1 becomes tyrosine phosphorylated by the insulin receptor kinase, it acts as a multisite docking protein via an interaction of its phosphotyrosine residues with src-homology 2 (SH2) domains of several target proteins (10). SH2-containing proteins that interact with IRS-1 on insulin stimulation include the p85 α subunit of phosphatidylinositol 3'-kinase (PI3K), the tyrosine phosphatase Syp/SH-PTP2/PTP1D, growth factor

receptor bound protein 2 (GRB2), and Nck (10,91,116-120). A schematic diagram of this is shown in fig. 1, adapted from White and Khan, 1994 (10). The specificity of these interactions is determined by the sequences surrounding

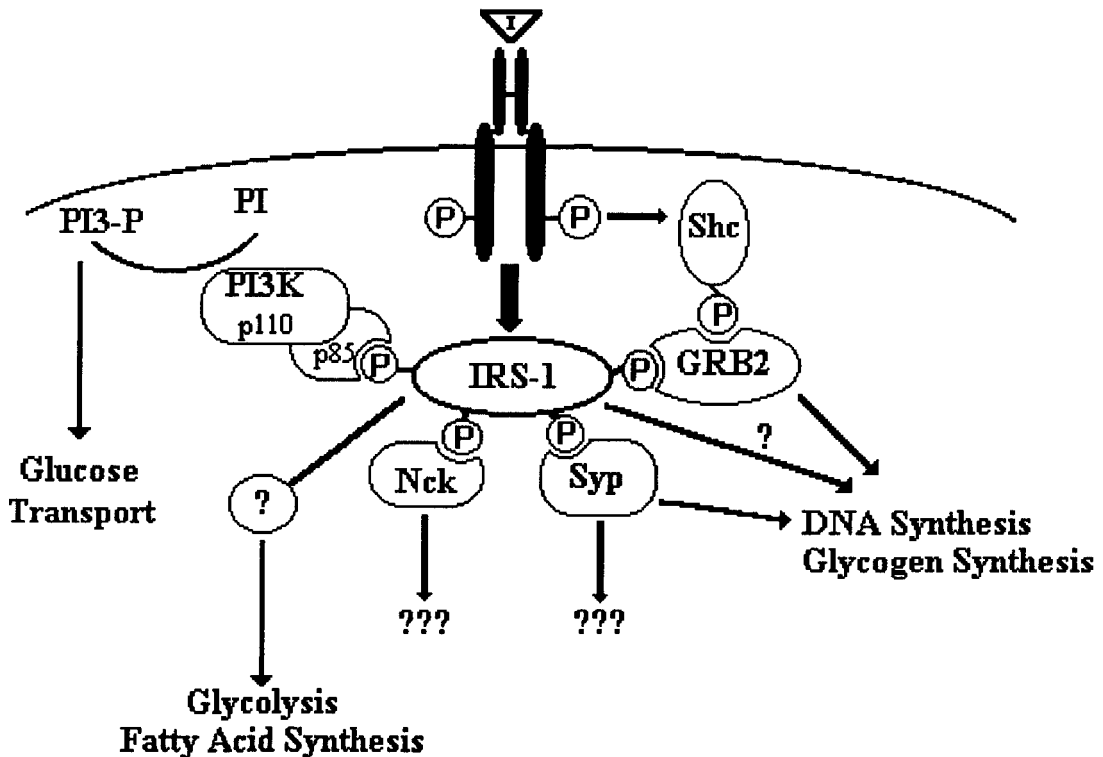


Fig. 1. Early steps in insulin signal transduction.

the phosphorylated tyrosines (pY) of IRS-1 and the sequence of each SH2 domain on the target proteins. The p85 α subunit of PI3K prefers pYMXM motifs (phosphotyrosine-methionine-any amino acid-methionine), specifically pY608 and pY939 of IRS-1 (91). GRB2 binds to pY(895)VNI (phosphotyrosine-valine-asparagine-isoleucine) (91), while Nck binds most strongly to pY(147)DTG (phosphotyrosine-aspartate-threonine-glycine) (118). Syp has two SH2 domains that bind to pY(1172)IDL (phosphotyrosine-isoleucine-aspartate-leucine) and pY(1222)ASI (phosphotyrosine-alanine-serine-isoleucine), respectively (121).

Mutations in IRS-1

When the incidence of amino acid mutations in the IRS-1 gene was compared between NIDDM patients and nondiabetic control subjects, two mutations were found: a glycine to arginine transition at position 972 and an alanine to proline transition at amino acid 513 (122). Of the 86 NIDDM patients and 76 normoglycemic controls studied, ten NIDDM patients and 3 controls were heterozygous for the position 972 polymorphism, while 6 NIDDM patients and 2 controls were heterozygous for the position 513 polymorphism. There were no homozygotes or double heterozygotes with both polymorphisms. Another study of French NIDDM families found that these same polymorphisms did not cosegregate with diabetes (123). A different study compared tandem repeat

mutations in the IRS-1 gene between Japanese NIDDM families and controls, and found that tandem repeat polymorphisms were not associated with a higher risk of NIDDM (124). Therefore, no direct link exists between these naturally occurring IRS-1 mutations and NIDDM.

Proteins which Associate with Phosphorylated IRS-1

Phosphatidylinositol 3'-Kinase (PI3K)

The phosphatidylinositol 3'-kinase (PI3K) is composed of an 85 kDa adaptor subunit and a 110 kDa catalytic subunit (52,125-128). The 110 kDa subunit is a 1068 amino acid protein which is related to Vps34p, a *Saccharomyces cerevisiae* protein involved in the sorting of proteins to the vacuole (127). It catalyzes the phosphorylation of the D-3 position of the inositol ring of phosphatidylinositol 4-phosphate and phosphatidylinositol 4,5-bisphosphate (52,125, 126). This reaction would yield phosphatidylinositol 3,4-bisphosphate and phosphatidylinositol 3,4,5 trisphosphate, respectively. The biological function of these products is unknown, but as mentioned above, inhibition of the p110 catalytic activity with the fungal toxin wortmannin inhibited insulin-stimulated glucose uptake by blocking recruitment of vesicles containing GLUT4 transporter proteins to the plasma membrane via an unknown mechanism (95,96,99,102,129). The phosphatidylinositol 3'-phosphate

products of PI3K action are not cleaved by phospholipase C, but they have been shown to activate the ζ , δ , η , and ϵ isoforms of protein kinase C (130,131).

PI3K may also be involved in insulin-stimulated mitogenesis (106,107). The stimulation of *Xenopus laevis* oocyte maturation by IGF-I or insulin requires the presence of IRS-1 and the activation of PI3K through its association with IRS-1 (106). Also, microinjection of N- or C-terminal SH2 domains of p85 α into rat-1 fibroblasts stably transfected with human insulin receptors inhibited insulin-stimulated DNA synthesis (107). Likewise, microinjection of pYMXM or pYXXM phosphonopeptides into the same cell line inhibited DNA synthesis from 61-68% as compared to control cells (107).

The p110 subunit requires the p85 α subunit in order to function (127). The p85 α subunit contains 2 SH2 domains and 1 SH3 domain (85,94,125,132), and may be phosphorylated on insulin stimulation, although this is controversial (85,94,100,114,125,133). There is an overwhelming amount of data showing that the p85 α subunit of PI3K associates with tyrosine-phosphorylated IRS-1 on insulin stimulation, and that this association causes PI3K activation (10,91,100,102,106,111-113,115,119,134-137). Strong evidence in favor of the importance of the association of IRS-1 with p85 α in PI3K activation involves the use of synthetic peptides. *In vitro* activation of immunopurified PI3K by recombinant IRS-1 was

inhibited by the addition of bacterial fusion proteins containing the SH2 domains of p85 α (100,119). Likewise, addition of phosphorylated pYMXM motifs from IRS-1 activated PI3K *in vitro* (100,112,119). In addition to these data, PI3K activity was found in anti-IRS-1 immunoprecipitations from insulin stimulated cells of a variety of types (10,101,111,126,135,136,138,139).

Growth Factor Receptor Bound Protein-2 (GRB2)

Growth factor receptor bound protein-2 (GRB2) is a 24 kDa protein containing one SH2 domain flanked by two SH3 domains, and has no known catalytic function of its own (140). As mentioned above, GRB2 associates with IRS-1 on insulin stimulation through its SH2 domains and the pY(895)VNI motif of IRS-1 (10,91,120,141,142).

GRB2 also associates with another protein, Shc, on insulin stimulation (10,105,116,141-145). Shc, or src-homology/collagen protein, has one SH2 domain and a glycine/proline rich stretch which is homologous to collagen. It has no SH3 domain and no catalytic function of its own (145). Shc is also tyrosine phosphorylated on insulin stimulation by the insulin receptor kinase, and it is the tyrosine-phosphorylated form of Shc which binds the SH2 domain of GRB2 (143,145). This is shown in fig. 1.

The function of GRB2 lies in its ability to bind to other proteins. The N- and C-terminal SH3 domains bind to a

proline-rich stretch in the C-terminus of the guanine nucleotide exchange factor son of sevenless (SOS) (144,146). SOS then activates ras, which binds the serine/threonine kinase raf-1 (10). Raf-1 is then activated to phosphorylate MAP kinase kinase, leading to activation of MAP kinase (10,105,116,140,144,146-148) and DNA synthesis (10,116,141,148). Another consequence of increased activation of ras or raf-1 is the increased expression and activity of the glucose transporter GLUT1 but not GLUT4. This results in increased basal glucose uptake regardless of insulin levels (149-151). The SH3 domains of GRB2 are also responsible for localization of GRB2 to membrane ruffles (152). Recent evidence has shown that a substrate of MAP kinase, PHAS-I, is involved in insulin activation of translation initiation (153), suggesting yet another downstream effect of insulin signaling through GRB2 and ras or raf-1.

A third function of the SH3 domains of GRB2 is to associate with the proline-rich stretch of the GTPase protein dynamin. GRB2 associates with dynamin in unstimulated cells, and this complex then associates with phosphorylated IRS-1 on insulin stimulation via the SH2 domain of GRB2 (140,154). Association of the GRB2-dynamin complex with phosphorylated IRS-1 or phosphopeptides containing the sequence of IRS-1 which binds to the GRB2 SH2 domain activated the GTPase activity of dynamin (154). The significance of this complex in insulin signaling is

unknown, but dynamin may be involved in the pinching off of coated vesicles from the plasma membrane for endocytosis, and thus it could possibly be involved in receptor internalization (154). Transfection of mammalian cells with mutant dynamin blocked receptor-mediated endocytosis (154).

Nck

Another protein found to associate with IRS-1 on insulin stimulation is Nck, a 47 kDa protein composed almost entirely of one SH2 and three SH3 domains (155). The function of Nck is unknown, but it may bind to a protein with serine/threonine kinase activity via its SH3 domains (156), and overexpression of Nck causes cell transformation and cell proliferation (155,157).

Syp/PTP1D/SH-PTP2

Syp is a 65-72 kDa protein tyrosine phosphatase with two SH2 domains in its N-terminus, and differs from the other IRS-1 binding proteins in that it has a well-characterized catalytic domain (117). It has also been called PTP1D or SH-PTP2 by separate groups. Syp has been shown to bind to tyrosine-phosphorylated IRS-1 (91,117), and incubation with IRS-1 phosphopeptides caused up to a 50-fold stimulation of the phosphotyrosine phosphatase activity of Syp *in vitro* (121). Syp also binds to and is tyrosine-phosphorylated by the insulin receptor *in vitro* on insulin

stimulation (158-160). Recent studies have provided evidence indicating that Syp is linked to insulin, IGF-1, or EGF stimulation of DNA synthesis. Xiao, et al. showed that in rat-1 fibroblasts stably expressing the insulin receptor, insulin-stimulated DNA synthesis was inhibited by microinjection of anti-Syp antibodies, phosphonopeptides containing the IRS-1 phosphotyrosine binding sites for Syp SH2 domains, or Syp SH2-GST fusion proteins by 60-90%, 50-60%, and 90%, respectively (161). Similar inhibition of DNA synthesis was seen with IGF-I and EGF stimulation of these cells under the same conditions, although serum-stimulated DNA synthesis was not affected by these inhibitors (161). Therefore, there are factors in serum other than insulin, IGF-I, or EGF that stimulate DNA synthesis independently of Syp.

Hypothesis and Specific Aims

Because NIDDM is associated with a variety of metabolic derangements (2-5,120), and because the cause of insulin resistance probably lies in a post-receptor defect in most cases, this project focused on studying early insulin signaling events as possible sites of defects leading to insulin resistance and NIDDM. The rationale for our hypothesis is that early defects would lead to a greater variety of derangements downstream, before insulin's signal branched off to elicit its many different effects. Such a

rationale is supported by the observation that two rare but very severe forms of NIDDM, leprechaunism and Rabson-Mendenhall Syndrome, result from defects in insulin's initial signaling events; i.e., receptor binding and autophosphorylation (83).

Hypothesis

The overall hypothesis of this dissertation is that a primary defect in insulin resistance is an altered expression or function of an early insulin signaling component, and that this defect is corrected or compensated for by the antihyperglycemic agent pioglitazone.

Specific Aims

To test this hypothesis, two models of insulin resistant diabetes were used. The insulin resistant KKA^y mice were used as an animal model for insulin resistant diabetes because such mice are obese, glucose intolerant, and exhibit hyperglycemia and hyperinsulinemia (36). Differentiated 3T3-L1 adipocytes pre-fed with high glucose and high insulin concentrations were used as an *in vitro* model of insulin resistance. In addition, rats made insulin deficient with streptozotocin treatment were studied to determine the effect of hyperglycemia in the absence of hyperinsulinemia on early insulin signal transduction events.

Specific Aim 1

To determine if the expression of the insulin receptor, IRS-1, PI3K p85 α , GRB2, Nck, or Syp is altered in liver and fat tissues of KKA^y mice as compared to control nondiabetic mice.

Protein levels. First, the protein levels of these insulin signaling components were compared between KKA^y diabetic mice and control diabetic mice.

mRNA levels. When the protein levels were found to be altered between diabetic and nondiabetic animals, the mRNA levels were examined to determine if the alteration was a result of a difference in the abundance of the mRNA for these genes.

Specific Aim 2

To determine if the insulin-stimulated tyrosine phosphorylation of the insulin receptor or IRS-1 is defective in KKA^y mice as compared to nondiabetic control mice.

Isolated epididymal adipocytes. The acute insulin-stimulated tyrosine phosphorylation of the insulin receptor and IRS-1 was examined in isolated epididymal adipocytes from KKA^y and control mice by immunoblotting cell extracts

with anti-phosphotyrosine antibodies.

Specific Aim 3

To determine if the insulin-stimulated association of IRS-1 to PI3K p85 α is defective in KKA^y mice as compared to nondiabetic mice.

Isolated epididymal adipocytes. Cell extracts from isolated epididymal adipocytes were acutely stimulated with insulin, immunoprecipitated for IRS-1, and immunoblotted for PI3K p85 α .

Specific Aim 4

To determine if any of the alterations observed in aims 1-3 were corrected by treatment of animals with the insulin-sensitizing agent pioglitazone.

Pioglitazone treatment of KKA^y mice. A third group was included in the studies in aims 1-3 which consisted of KKA^y mice treated with pioglitazone. Because the cellular mechanism of pioglitazone action is unknown, the purpose of this aim was to determine if pioglitazone treatment affected early insulin signaling events.

Specific Aim 5

To determine if the alterations observed above in KKA^y

mice were due to the high levels of insulin and glucose associated with the diabetic condition.

High glucose and high insulin. Differentiated 3T3-L1 adipocyte cell cultures were treated overnight with medium containing high levels of glucose and insulin, thus representing the hyperglycemic and hyperinsulinemic state seen in the diabetic KKA^y mice. The expression of early insulin signaling components in this model was compared to the expression of these factors in control cells pre-fed for the same time interval with low glucose and low insulin levels. In addition, the ability of insulin to stimulate receptor autophosphorylation and IRS-1 phosphorylation was also analyzed in this model.

High glucose. To determine if any alterations observed in insulin-resistant mice were due to high blood glucose levels, the expression of these insulin signaling mediators was studied in rats made insulin-deficient by streptozotocin treatment.

Significance

Because the cause of NIDDM is unknown in the majority of cases, the search for defects leading to this condition is of extreme importance for developing preventive and therapeutic strategies. Identification in the last few

years of proteins involved in insulin signaling has provided a starting point for the search for defects in insulin signaling leading to insulin resistance. Once the likely defects are identified, it is possible that the development of new antidiabetic compounds could be aimed at these points of signal breakdown. This study has included the antidiabetic agent pioglitazone, a member of a novel class of insulin-sensitizing compounds. This class of compounds is known to lower blood glucose levels of diabetic mice by an unknown mechanism that operates post insulin-receptor binding.

CHAPTER III
MATERIALS AND METHODS

Materials

General Chemicals and Supplies

Chemicals

Guanidinium thiocyanate and formamide were purchased from International Biotechnologies, Inc. (New Haven, CT). Acrylamide/Bis (40%), ammonium persulfate, and TEMED were obtained from Bio-Rad (Richmond, VA). Protein A-Sepharose was purchased from Pharmacia (Milwaukee, WI). Nytran nylon membranes (Schleicher and Schuell, Keene, NH) and Immobilon PVDF membranes (Millipore, Bedford, MA) were used for northern and western blotting, respectively. Tris and glycine were purchased from Fisher Scientific (Pittsburgh, PA). The Riboprobe kit, including all nucleotides, polymerases, and transcription buffers were obtained from Promega Corp. (Madison, WI). ^{32}P -CTP, ^{14}C -Deoxyglucose, and the Enhanced ChemiLuminescence reagents were purchased from Amersham (Arlington Heights, IL). Luria-Bertani broth (dehydrated) was obtained from Difco (Detroit, MI). All

other chemicals were purchased from Sigma Chemical Co. (St. Louis, MO).

Culture Reagents

Dulbecco's Modified Essential Medium (DMEM) with high glucose (25 mM) or low glucose (5 mM) were obtained from BioWhittaker (Walkersville, MD). Fetal Calf Serum and Calf Serum (heat inactivated), glutamine, trypsin-EDTA, dexamethasone, IBMX (3-isobutyl-1-methylxanthine), endotoxin-free water, Antibiotic/Antimycotic solution (100X), and no-glucose DMEM (for glucose transport assays) were all obtained from Sigma Chemical Corp. (St. Louis, MO). Porcine insulin obtained from Eli Lilly (Indianapolis, IN) was used for the acute stimulation studies, and bovine insulin (Sigma Chemical Corp. (St. Louis, MO) was used during differentiation of 3T3-L1 adipocytes.

cDNA Constructs

The Insulin Receptor

Mouse insulin receptor cDNA was obtained from Dr. Graeme Bell (University of Chicago, Chicago, IL) in pUC, and a 775 bp insert was subcloned into the EcoRI site of pGEM3Z (2743 bp) giving a total construct size of 3518 bp. For Riboprobe preparation, the plasmid was linearized with HindIII and T7 polymerase was used to make antisense mRNA.

This probe hybridizes to two transcripts of 9.5 and 7.5 kb, which differ by alternate poly-A site selection (59).

The Insulin Receptor Substrate-1

A rat cDNA insert of 5.5 kb in pBluescript was obtained from Dr. Morris White (Joslin Diabetes Center, Boston, MA) (85). For Riboprobe preparation, the construct was linearized with BamHI and T7 polymerase was used to make antisense mRNA. The size of the transcript that hybridizes with this Riboprobe is 9.5 kb.

Phosphatidylinositol 3'-kinase p85 α

A rat cDNA insert of 1550 bp in pBluescript SK+/- was obtained from Dr. Lewis Cantley (Harvard Medical School, Boston, MA). Digestion of this construct for Riboprobe preparation with PvuII generates 3 fragments: a ~2900 bp vector fragment, a ~700 bp fragment, and a ~900 bp fragment. The antisense mRNA probe created with T7 polymerase is approximately 760 bp, transcribed from the ~700 bp fragment. The main transcript recognized by northern blotting in most tissues is 7.5 kb.

Antibodies

Anti-Insulin Receptor β -subunit

A polyclonal antibody directed against the C-terminus of the insulin receptor β subunit was obtained from Dr. Morris White (Joslin Diabetes Center, Boston, MA).

Anti-Insulin Receptor Substrate-1

Immunoprecipitations. A polyclonal antibody directed against a C-terminal 14 amino acid peptide from rat liver IRS-1 was purchased from Upstate Biotechnologies, Inc. (Lake Placid, NY) and used for immunoprecipitation of IRS-1 from mouse primary adipocytes. For immunoprecipitation of IRS-1 from mouse tissue, a polyclonal antibody directed against a baculovirus-overexpressed IRS-1 was obtained from Morris White (Joslin Diabetes Center, Boston, MA).

Western blotting. For primary adipocyte experiments, rat experiments, and 3T3-L1 experiments, the anti-C-terminus antibody described above was used for western blotting. For western blotting of mouse tissue immunoprecipitates, a monoclonal antibody directed against IRS-1 was obtained from Morris White (Joslin Diabetes Center, Boston, MA).

Anti-Phosphotyrosine

Tyrosine phosphorylation of the insulin receptor and IRS-1 was detected using a monoclonal anti-phosphotyrosine antibody, which was purchased from Upstate Biotechnologies, Inc. (Lake Placid, NY). This antibody, named 4G10, was generated using phosphotyramine, and recognizes tyrosine-phosphorylated proteins.

Anti-Phosphatidylinositol 3'-kinase p85 α

For detection of PI3K p85 α in all experiments except for the primary adipocytes, a monoclonal antibody directed against the N-terminal SH2 domain was obtained from Upstate Biotechnologies, Inc. (Lake Placid, NY). In the primary adipocyte experiments, a monoclonal antibody specific for the SH3 domain of PI3K p85 α , also purchased from Upstate Biotechnologies, Inc., was used to measure PI3K p85 α in anti-IRS-1 immunoprecipitates.

Anti-Growth Factor Receptor Bound Protein-2

Anti-GRB2 monoclonal antibody was obtained from Transduction Laboratories (Lexington, KY). This antibody was generated using the entire rat brain GRB2 protein as an immunogen.

Anti-Nck

Anti-Nck monoclonal antibody was obtained from Transduction Laboratories (Lexington, KY). It was generated using an 11.5 kDa fragment corresponding to amino acid positions 279-377 of the human Nck protein. This antibody cross-reacts with Nck in mouse and rat lysates.

Anti-Syp

For detection of Syp in all experiments, an anti-Syp monoclonal antibody was obtained from Transduction Laboratories (Lexington, KY). The anti-Syp antibody was produced using a polypeptide consisting of the N-terminal 177 amino acids of the human Syp protein.

Anti-Mouse

Anti-mouse Ig antibody (from sheep) was purchased from Amersham (Arlington Heights, IL). This antibody was conjugated to horseradish peroxidase (HRP) for use as a secondary antibody in enhanced chemiluminescence detection (ECL) of proteins which are recognized by monoclonal (mouse) primary antibodies.

Anti-Rabbit

Anti-rabbit Ig antibody (from donkey) was purchased from Amersham (Arlington Heights, IL). This antibody was conjugated to horseradish peroxidase for use as a secondary

antibody in ECL detection of proteins which are recognized by a polyclonal (rabbit) primary antibody.

Positive Controls

Insulin Receptor Substrate-1

Chinese hamster ovary cells overexpressing IRS-1 were obtained from Morris White (Joslin Diabetes Center, Boston, MA). An aliquot of total cell lysate from these cells was used as a positive control for all experiments involving the detection of IRS-1.

Phosphatidylinositol 3'-kinase

Baculovirus-overexpressed PI3K p85 α was obtained from Dr. Lewis Cantley (Harvard Medical School, Boston, MA), and an aliquot of this protein extract was used as a positive control for all experiments involving detection of PI3K p85 α . This protein migrated on SDS-PAGE as 85 kDa and was recognized by the anti-PI3K p85 α antibodies with high affinity.

Experimental Models and Design

Insulin Resistant Model (NIDDM)

All animal work up until the point of protein or RNA extraction was performed at The Upjohn Company, including blood glucose and serum insulin determinations.

C57 Control Mice

Male C57Bl-J6 mice 10-12 weeks of age were obtained from Charles Rivers (Portage, MI) as control animals with normal blood glucose (170 ± 6 mg/dl or 9.4 ± 0.3 mM) and normal serum insulin levels (26 ± 3 μ U/ml or 1.9×10^{-10} M).

KKA^y Diabetic Mice

Obese male KKA^y mice 10-12 weeks of age were obtained from the Upjohn Company (Kalamazoo, MI) for use as an animal model of insulin-resistant diabetes (NIDDM). KKA^y mice result from a cross between glucose-intolerant black KK female mice and yellow obese male A^y mice. The yellow offspring KKA^y mice are obese and insulin resistant, and display marked hyperinsulinemia and hyperglycemia (19,36).

Due to the diabetic characteristics of the parental strains, no genetically matched control exists for this model for this model. Therefore, C57Bl/6J mice were used as controls because of the relatively normal glucose regulation in the C57 strain.

Feeding and Pioglitazone Treatment

All animals were housed individually and fed *ad libitum* for four days prior to the experiment with or without pioglitazone delivered as a food admixture at about 20 mg/kg/day. It was previously determined that this dose and delivery method produced maximal changes in blood glucose and insulin sensitivity in mice within four days (Jerry Colca, The Upjohn Company, Kalamazoo, MI, unpublished observations).

Tissue Extraction and Animal Processing

On the fifth day from the start of drug treatment, the mice were bled from the orbital sinus for measurement of blood glucose concentrations and serum insulin levels, decapitated, and liver and epididymal fat pads were excised. The tissues were rapidly frozen in liquid nitrogen, shipped to us on dry ice, and stored at -70° C until they were processed by the RNA preparation or protein preparation protocols. Blood glucose levels were determined with an Alpkem Glucose AuotoAnalyzer (Alpkem, Clackamas, OR), and serum insulin levels were determined by radioimmunoassay as previously described (162).

Primary Adipocytes

Isolated/Primary Adipocyte Preparation

Animals used for the isolated adipocyte studies were treated exactly as the above animals regarding feeding, pioglitazone treatment, and animal sacrifice until the point of tissue excision. Epididymal fat pads from C57 and KKA^y mice treated with or without pioglitazone were placed into KRB buffer (Krebs-Ringer-Bicarbonate-BSA = 128 mM NaCl, 5 mM KCl, 1.4 mM CaCl₂, 1.3 mM MgSO₄•7H₂O, 5 mM NaHCO₃, 1.1 mM glucose, and 2% BSA), quickly minced, and incubated in KRB with 200 units/ml collagenase for 20 minutes. Epididymal fat pads from six animals from each group were combined to generate a pool of adipocytes which were later split into five samples to be individually stimulated with insulin. The entire experiment was performed twice. The collagenase-digested fat pads were then passed through a cell strainer which allowed digested cells and buffer to flow through. The cells were washed twice in KRB buffer, then aliquots were delivered into 0.4 ml microfuge tubes containing 0.1 ml dinonylphthalate oil and centrifuged briefly at 3000 x g to separate the buoyant fat cells from the non-adipose cells. Adipocytes were then pooled again, pre-incubated in KRB for five minutes, and cells were distributed in equal volume aliquots (0.25 ml) for insulin stimulation.

Insulin Stimulation

Equal volume aliquots of adipocytes (5 samples per group) were incubated with 1×10^{-7} M insulin for two minutes at 37° C with gentle shaking. The samples were then quickly frozen in a dry ice-acetone bath and stored at -70° C until the time of the protein extraction.

Insulin Deficient Model (IDDM)

As with the insulin-resistant model, all animal work up until the point of protein or RNA preparation was performed at The Upjohn Company.

Control Rats

Male Sprague-Dawley rats (160-180g) (Charles Rivers, Portage, MI) were used as control animals for the experiments dealing with insulin-deficient diabetes.

Insulin-Deficient Rats

Male Sprague-Dawley rats (160-180g) were made insulin deficient by tail-vein injection of streptozotocin (65 mg/kg) and allowed to recover for 7 days prior to tissue extraction for protein or RNA preparation. These animals displayed serum insulin levels of 4.2 ± 1.0 μ U/ml ($3.1 \times 10^{-11} \pm 0.7 \times 10^{-11}$ M) compared to 22.8 ± 1.8 μ U/ml ($1.7 \times 10^{-10} \pm 0.1 \times 10^{-10}$ M) in the controls. Streptozotocin-treated rats also possessed

high blood glucose levels (459 ± 10 mg/dl or 25.5 ± 0.5 mM) as compared to control rats (151 ± 2 mg/dl or 8.4 ± 0.1 mM).

Tissue Extraction and Animal Processing

On the day of the experiment, the rats were bled from the orbital sinus for measurement of blood glucose concentrations and blood insulin levels, decapitated, and liver and epididymal fat pads were excised. The tissues were rapidly frozen in liquid nitrogen, shipped to us on dry ice, and stored at -70° C until they were processed by the RNA preparation or protein preparation protocols. Blood glucose levels were determined with an Alpkem Glucose AuotoAnalyzer (Alpkem, Clackamas, OR), and serum insulin levels were determined by radioimmunoassay as previously described (162).

3T3-L1 Cells

Culture Conditions

3T3-L1 cells were obtained from the laboratory of Dr. Howard Green (Harvard Medical School, Boston, MA). 3T3-L1 cells were cultured on 100 mm plates (Corning, Oneonta, NY) in a Napco Model 6200 incubator (Napco Scientific Co., Tualatin, OR) at 37° C and 10% CO_2 , and fed with the appropriate medium every 2-3 days. In the culturing of 3T3-L1 adipocytes, "high glucose" medium refers to Dulbecco's

Modified Eagle's Medium (DMEM) containing 4.5 g/L glucose (450 mg/dl or 25 mM), and "low glucose" medium refers to DMEM containing 1.0 g/L glucose (100 mg/dl or 5.5 mM).

Differentiation

Undifferentiated preadipocytes were grown to confluence in high glucose DMEM + 10% calf serum. Two days post-confluence, the cells were cultured in differentiation medium (high glucose + 10% fetal calf serum, 1.6×10^{-7} M insulin, $0.25 \mu\text{M}$ dexamethasone, and 0.5 mM IBMX). After two days in differentiation medium, the cells were fed with high glucose DMEM + 10% fetal calf serum and 1.6×10^{-7} M insulin for an additional two days. The cells were then cultured in high glucose DMEM + 10% fetal calf serum for 6 days, at which time they were determined to be at least 90% confluent by visual assessment.

Pre-feeding Conditions

Control Cells - Low Glucose, No Insulin.

Differentiated control cells were cultured in low glucose DMEM + 0.5% serum substitute for 20-24 hours prior to the experiment.

Insulin Resistant Cells - High Glucose, High Insulin.

Differentiated cells to be used as a model of the insulin

resistant condition were cultured in high glucose DMEM + 0.5% serum substitute and 2×10^{-6} M insulin for 20-24 hours prior to the experiment.

Insulin debinding procedure. This procedure was used to release any bound insulin from the overnight high insulin incubation, and was related to our laboratory through personal communication (Jonathan Whittaker, SUNY Health Science Center, Stonybrook, NY, phone conversation in April, 1992). It is a variation on a method which was previously published (163). Immediately prior to glucose transport assays or acute insulin stimulation of cells for protein preparations, all cell groups were rinsed twice in PBS (pH 6.8), incubated in PBS (pH 6.8) + 1% BSA for 45 minutes, and then rinsed again in PBS (pH 6.8).

Glucose Transport Assay

3T3-L1 cells were grown in Costar 6-well plates (Cambridge, MA), differentiated, pre-fed, and incubated with insulin debinding buffer prior to glucose transport assays. The cells were then washed once with PBS (pH 7.4), followed by a 15-minute incubation in a 22° C environmental shaker in 1 ml assay media (1 packet of Sigma DMEM base, 10 ml 100mM sodium pyruvate, 3.1 ml 0.5% phenol red, 5.96 g HEPES, 0.42 g sodium bicarbonate, 10 ml 200mM glutamine, 1 L pyrogen-free water, 0.1% BSA, pH 7.4) per well containing increasing

amounts of insulin (0, 1×10^{-10} M, 1×10^{-9} M, 1×10^{-8} M, 1×10^{-7} M, 1×10^{-6} M; or 0, 1×10^{-11} M 1×10^{-10} M, 1×10^{-9} M, 1×10^{-8} M, 1×10^{-7} M) for each group of three wells. 100 μ l 14 C-deoxyglucose was then added for a final concentration of 0.5 μ Ci/ml, and the cells were incubated for an additional 15 minutes. The cells were then washed three times in ice-cold PBS (pH 7.4) containing 10 mM glucose, 0.9 ml 0.5 N NaOH was added to each well, and the plates were incubated at 37° for 30 minutes. These cell lysates were then removed to 18 ml liquid scintillation vials, and 105 μ l of glacial acetic acid plus 10 ml of Beckman Ready Value Scintillation Fluid (Beckman, Inc. Fullerton, CA) was added prior to reading the amount of 14 C-deoxyglucose uptake on a Beckman LS5801 liquid scintillation counter. This insulin dose response curve was performed with each 3T3-L1 experiment to be certain that the high insulin/high glucose pre-incubation made the cells insulin resistant, and also to ensure that the control cells were indeed responsive to insulin.

RNA Preparation

Extraction Methodology

RNase Inactivation of Supplies

Glassware. All Corex tubes (Dupont, Wilmington, DE) and glassware were baked at 225° C overnight to inactivate RNases.

Plasticware and water. To inactivate RNases, all pipet tips and aqueous solutions were treated with diethyl pyrocarbonate (DEPC) and autoclaved prior to use.

Isolation of RNA from Animal Tissue

Isolation of total RNA was performed essentially by the method of Chomczynski and Sacchi (120,164). Frozen tissue pieces of 0.1-0.4 g (liver) or 0.2-1.1 g (epididymal fat) were homogenized for 10 seconds with a Tekmar Tissuemizer (Cincinnati, OH) in 5 ml of ice-cold RNA homogenization buffer (4 M guanidinium thiocyanate, 22 mM sodium citrate, 0.5% Sarkosyl, and 0.1 M 2-mercaptoethanol) in a 15 ml polystyrene Falcon tube (Becton Dickinson Labware, Franklin Lakes, NJ). Following homogenization, samples were centrifuged at 8000 x g at 4° C for 15 minutes in a Sorvall RC2B high speed centrifuge (Dupont, Wilmington, DE). The infranatants from this spin, between the cell debris and the uppermost lipid layer, were then transferred to a Corex tube and mixed vigorously with 0.5 ml 2 M NaOAc (pH 4.0), 5 ml phenol, and 1 ml chloroform:isoamyl alcohol (49:1), followed by an incubation on ice for 15 minutes. Samples were then centrifuged at 8000 x g at 4° C for 30 minutes, the top

aqueous fraction was transferred to another Corex tube, and an equal volume (4 ml) of isopropanol was added. Samples were mixed thoroughly, then incubated for 2 hr at -70° C. Following this precipitation, the samples were spun at 8000 x g at 4° C for 45 minutes. The supernatant was poured off, the pellet was resuspended in 1 ml of RNA homogenization buffer, and 100 μ l of 3 M NaOAc (one tenth volume) plus 1 ml isopropanol (equal volume) were added to the samples. Following another 2 hr incubation at -70° C, the samples were spun for 45 minutes at 8000 x g and 4° C to precipitate the RNA. The supernatant was then poured off and the pellet was washed with 1 ml of 70% ethanol followed by a 3 minute spin at 8000 x g at 4° C. The ethanol supernatants were poured off, the pellets were allowed to dry, and then the RNA samples were resuspended in 0.2-1 ml DEPC-treated water. Samples were stored at -70° C.

Isolation of RNA from 3T3-L1 Cells

Two 100mm plates of differentiated, pretreated 3T3-L1 cells were combined for each data point. The prefeed media was aspirated, the cells were washed once with PBS, and then 5 ml of RNA homogenization buffer was split between the two plates. Cells were scraped from the two plates with a sterile rubber policeman and combined into a Corex tube. To ensure that the cells were lysed, the samples were pipetted up and down in a 10 ml pipette 5 times. From this point on,

the samples were treated exactly as the infranatants from the first spin in the animal tissue extractions as described above.

Concentration Determination

The UV absorbance of the RNA sample was read at 260 λ on a Beckman DU-64 Spectrophotometer (Beckman Instruments, Inc., Arlington Heights, IL) using the Nucleic Acid Soft-Pac Module software (Beckman Instruments, Inc.). The conversion factor used to determine the concentration of the RNA samples was 1 Optical Density unit = 40 $\mu\text{g/ml}$.

Northern Blot Analysis

Electrophoresis

Electrophoresis was performed essentially by the method of Fourney, *et al.* (165). 10 μg of total RNA at a concentration of 1 $\mu\text{g}/\mu\text{l}$ in RNA loading buffer (0.04 mg/ml ethidium bromide, 53% formamide, 17% formaldehyde, 7% glycerol, and 5.6% saturated bromophenol blue in 1x 3-[N-morpholino]propanesulfonic acid (MOPS)) was loaded per lane on 1.1% agarose gels. An RNA ladder was run on each gel to ensure that the band resulting from hybridization was the correct transcript size, and also to maintain the correct orientation of the samples. The gels were electrophoresed at 90V for 4 hours in 1X MOPS (0.02 M MOPS, 5 mM NaOAc, 1 mM

EDTA, pH 7.0), after which the gels were washed twice in 10X SSC (1.5 M NaCl, 0.15 M citrate, pH 7.0) at room temperature for 20 minutes.

Transfer of RNA to a Membrane by Northern Blotting

Following the two 10X SSC washes described above, the RNA was transferred overnight by capillary action to a Nytran nylon membrane (Schleicher and Schuell, Keene, NJ) by the method of Fourney and coworkers (165). The RNA was then UV crosslinked to the membrane using a Stratagene UV Stratalinker™ 1800 (Stratagene, La Jolla, CA). The nylon membranes were then placed on a UV transilluminator and photographed with a Polaroid MP-3 Land Camera, with an orange filter and Polaroid Type55 positive/negative black and white film. Exposure was for 25 seconds, with an aperture setting of f/8, followed by a 20 second development.

Loading Correction

Loading correction for RNA blots was based on the amount of 28S ribosomal RNA per lane, as measured by 2-dimensional densitometric analysis of the negative from the photograph of the northern blot. The 28S signal on the negative from the amount of RNA loaded per lane (10 μ g) was determined to be in the linear range of the film under our photographic conditions, as determined by Bonini and Hofmann (166).

Riboprobe Preparation and Hybridization

DNA Template Preparation

DNA templates for Riboprobe preparation were isolated from bacterial slushes containing the appropriate plasmid using the QIAGEN kit (Chatsworth, CA). Ten μ l of the appropriate bacterial slush stock (which has an OD of 1.0 when read at 600 λ with a spectrophotometer) was used to inoculate 200 ml of Luria-Bertani broth with 150 μ g/ml ampicillin. The culture was grown overnight to a concentration of cells which had an optical density of 1.0 when read at 600 λ . The 200 ml culture was then split into four 50 ml conical centrifuge tubes in equal aliquots and centrifuged at 1000 rpm at 4°C in a table-top Sorvall RT6000B. The supernatant was discarded, and each pellet was resuspended in 10 ml P1 buffer (100 μ g/ml RNase A, 50 mM Tris/HCl, and 10 mM EDTA pH 8.0). Ten ml of P2 buffer (200 mM NaOH, 1% SDS) was added to the samples, and after a gentle shaking, the samples were incubated for 5 minutes at room temperature. Ten ml of P3 was added, the samples were gently mixed, incubated on ice for 20 minutes, and then spun at 10,000 x g for 30 min. The supernatant was then passed through a cell strainer (Beckton Dickinson Labware, Franklin Lakes, NJ) into the Qiagen Q500 column, which was pre-equilibrated with 10 ml of QBT buffer (750 mM NaCl, 50 mM MOPS, 15% ethanol, pH 7.0, and 0.15% Triton X-100). The

column was then washed with 30 ml of buffer QC (1.0 M NaCl, 50 mM MOPS, 15% ethanol, pH 7.0), followed by elution with 15 ml buffer QF (1.25 M NaCl, 50 mM MOPS, 15% ethanol, pH 8.2). The DNA samples were then precipitated with 0.7 volume of isopropanol, spun at 16,000 x g for 30 minutes at room temperature, washed with 70% ethanol, and resuspended in 50 μ l TE (10 mM Tris-Cl, pH 7.4, 1 mM EDTA, pH 8.0). The concentration of the purified plasmid was determined by reading the absorbance of the sample at 260 λ . The conversion factor used to determine the concentration of the DNA was 1 OD unit equals a concentration of 50 μ g/ml. DNA templates were then linearized using 0.5 μ g/ μ l DNA, 20 units restriction enzyme, 4 μ l 10X REACT Buffer, and 12 μ l DEPC-H₂O).

Probe Preparation

³²P-labeled Riboprobes were prepared according to the recommendations of the supplier (Promega, Madison, WI). Linearized DNA was incubated with the transcription reagents (1.2 mM ATP, 1.2 mM GTP, 1.2 mM UTP, 10 mM DTT, 25 units/ μ l RNAsin, 1X transcription buffer, 5 μ M CTP, 5-10 units T7 RNA polymerase, and 50 μ Ci of α -³²P-CTP) for 1 hour at 37° C, after which RNase-free DNase (1U/ μ l) was added, and the probes were incubated for an additional 15 minutes to remove any remaining template. Riboprobes were then subjected to a phenol-chloroform extraction and precipitated with 1/10

volume NaOAc and 2.5 volumes of 100% ethanol by incubation for 1-2 hours -70° C. The supernatant was poured off, the pellet was resuspended in 50 μ l TE, and then the probe was passed over a 5 Prime-3 Prime column (Westchester, PA). The effluent from a 4 minute spin at 1670 x g through this column was used as the purified 32 P-labeled Riboprobe for hybridization.

Hybridization

Hybridization of Riboprobes to the Nytran-bound RNA was performed as previously described (18). Nytran membranes were pre-wet in 2X SSC prior to prehybridization for 2 hours at 65° C with 10 ml hybridization buffer (4X SSPE, 50% formamide, 10% dextran sulfate, 5X Denhart's solution, 0.1% SDS, and 0.1 mg/ml sonicated denatured salmon sperm DNA) in a Hybaid Mini Hybridization Oven (Hybaid, Middlesex, UK). 100X Denhart's (2% polyvinylpyrrolidone, 2% BSA, 2% Ficoll) and 20X SSPE (3 M NaCl, 0.17 M $\text{NaH}_2\text{PO}_4 \cdot \text{H}_2\text{O}$, 0.02 M EDTA) were used as stock solutions to make the hybridization buffer.

Following prehybridization, 32 P-labeled Riboprobes were denatured by boiling for 5 minutes with an additional 1 mg of denatured sonicated salmon sperm DNA, and added to the hybridization buffer for an overnight hybridization (16-18 hours) in the Hybaid oven. After the hybridization, northern blots were washed twice at room temperature for 5 minutes (2X SSC, 0.1% SDS), twice at 70° C (2X SSC, 0.1%

SDS) for 30 minutes, and twice at 70° C in 0.1X SSC, 0.1% SDS for 30 minutes. Blots were then either filmed with Amersham Hyperfilm MP (Arlington Heights, IL) at -70° C with an intensifying screen for 16-72 hours, or washed further with 100 ml of 2X SSC containing 3 µg/ml RNase A and 0.005 units RNase T1/ml to remove nonspecific binding.

Protein Preparation

Extraction Methodology

Animal Tissue

Total protein was prepared from animal tissue by an adaptation of the method previously described by Rice, *et al.* (84). Liver and epididymal fat tissue pieces of 0.1-1.2 g were homogenized with a Tekmar Tissuemizer (Cincinnati, OH) in 3 ml of ice cold homogenization buffer (0.02 M Tris base, 0.15 M NaCl, 1% Triton X-100, 0.03 M Na₄P₂O₇•10 H₂O, 1 mM Na₃VO₄, 10 µM E-64, 1 mM PMSF, 3 mM EDTA, 50 µM leupeptin, and 10 µg/ml aprotinin). Cell lysates were then centrifuged at 30,000 x g for 30 minutes at 4° C, and the infranatant was passed through a Millex AP20 Syringe filter (Millipore Corp., Bedford, MA) to remove any remaining lipids. Concentration determinations were made, sample aliquots were taken for immunoprecipitation or dilution in Laemmli buffer, and the samples were stored at -70° C.

3T3-L1 Cells

Four 100mm plates of confluent, differentiated, prefed 3T3-L1 adipocytes were used per data point. One ml of ice-cold homogenization buffer was added to each plate, the cells were scraped with a rubber policeman, and pipetted up and down repeatedly to ensure cell lysis. The lysates from the four plates were then combined into one tube, centrifuged at 30,000 x g for 30 minutes at 4° C, and passed through a Millex AP20 syringe filter. Samples were stored at -70° C.

Isolated Mouse Adipocytes

Equal amounts of isolated mouse adipocytes were homogenized in 500 μ l of ice-cold homogenization buffer using a teflon Dounce homogenizer connected to a Glas-Col variable speed laboratory motor (Terre-Haute, IN) at speed 2 for 10 seconds, followed by centrifugation at 16,000 x g for 30 minutes. The infranatant was passed through a Millex AP4 syringe filter, and the samples were then stored at -70° C.

Concentration Determination

The concentration of each protein sample was determined the day of the experiment, and sample aliquots were taken for immunoprecipitation and SDS-polyacrylamide gel electrophoresis. Concentrations were determined by the Lowry method (167) using the BioRad D_c Assay (Bio-Rad,

Hercules, CA). The absorbance of the samples at 750λ was compared against a standard curve of varying concentrations of BSA in homogenization buffer.

Immunoprecipitation

Sample and Antibody Concentrations

For immunoprecipitation of IRS-1 from isolated primary adipocytes, 1 mg total protein in 500 μ l was incubated with 8 μ g anti-IRS-1 antibody (Upstate Biotechnologies, Inc.). For immunoprecipitation of IRS-1 from animal tissue, 10 μ l of the anti-baculovirus IRS-1 antibody was added to 1 mg total protein in 400 μ l, as recommended by the supplier (Morris White, Boston, MA).

Methodology

Cell lysates were incubated with anti-IRS-1 antibodies overnight (16-18 hours) at 4° C with gentle rocking. Following the overnight incubation, 100 μ l of protein A-Sepharose (Pharmacia, Milwaukee, WI) was added and the samples were rocked for an additional 2 hours at 4° C. The samples were then centrifuged at 16,000 x g for 2 minutes, and the pellets were washed twice with 1 ml wash buffer (140 mM NaCl, 2.7 mM KCl, 10 mM Na_2HPO_4 , 1.8 mM KH_2PO_4 , 100 μ M Na_3VO_4 , and 1% NP40), with a 2 minute centrifugation at 16,000 x g between washes. After the second wash, the

pellet was resuspended in 100 μ l of 2X Laemmli Sample Buffer(1X = 62.5 mM Tris, 10% glycerol, 2% SDS, 10% 2-mercaptoethanol, and .001% bromophenol blue) and boiled for 6 minutes prior to electrophoresis.

Western Blot Analysis

SDS-PAGE

Total cell lysates in 1X Laemmli sample buffer or immunoprecipitates were electrophoresed on 7.5% or 12% polyacrylamide gels essentially according to the method of Laemmli (168). Equal amounts of protein (between 10 and 30 μ g for total lysates) or equal volumes of immunoprecipitate were electrophoresed on duplicate gels at 150 V for 1.5 hours using the Bio-Rad Mini-Protean II Dual Slab Cell (Bio-Rad, Richmond, CA). On each gel a molecular weight marker (Bio-Rad, Richmond, CA) was included for orientation and size determination purposes. Where appropriate, a positive control for IRS-1 or PI3K p85 α was used to confirm that the correct protein was visualized during immunostaining. Proteins were then electrophoretically transferred to Immobilon P membranes (Millipore Corp., Bedford, MA) using the Bio-Rad Mini-Transblot electrophoretic transfer cell (Bio-Rad, Richmond, CA) for 3-4 hours at 100 V. One set of the duplicate blots was used for Coomassie staining, followed by total protein quantitation of the stained blot.

This quantitation was used for normalizing for differences in loading between lanes. The other set of blots was immunostained as described below with the appropriate antibodies.

Immunostaining

Western blots were blocked 2 hours or overnight in Tris-Buffered Saline (TBS = 0.9% NaCl, 20 mM Tris, pH 7.4) with 5% BSA, then washed four times for 10 minutes with TBS-tween (TBST) wash buffer (TBS, 0.05% Tween-20, 0.1% BSA) and incubated with primary antibody for 2 hours in antibody dilution buffer (TBS, 0.05% Tween-20, 1% BSA). Blots with mouse tissue anti-IRS-1 immunoprecipitates were probed with the monoclonal anti-IRS-1 antibody and required an overnight incubation with the primary antibody. Following the primary antibody incubation, the blots were washed four times for 10 minutes in TBST, then incubated for 30 minutes in antibody dilution buffer with the appropriate secondary antibody. After the incubation with the secondary antibody, the blots were washed four times for 15 minutes in TBST before exposure to the ECL reagents for 1 minute. The excess ECL liquid was allowed to drain off, and the blots were placed between two sheets of acetate and exposed to Hyperfilm MP or Hyperfilm ECL for a period of 10 seconds to 45 minutes.

Primary antibody dilutions. The anti-IR β -subunit antibody was used at a 1:2000 dilution. The anti-IRS-1 monoclonal antibody and anti-phosphotyrosine antibody were used at a 1:1000 dilution, and the anti-IRS-1 C-terminal polyclonal antibody was used at a 1:1500 dilution. Both anti-PI3K p85 α antibodies were used at a dilution of 1:8000. Anti-GRB2, anti-Nck, and anti-Syp antibodies were used at a 1:4000 dilution.

Secondary antibody dilutions. The anti-mouse HRP-linked secondary antibody was used at a dilution of 1:7500. The anti-rabbit HRP-linked secondary antibody was used at a 1:6000 dilution.

Image Analysis

All autoradiographs from northern blots and ECL western blots were quantitated by video densitometry using the Ambis Image Acquisition Analysis system (San Diego, CA). This system was also used for determination of molecular weights of proteins and sizing of mRNA transcripts by comparison of sample lanes with molecular weight lanes or RNA ladder lanes.

Statistics

All data were analyzed for statistical significance using the Graphpad InStat software (Graphpad Software, San Diego, CA).

Two-Group Experiments

Parametric Test

For most experiments with two groups, such as the rat experiments (control vs. streptozotocin-treated) or the 3T3-L1 cell culture experiments (low glucose/no insulin vs. high glucose/high insulin), the data was analyzed with an unpaired Student's T-Test using a two-sided p-value. A p-value less than 0.05 was considered significant.

Nonparametric Test

For two-group experiments in which the standard deviations were significantly different between groups and were also not normalized by log, square-root, or reciprocal transformation of the data, the Mann-Whitney nonparametric test with a two-sided p-value was used to analyze the data. A p-value less than 0.05 was considered significant.

Experiments with More Than Two Groups

Ordinary ANOVA

In most experiments with more than two groups, such as the mouse, primary adipocyte, or 3T3-L1 acute insulin studies, the data was analyzed using ANOVA with the Tukey multiple comparisons post-test. A p-value of less than 0.05 was considered significant.

Kruskal-Wallace Nonparametric Test

For experiments with more than two groups in which the standard deviations were significantly different between groups and were also not normalized by log, square-root, or reciprocal transformation of the data, the Kruskal-Wallace nonparametric test with the Dunn's multiple comparisons test was used to analyze the data. A p-value less than 0.05 was considered significant.

CHAPTER IV

RESULTS

Glycemic State and Insulin Levels of KKA^y Mice

The blood glucose and serum insulin levels were determined from blood samples taken from the animals at the time of tissue extraction at The Upjohn Company. The blood glucose level for the control C57 mice was 170 ± 6 mg/dl or 9.4 ± 0.3 mM (\pm SEM), while the average blood glucose level in KKA^y mice was 494 ± 25 mg/dl or 27.4 ± 1.3 mM. Pioglitazone treatment of KKA^y mice lowered the blood glucose level to 257.4 ± 18.3 mg/dl (14.3 ± 1.0 mM).

Serum insulin levels were similarly elevated in the KKA^y mice as compared to control C57 mice, and these levels were also partially corrected by pioglitazone treatment. C57 mice had an average serum insulin concentration of 25.8 ± 2.7 μ U/ml or $1.9 \times 10^{-10} \pm 0.2 \times 10^{-10}$ M (\pm SEM), while the average serum insulin level of KKA^y mice was 476.9 ± 54.4 μ U/ml or $3.5 \times 10^{-9} \pm 0.4 \times 10^{-9}$ M. Pioglitazone treatment of KKA^y mice corrected the average serum insulin levels to 299.5 ± 33.2 μ U/ml ($2.2 \times 10^{-9} \pm 0.2 \times 10^{-9}$ M).

Expression of Insulin Signaling Components in Animal NIDDM

The expression of the insulin receptor (IR), IRS-1, PI3K p85 α , GRB2, Nck, and Syp was analyzed in three animal groups: C57 control mice (C), KKA^y diabetic mice (D), and KKA^y mice treated with pioglitazone (D+P). The observed protein and transcript sizes are shown in table 1. All data in figs. 2 and 3 are expressed as percent of control C57 expression for each group, \pm standard error of the mean (SEM).

Protein Levels of Insulin Signal Components

In order to determine if the protein levels of IR, IRS-1, p85 α , GRB2, Nck and Syp were altered in insulin resistant animals as compared to control nondiabetic animals, and to determine if pioglitazone treatment corrected these alterations, protein extracts of epididymal fat and liver tissue from nondiabetic C57 mice, obese KKA^y insulin-resistant mice, and KKA^y mice treated with pioglitazone were analyzed by western blotting. The abundance of the proteins studied was determined to be roughly the same between liver and adipose in the control animals.

Table 1.-- Observed Protein and mRNA Transcript Sizes of
Signaling Components

Gene	Protein size (kDa)	mRNA size (kb)
IR	96.5	9.5, 7.5
IRS-1	162.9	9.5
P85 α	84.9	7.5
GRB2	25.7	-
Nck	44.2	-
Syp	69.6	-

The Insulin Receptor

In both epididymal fat and liver, the IR levels in KKA^y mice were reduced to 17 \pm 3% and 33 \pm 4% of C57 control levels, respectively, and these were increased significantly with pioglitazone treatment to 32 \pm 3% and 57 \pm 5% of control levels (fig. 2, upper panels).

IRS-1

IRS-1 protein levels were not significantly different between C57 and KKA^y mice, and pioglitazone treatment did

not significantly alter IRS-1 protein abundance in either tissue (fig. 2, middle panels).

PI3K p85 α

The expression of PI3K p85 α was measured using a monoclonal antibody directed against the SH2 domains of p85 α . As seen in fig. 2, two major bands of approximately the same size are recognized by this antibody in fat tissue. This may be due to cross-reactivity with another protein, p87 β , which has high homology to p85 α (128). While both proteins may associate with the p110 subunit (128), we found that only the lower band (p85 α) associated with IRS-1 on insulin stimulation of isolated adipocytes (fig. 11). In addition, the lower band lined up with the baculovirus-expressed p85 α positive control, while the upper band did not. Also, the recent availability of an antibody specific for the SH3 domains of only p85 α detected only the lower of the two bands in fat tissue (data not shown). For these reasons, the lower band observed in fat tissue was quantitated as p85 α .

PI3K p85 α protein levels were significantly lower in KKA^y fat (47 \pm 3 % of control) and fully corrected by pioglitazone administration to 103 \pm 15% of control levels (fig 2, panel E). However, p85 α levels in liver were not significantly different between C57 and KKA^y mice, and were not altered by pioglitazone treatment (fig. 2, panel F).

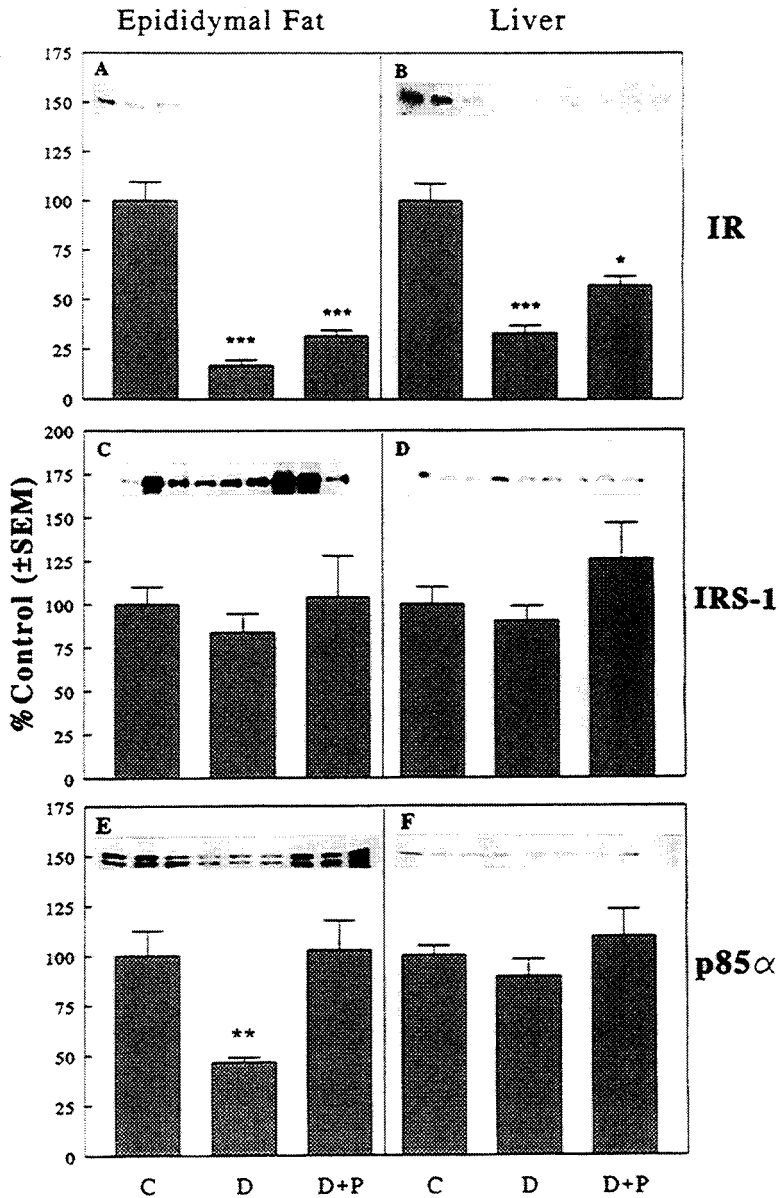


Fig. 2. The protein levels of the insulin receptor (IR), IRS-1, and PI3K p85α are depicted in C57 (C), KKA^y (D), and KKA^y + pioglitazone (D+P) as % Control C57, with fat data on the left and liver data on the right. Inside each graph is a representative western blot for the respective protein, shown with an n=3 for C, D, and D+P. The upper panels represent protein levels of IR, the center panels represent the protein levels of IRS-1, and the lower panels show the protein levels for PI3K p85α. For all experiments, n=12 and all values represent the mean ± SEM (* indicates p<0.05, ** indicates p<0.01, and *** indicates p<0.001).

Pioglitazone treatment did not significantly alter the expression of the insulin receptor, IRS-1, or p85 α proteins in the control animals (data not shown).

GRB2, Nck, and Syp

GRB2, Nck, and Syp levels were regulated in an opposite manner from IR, IRS-1, and p85 α levels.

GRB2. GRB2 protein abundance was significantly elevated in KKA y epididymal fat (321 \pm 25% control - fig. 3, panel A). In liver tissue this elevation was not as great (118 \pm 6% control), although it was significant (fig 3, panel B). Pioglitazone administration did not alter GRB2 levels to a large extent, but it did lower the slightly elevated KKA y liver GRB2 levels to control levels.

Nck. Like GRB2, Nck levels were much higher in KKA y fat as compared to C57 (186 \pm 12% control), and there was a smaller but significant elevation of Nck in KKA y liver compared to C57 (124 \pm 7% control - fig. 3, middle panels). Again, there was little effect of pioglitazone treatment on Nck protein levels in the treated KKA y tissues.

Syp. Syp protein levels were 43 \pm 11% higher in KKA y fat than in C57, and 25 \pm 4% higher in KKA y liver compared to C57. Both of these increases were statistically significant

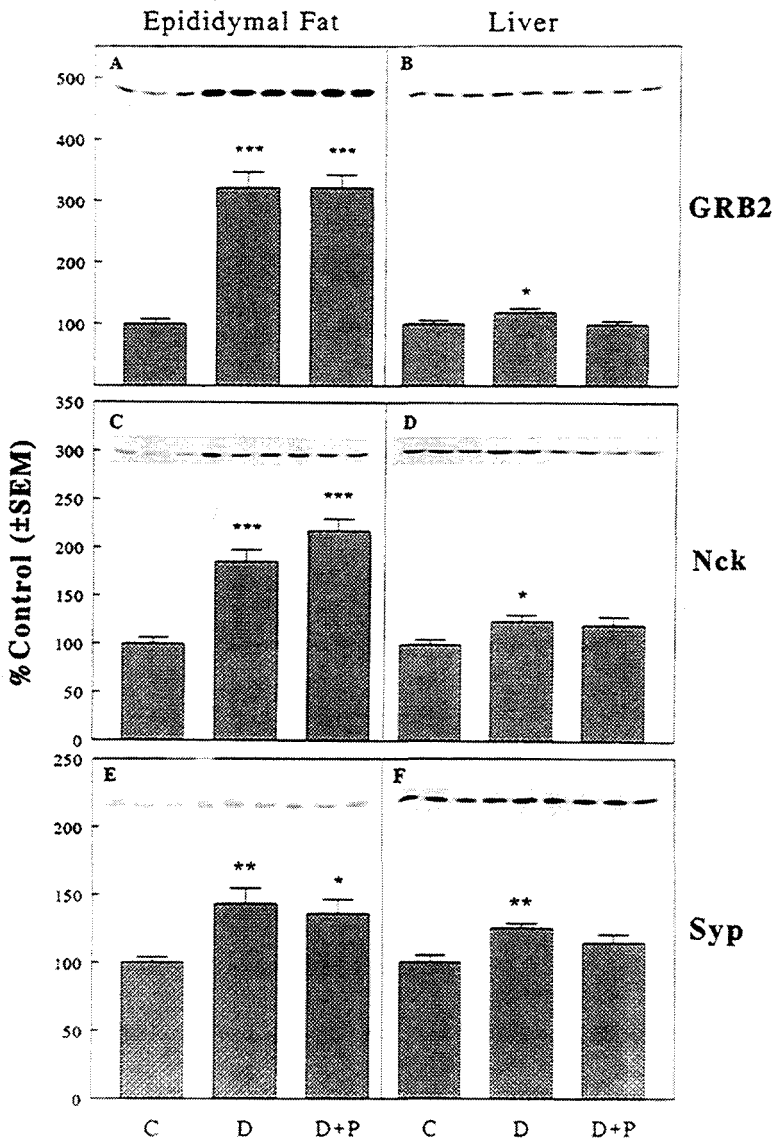


Fig. 3. The protein levels of the GRB2, Nck, and Syp are depicted in C57 (C), KKA^y (D), and KKA^y + pioglitazone (D+P) as % Control C57, with fat data on the left and liver data on the right. Inside each graph is a representative western blot for the respective protein, shown with an n=3 for C, D, and D+P. The upper panels represent the protein levels of GRB2, the center panels represent the protein levels of Nck, and the lower panels show the protein levels for Syp. For all experiments, n=12 and all values represent the mean ± SEM (* indicates p<0.05, ** indicates p<0.01, and *** indicates p<0.001).

($p < 0.05$). Pioglitazone treatment did not significantly change Syp levels in fat, but it did lower liver Syp levels in liver tissue toward control levels (fig. 3, lower panels). Pioglitazone treatment did not significantly alter the expression of GRB2, Nck, or Syp in control animals (data not shown).

mRNA Levels of Insulin Signaling Components

PI3K has been implicated in insulin stimulated glucose transport (99,102), and KKA^y mice display a defect in insulin's ability to promote glucose uptake in fat and muscle (18). Therefore, potential mechanisms for lowered levels of IR and p85 α proteins were determined by analyzing the mRNA abundance of these transcripts in tissues of nondiabetic C57 mice, obese KKA^y insulin-resistant mice, and KKA^y mice treated with pioglitazone. IRS-1 mRNA abundance was also determined in the same groups. A northern blot for the insulin receptor showed transcripts of two lengths: 9.5 kb and 7.5 kb. The difference in size between these two transcripts results from differential poly-A site selection and there is no known functional difference between the 9.5 and 7.5 kb transcripts (59). The IRS-1 mRNA transcript is 9.5 kb long, and the primary p85 α mRNA size is 7.5 kb. The abundance of these transcripts was determined as described in Materials and Methods above. Data are summarized in figures 4, 5, and 6.

Insulin Receptor

In epididymal fat and liver, receptor mRNA levels were slightly less in the KKA^y mice as compared to C57, although the only significant difference was in the liver with the 7.5 kb transcript (figure 4). Pioglitazone administration did not have a significant effect on receptor mRNA levels. There was no detectible difference in the 9.5/7.5 kb ratio between any of the groups.

IRS-1

IRS-1 mRNA levels were significantly lower in KKA^y fat and liver (53.3 ± 4.3 and $50.7 \pm 6.2\%$ control, respectively) than in the C57 controls, with no correction by pioglitazone treatment (figure 5). However, this difference in IRS-1 mRNA abundance was not associated with a significant change in the IRS-1 protein levels (fig. 2, middle panels).

PI3K p85 α

In epididymal fat, p85 α mRNA abundance was not significantly different between the C57 and KKA^y mice, although the mean p85 α mRNA level was 75% of control. Pioglitazone treatment did not significantly alter the p85 α mRNA levels in the treated KKA^y group as compared to the untreated KKA^y group (fig. 6). The mRNA levels of p85 α were not determined in liver because there was no difference in the level of p85 α protein in this tissue.

Insulin Receptor RNA

Mouse Tissue

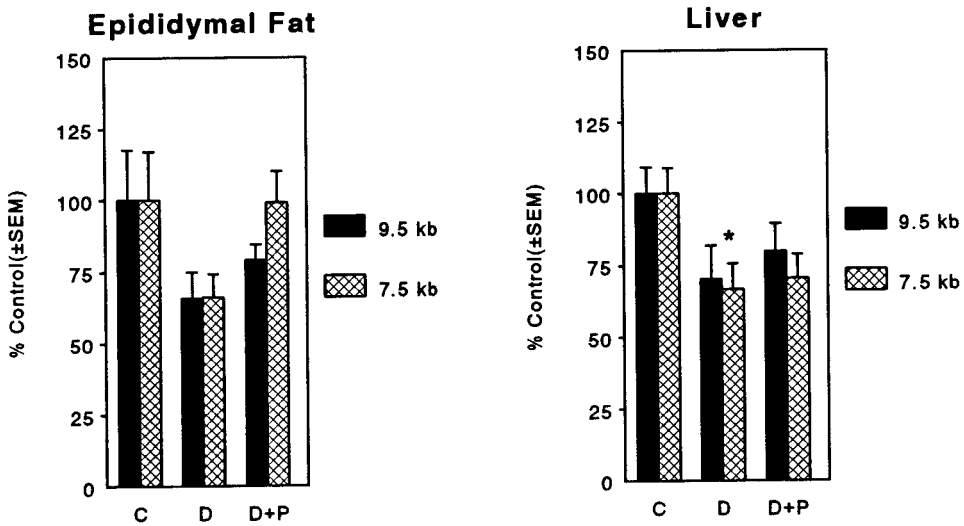


Fig. 4. The mRNA levels for the insulin receptor in C57 (C), KKA^y (D), and KKA^y + pioglitazone (D+P) are depicted as mean % control C57, \pm SEM. Left, IR RNA abundance in fat; right, IR RNA in liver. Solid bars represent the abundance of the 9.5 kb receptor transcripts and hatched bars represent the 7.5 kb transcript abundance. $n=12$ for both fat and liver data. * represents a statistical difference with a p value less than 0.05.

IRS-1 RNA Mouse Tissue

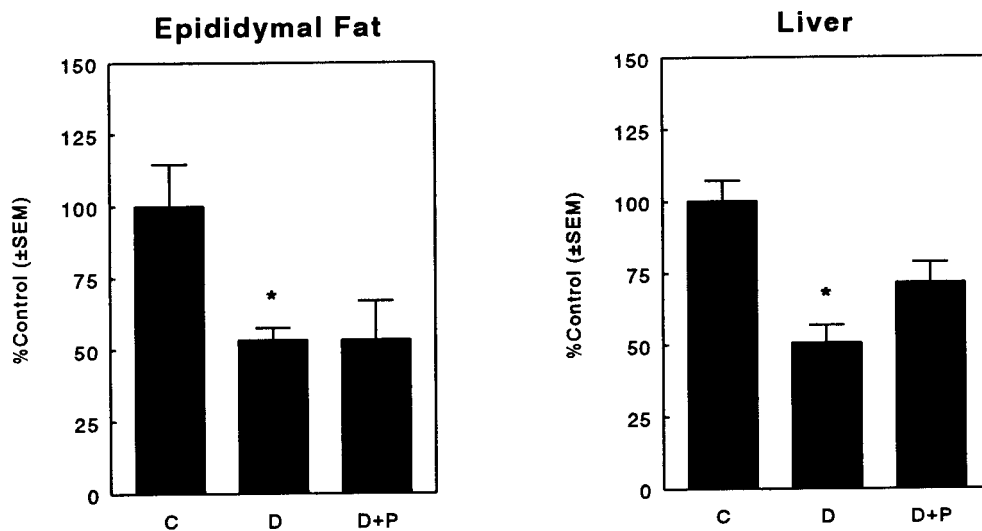


Fig. 5. The mRNA levels for IRS-1 in C57 (C), KKA^y (D), and KKA^y + pioglitazone (D+P) are depicted as mean % control C57, ± SEM. Left, IRS-1 RNA abundance in fat; right, IRS-1 RNA in liver. n=12 for both tissues, and * represents a statistical difference with a p value less than 0.05 relative to control.

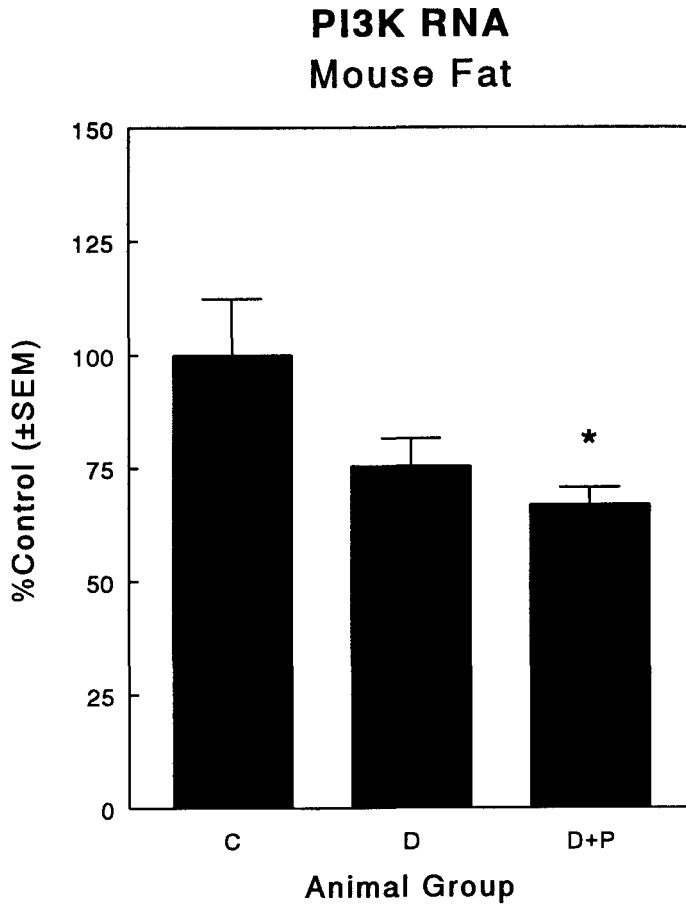


Fig. 6. The levels of mRNA transcripts PI3K p85 α in epididymal fat from C57 (C), KKA^y (D), and KKA^y + pioglitazone (D+P) are depicted as mean % control C57, \pm SEM. n=12 for both tissues, and * represents a statistical difference with a p value less than 0.05 relative to control.

GRB2, Nck, and Syp

The cDNA for GRB2, Nck, and Syp were not available at the time of the study; thus, the RNA levels for these components in this model are unknown. Since the differences in GRB2 and Nck protein levels between C57 and KKA^y mice were very large, in the future it would be interesting to determine if such differences also exist at the RNA level.

Function of the Insulin Receptor and IRS-1 in Animal NIDDM

Insulin-Stimulated Tyrosine Phosphorylation of the Insulin Receptor And IRS-1

In order to study the role of insulin receptor function in insulin resistance, primary adipocytes were isolated from epididymal fat of C57 mice, KKA^y mice, and KKA^y mice pretreated with pioglitazone. These adipocytes were then stimulated acutely with insulin, and the tyrosine phosphorylation of the insulin receptor β subunit and IRS-1 was assayed by western blotting with an anti-phosphotyrosine antibody. A representative blot is shown in fig. 7, and the graphed results of the cumulative data are illustrated in figures 8, 9, and 10. Although the representative blot shows an n of 2, The n for these experiments was 10 cell aliquots per group. The data are represented as the percent phosphorylation of the unstimulated C57 control group, \pm SEM.

Insulin Receptor Phosphorylation

In control C57 mice, acute insulin stimulation resulted in an 11.4-fold increase in insulin receptor β subunit tyrosine autophosphorylation (fig. 8). In adipocytes from KKA^y mice, insulin stimulation failed to increase the tyrosine phosphorylation of the insulin receptor relative to the KKA^y basal tyrosine phosphorylation, and the receptor was not made any more sensitive to insulin in stimulating tyrosine phosphorylation of its β subunit by prior pioglitazone treatment of the mice (fig. 8). Also, basal phosphorylation of the receptor in KKA^y mouse adipocytes was significantly higher (about 6-fold) than basal tyrosine phosphorylation of the receptor in C57 mice. This is likely due to the higher level of circulating insulin in the KKA^y mice relative to the control mice. Pioglitazone treatment did not significantly lower the basal phosphorylation of KKA^y insulin receptors. Therefore, there appears to be both a decreased number of receptors (fig. 2) and a decrease in the responsiveness of the receptors to insulin in KKA^y mice.

Because pioglitazone treatment partially corrects receptor number back toward control levels, the mean phosphorylation per unit receptor appears to be lowered to approximately a third of the phosphorylation per receptor in untreated KKA^y mice (fig.9), although this change was not quite significant ($p=0.0594$). However, the analysis of the data as phosphorylation per receptor did emphasize the

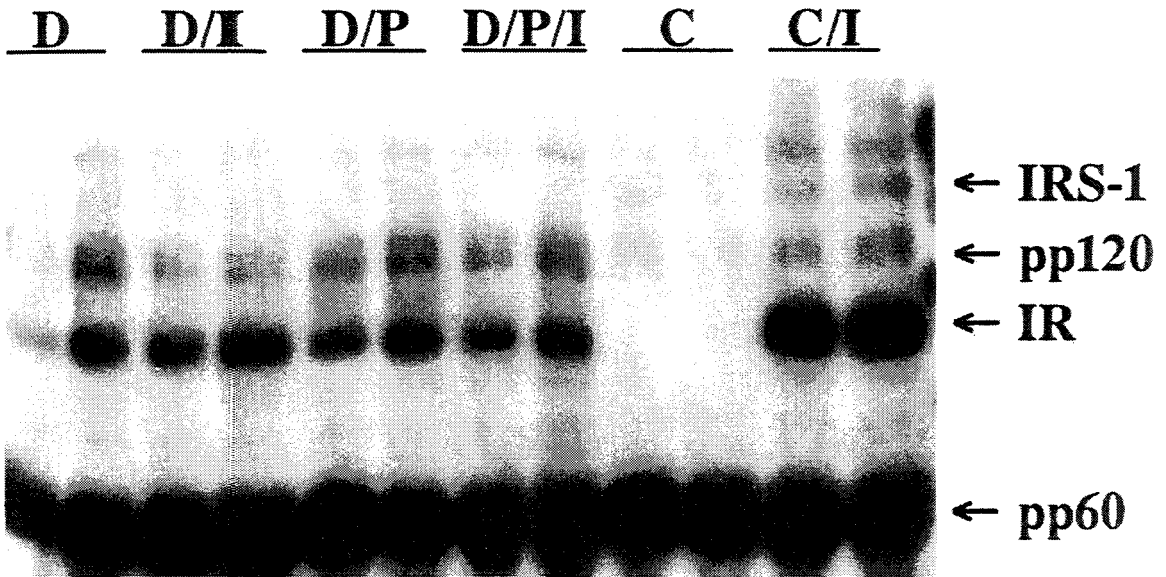


Fig. 7. Phosphotyrosine content of the insulin receptor (IR) and IRS-1 was detected by western blotting with anti-phosphotyrosine antibodies of lysates from isolated adipocytes unstimulated or stimulated acutely with 100 nM insulin for 2 minutes. This representative blot shows an $n=2$ for each group: D= KKA^y (unstimulated), D/I= KKA^y (stimulated), D/P= KKA^y pretreated with pioglitazone (unstimulated), D/P/I= KKA^y pretreated with pioglitazone (stimulated), C=C57 (unstimulated), C/I=C57 (stimulated). IR and IRS-1 bands are indicated by arrows to the right of the blot.

IR Phosphorylation Isolated Adipocytes

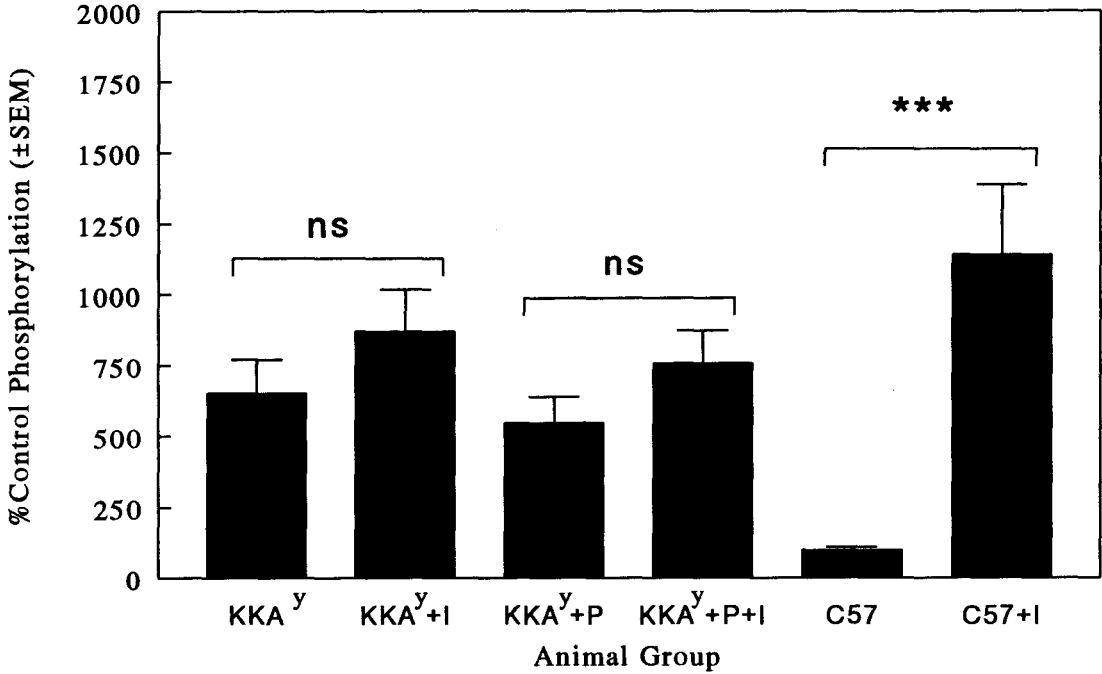


Fig. 8. Cumulative graphed results of acute insulin-stimulated phosphorylation of the insulin receptor β subunit in isolated adipocytes are depicted as mean % unstimulated control (C57) \pm SEM, $n=10$. Data were accumulated from anti-phosphotyrosine western blots such as is shown in fig. 7. *** represents a statistical difference ($p<0.001$) between the bracketed groups. ns=not significant ($p>0.05$)

IR Phosphorylation/Receptor Isolated Adipocytes

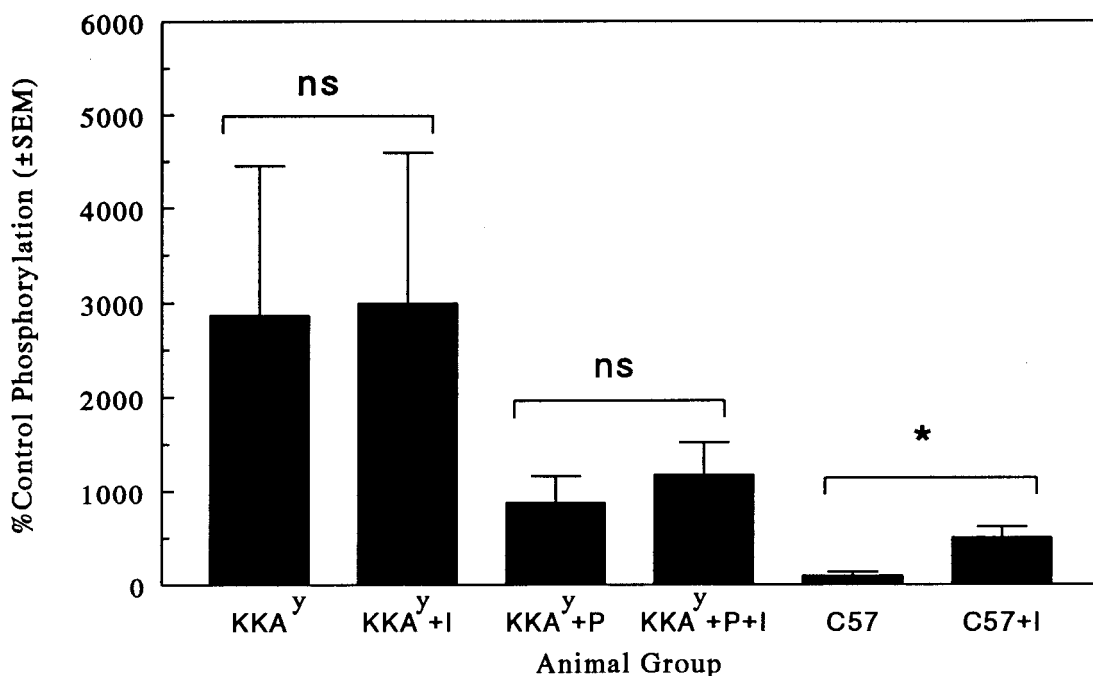


Fig. 9. Cumulative graphed results of receptor tyrosine phosphorylation per unit receptor in isolated adipocytes are depicted as mean % unstimulated control (C57) \pm SEM, $n=10$. Data were accumulated from anti-phosphotyrosine western blots such as is shown in fig. 7 and anti-IR β western blots of the same samples. *** represents a statistical difference ($p<0.001$) between the bracketed groups. ns=not significant ($p>0.05$).

IRS-1 Phosphorylation Isolated Adipocytes

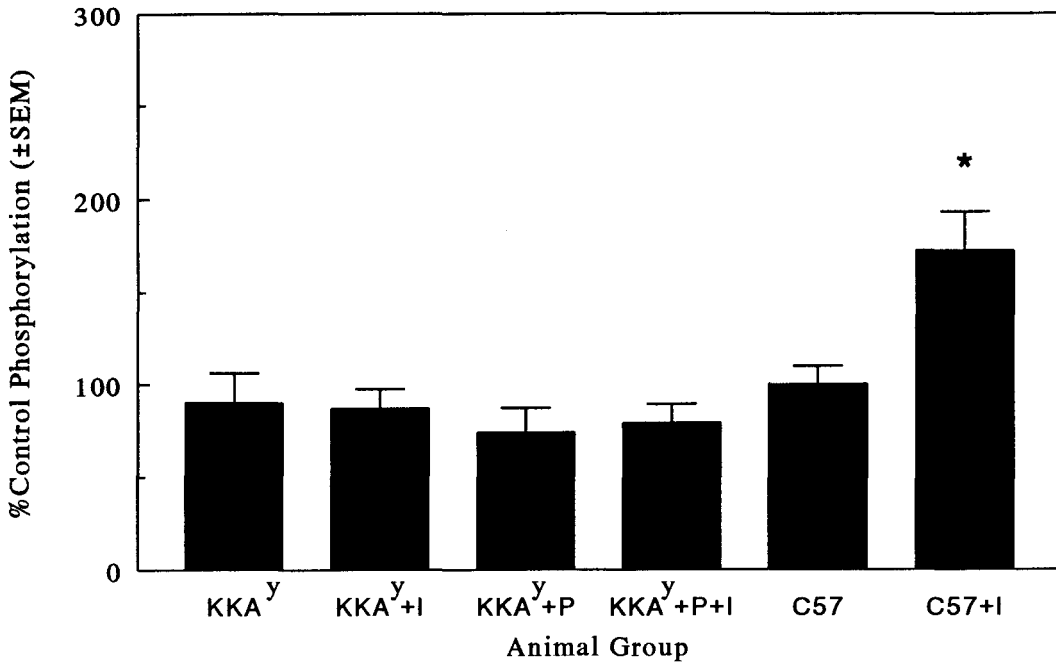


Fig. 10. Cumulative graphed results of acute insulin-stimulated phosphorylation of IRS-1 in isolated adipocytes are depicted as mean % unstimulated control (C57) \pm SEM, $n=10$. Data were accumulated from anti-phosphotyrosine western blots such as is shown in fig. 7. * represents a statistical difference ($p<0.05$) as compared to the unstimulated control group.

increased basal phosphorylation of the receptor in the KKA^y mice as compared to control.

IRS-1 Phosphorylation

The insulin-stimulated tyrosine phosphorylation of IRS-1 in control mice was not as pronounced as that of the insulin receptor (fig. 7 and fig. 10). Insulin stimulation of the control isolated adipocytes caused an increase in tyrosine phosphorylation of IRS-1 by $72.4 \pm 21.1\%$ over nonstimulated cells (fig. 10), while in KKA^y adipocytes insulin failed to stimulate tyrosine phosphorylation over the nonstimulated KKA^y adipocytes. As with the insulin receptor phosphorylation, pioglitazone treatment did not make the KKA^y cells any more sensitive to insulin in phosphorylating IRS-1. In contrast to receptor phosphorylation, the basal tyrosine phosphorylation of IRS-1 in KKA^y adipocytes or pioglitazone-treated KKA^y adipocytes was not elevated relative to the IRS-1 tyrosine phosphorylation in unstimulated C57 adipocytes (fig. 10). The IRS-1 phosphorylation per unit IRS-1 was not determined since there was not a significant difference in IRS-1 protein levels between the three groups.

Insulin-Stimulated Association of IRS-1

with PI3K p85 α

Following insulin stimulation of the receptor tyrosine kinase and tyrosine phosphorylation of IRS-1, IRS-1 is known to associate with PI3K p85 α via the phosphorylated YMXM motifs on IRS-1 and the SH2 domains of p85 α . Therefore, the association of IRS-1 with p85 α on insulin stimulation was compared between C57 and KKA y mice. Since pioglitazone partially corrects blood glucose levels, and PI3K has been linked to glucose transport, the KKA y mice treated with pioglitazone were included in this comparison. In addition, as is shown in figure 2, pioglitazone corrected PI3K p85 α protein levels in epididymal fat to C57 levels and thus may result in increasing the association of PI3K p85 α with IRS-1.

However, given the above results from figures 7 and 10, one would expect that in the absence of insulin-stimulated IRS-1 phosphorylation in KKA y mice or pioglitazone-treated KKA y mice, there would be no insulin stimulation of p85 α associated with IRS-1 in either group. To determine if the pioglitazone correction of PI3K p85 α levels resulted in a correction of insulin signaling at this level, lysates from the isolated adipocytes from C57, KKA y , and pioglitazone-treated KKA y mice with or without acute insulin stimulation were subjected to an immunoprecipitation with a polyclonal anti-IRS-1 antibody. These immunoprecipitates were then

size-fractionated on SDS-PAGE and immunoblotted for PI3K p85 α to observe the amount of p85 α which associates with IRS-1 on insulin stimulation in each group. A representative blot is shown in fig. 11, and the cumulative data from an n of 10 are summarized in fig. 12. As is shown in fig. 12, acute insulin stimulation of C57 adipocytes caused p85 α to associate with IRS-1 to a level of $217.2 \pm 25.8\%$ of the amount of p85 α associated with IRS-1 in unstimulated control cells. Like the tyrosine phosphorylation of IRS-1, the basal association of p85 α with IRS-1 in KKA^y and pioglitazone-treated KKA^y groups was about the same as the basal level in unstimulated C57 adipocytes, and this association was not elevated by insulin stimulation.

The Effects of Insulin and Glucose on Signal Transduction Components

Expression of Insulin Signaling Components in the Presence of High Glucose or High Glucose plus High Insulin

To determine if the alterations in expression and function of insulin signaling components observed above in the KKA^y mice was due to the presence of the high glucose and high insulin levels in these animals, two other models were used. First, differentiated 3T3-L1 adipocytes

pretreated with high glucose (25mM or 450mg/dl) plus high insulin (2 μ M) medium overnight were used in an attempt to mimic the hyperglycemia and hyperinsulinemia of KKA^y mice. This caused the cells to be resistant to insulin stimulation of glucose uptake (fig. 13). 3T3-L1 cells pretreated overnight in low glucose (5.5 mM or 100 mg/dl) and very low insulin medium were used as control cells to represent the normoglycemic state.

In addition, a rat model of IDDM displaying high glucose (459 \pm 10 mg/dl) relative to control rats (151 \pm 2 mg/dl) was used to determine whether the presence of high circulating levels of glucose in the absence of high insulin levels could affect the expression of these proteins. Streptozotocin treatment of rats induces IDDM by causing destruction of the pancreatic β cells, and in this model lowered blood insulin levels to roughly 20% of the insulin levels in the control rats (data not shown).

3T3-L1 Cells

In the 3T3-L1 model, the expression of all six of the signaling components and insulin-stimulated phosphorylation of the insulin receptor and IRS-1 were studied. Fig. 13 shows the degree of insulin resistance caused by high insulin and glucose incubation as assayed by ¹⁴C-deoxyglucose uptake upon acute insulin stimulation with increasing

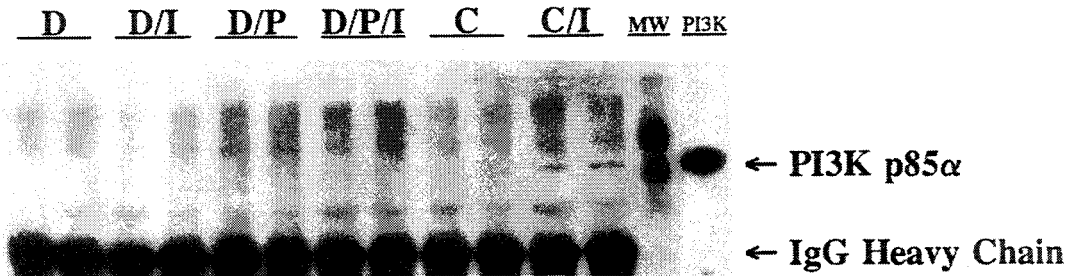


Fig. 11. The amount of PI3K p85 α associating with IRS-1 was detected by western blotting of anti-IRS-1 immunoprecipitates from isolated adipocytes unstimulated or stimulated acutely with 100 nM insulin for 2 minutes. This representative blot shows an n=2 for each group: D=KKA γ (unstimulated), D/I=KKA γ (stimulated), D/P=KKA γ pretreated with pioglitazone (unstimulated), D/P/I=KKA γ pretreated with pioglitazone (stimulated), C=C57 (unstimulated), C/I=C57 (stimulated). MW=molecular weight markers. The two bands in the MW lane are 106,000 (upper band) and 80,000 (lower band). The lane labeled PI3K was loaded with PI3K p85 α positive control. The labels on the right of the figure indicate the positions of PI3K p85 α migration and the IgG heavy chain of the precipitating antibody.

PI3K in Anti-IRS-1 IP Isolated Adipocytes

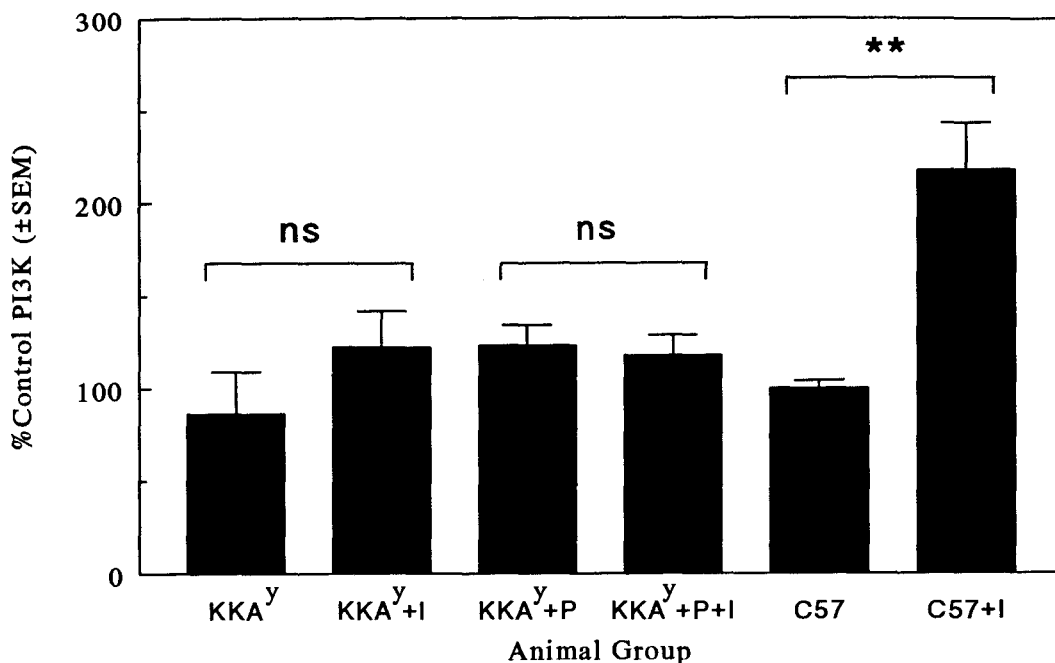


Fig. 12. Cumulative graphed results of acute insulin-stimulated association of PI3K p85 α with IRS-1 in isolated adipocytes are depicted as mean % unstimulated control (C57) \pm SEM, n=10. Data were accumulated from anti-p85 α western blots of IRS-1 immunoprecipitates such as is shown in fig. 11. ** represents a statistical difference (p<0.01) between the bracketed groups. ns=not significant (p>0.05).

Glucose Transport

Low vs. High Glucose; -, +I

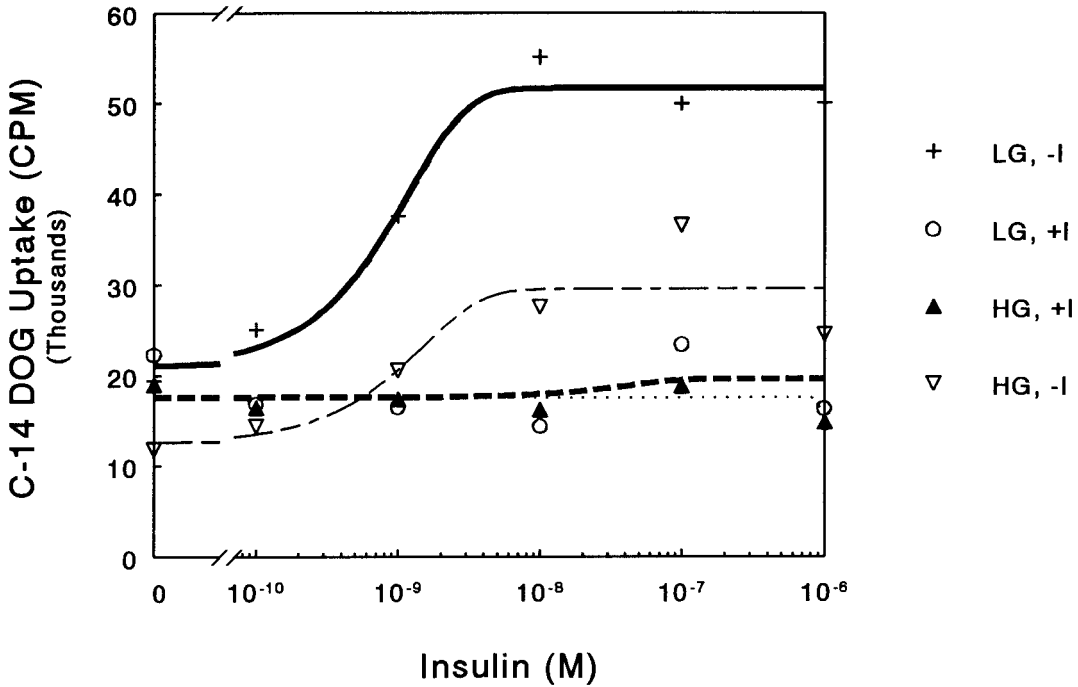


Fig 13. Representative insulin dose-response curves are shown for insulin-stimulated ^{14}C -deoxyglucose uptake in 3T3-L1 adipocytes pre-fed overnight with DMEM containing 5.5mM glucose (LG, -I, thick solid line, +), 5.5mM glucose + $2 \times 10^{-6}\text{M}$ insulin (LG, +I, thick dashed line, O), 24.4 mM glucose (HG, -I, thin dashed line, ∇), or 24.4 mM glucose + $2 \times 10^{-6}\text{M}$ insulin (HG, +I, thin dotted line, \blacktriangle). Each symbol represents the average amount of ^{14}C -deoxyglucose uptake ($n=6$) at the given insulin concentration, and the lines represent a sigmoidal regression of each data set.

amounts of insulin. High glucose in the absence of high insulin caused a decrease in the maximal insulin stimulation of glucose transport, while high insulin with or without high glucose fully attenuated the ability of the cells to take up glucose on insulin stimulation.

Insulin receptor. The expression and phosphorylation of the insulin receptor in insulin-resistant 3T3-L1 adipocytes were altered in a manner similar to the expression and phosphorylation of the receptor observed in KKA^y mice. The receptor protein levels in the insulin-resistant cells was lowered to $33.6 \pm 3.3\%$ of control cell receptor expression (fig. 14, left panel), much like the lower expression seen in KKA^y mice as compared to C57. The levels of 9.5 and 7.5 kb mRNA transcripts were significantly lowered to 58.75 ± 3.2 and $75.3 \pm 3.6\%$ of control cells (fig. 14, middle), a larger difference than was seen in the receptor RNA levels between the KKA^y and control mice. Another interesting observation was that the high glucose and high insulin incubation caused a shift in the ratio of the 9.5 to 7.5 kb transcripts. In control cells, there was an 11% difference between the percent 9.5 kb transcript in the total receptor RNA and the 7.5 kb transcript in the total. In the cells treated with high insulin and high glucose, this difference disappeared (fig. 14, right).

Insulin Receptor Expression

3T3-L1 Cells

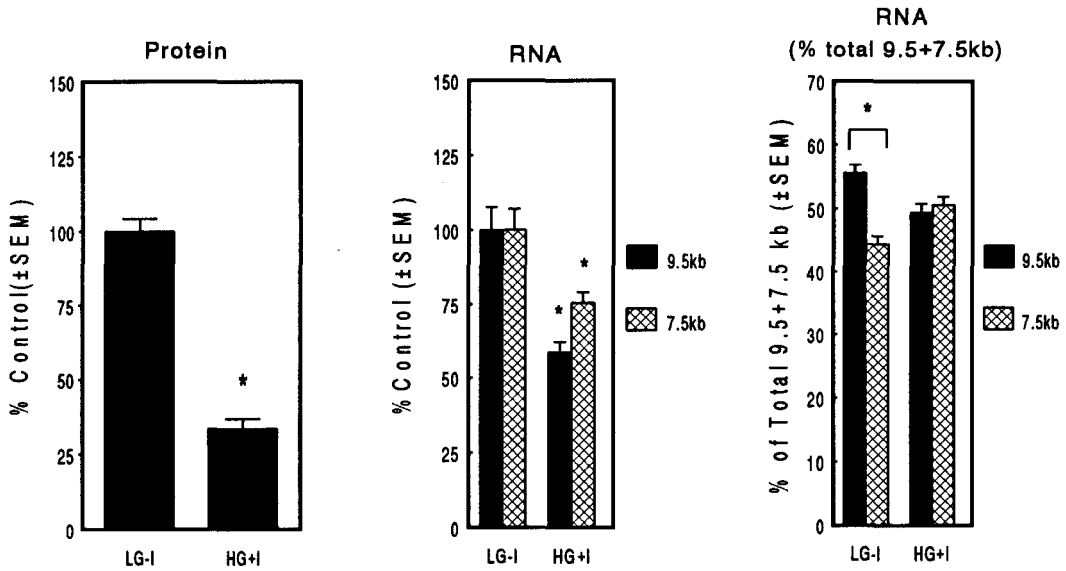


Fig. 14. Graphed results of the protein and RNA levels of the insulin receptor in 3T3-L1 cells. LG-I=3T3-L1 cells pre-fed overnight in low glucose (4.4 mM) DMEM; HG+I=3T3-L1 cells pre-fed overnight in high glucose (24.4 mM) DMEM with 2×10^{-6} M insulin. Left, protein levels are represented as % control (LG-I) \pm SEM, n=22. Center, the RNA levels are graphed as %control (LG-I) \pm SEM for both the 9.5 and 7.5 kb species, n=16. The solid bar represents the amount of 9.5 kb transcript, while the hatched bar represents the amount of 7.5 kb transcript. Right, the relative ratios of the 9.5 and 7.5 kb transcripts are shown as % of the total insulin receptor transcripts (9.5+7.5 kb) for both treatment groups. * indicates a significant difference ($p < 0.05$) as compared to control or between the bracketed groups.

The acute insulin stimulation of control 3T3-L1 cells resulted in a 25-fold increase in the tyrosine-phosphorylation of the insulin receptor β subunit, as detected by western blotting with anti-phosphotyrosine antibodies (fig. 15). A one-minute insulin stimulation was used in these experiments, since the receptor and IRS-1 tyrosine phosphorylation was maximal in control cells at one minute (fig. 16, lanes 4 and 5). Like the KKA^y isolated adipocytes, the insulin-resistant cells had a much higher level of basal tyrosine phosphorylation than the control cells, and were unable to respond to insulin by further phosphorylation of the receptors (fig. 15, left). Likewise, expression of data as phosphorylation per receptor exaggerated the basal phosphorylation of the receptor in the insulin resistant cells as compared to control (fig. 15, right), owing to decreased receptor numbers in insulin-treated cells. Such observations were consistent with those seen in adipocytes isolated from insulin-resistant KKA^y mice (fig. 9).

IRS-1. The expression of IRS-1 in the insulin-resistant 3T3-L1 cells was also regulated in much the same way as IRS-1 expression in KKA^y mice. The protein levels of IRS-1 were not significantly different between control and insulin-resistant cells, as shown in fig. 17 (left panel). In addition, like in the animal model of insulin resistance,

Insulin Receptor Tyrosine Phosphorylation

3T3-L1 Cells

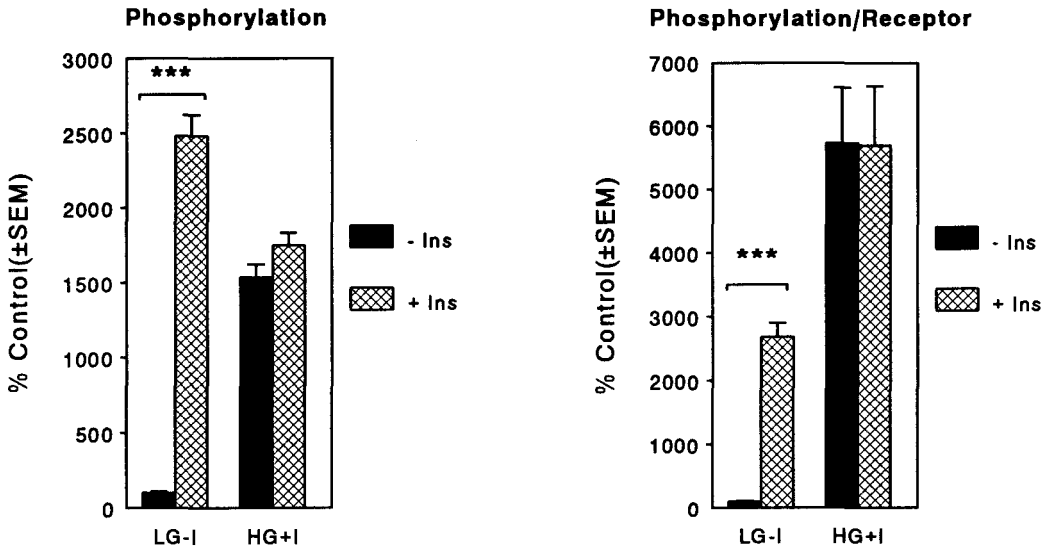


Fig. 15. Cumulative graphed results of acute insulin-stimulated phosphorylation of the insulin receptor β subunit in 3T3-L1 cells are depicted as mean % unstimulated control (LG-I) \pm SEM, $n=11$. Left, total phosphorylation of the insulin receptor β subunit as measured by western blotting of cell lysates with anti-phosphotyrosine antibodies. Right, phosphorylation per unit receptor. Solid bars represent unstimulated cells and hatched bars represent cells stimulated actually with 1×10^{-7} M insulin for 1 minute. *** represents a statistical difference ($p < 0.001$) between the bracketed groups.

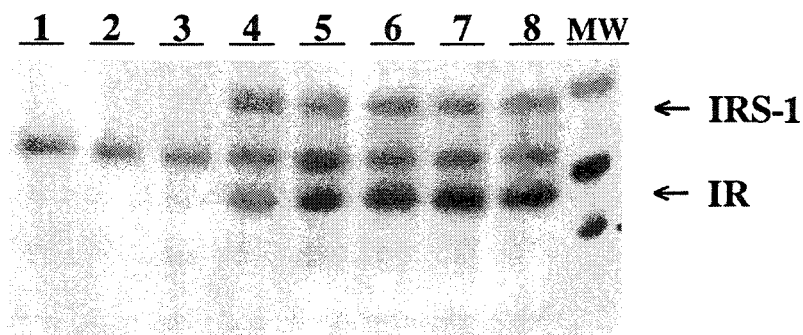


Fig. 16. The time course for insulin-stimulated tyrosine phosphorylation of IRS-1 and the insulin receptor in control 3T3-L1 cells, as observed with western blotting with anti-phosphotyrosine antibodies. Phosphorylated IRS-1 and IR bands are indicated by the arrows on the right. Lanes 1 and 2: no insulin stimulation; lane 3: 30 second insulin stimulation with 1×10^{-7} M insulin; lanes 4 and 5: 1 minute insulin stimulation; lanes 6 and 7: 5 minute insulin stimulation; lane 8: 10 minute insulin stimulation; MW: molecular weight markers 205, 106, and 80 kDa from top to bottom.

the mRNA abundance for IRS-1 in the insulin-resistant 3T3-L1 cells was significantly lower than in the control cells (fig. 17, right).

The insulin stimulated tyrosine phosphorylation of IRS-1 was attenuated by high insulin and high glucose incubation of 3T3-L1 cells, as shown in fig. 18. Although this was also seen in the KKA^y adipocytes, there was a difference between these two models in that the basal phosphorylation of IRS-1 was elevated in the *in vitro* model of insulin resistance relative to control cells (fig. 18). In the animals, there was not a difference in the basal tyrosine phosphorylation of IRS-1 between KKA^y and C57 mice. Because there was not a large difference in the protein levels of IRS-1 between control 3T3-L1 cells and the insulin-resistant 3T3-L1 cells, the results for phosphorylation per IRS-1 (fig. 18, right) did not differ greatly from the total phosphorylation data (fig. 18, left).

PI3K p85 α . As in the animal epididymal fat tissue, the PI3K monoclonal (anti-SH2) antibody recognized two bands. The lower of these two bands comigrated with the baculovirus-produced p85 α positive control on SDS-PAGE western blots. The expression of PI3K p85 α was not altered by incubation of 3T3-L1 cells with high glucose and high insulin (fig. 19, left), although this treatment caused an

IRS-1 Expression in 3T3-L1 Cells

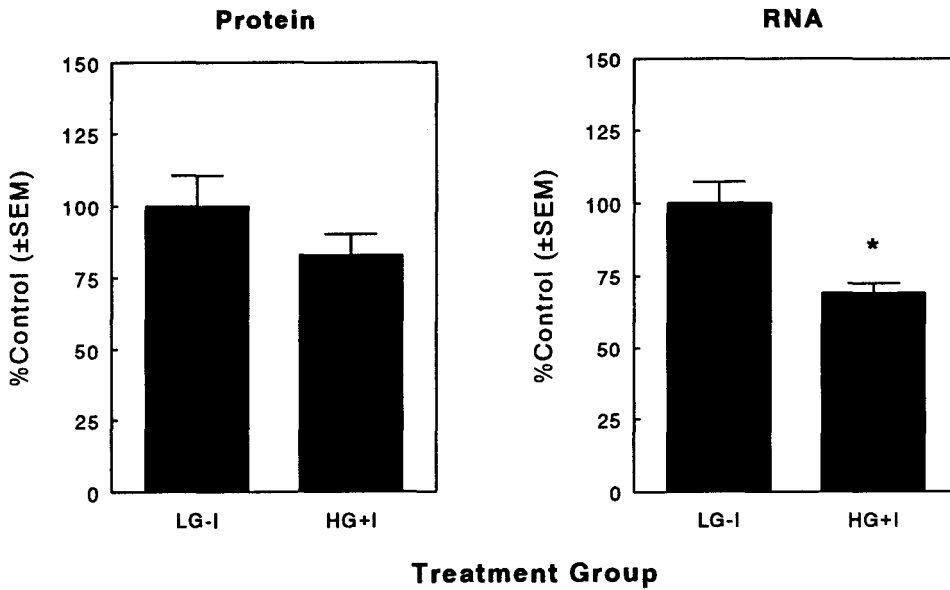


Fig. 17. Graphed results of the protein and RNA levels of IRS-1 in 3T3-L1 cells. LG-I=3T3-L1 cells pre-fed overnight in low glucose (4.4 mM) DMEM; HG+I=3T3-L1 cells pre-fed overnight in high glucose (24.4 mM) DMEM with 2×10^{-6} M insulin. Left, protein levels are represented as % control (LG-I) \pm SEM, n=22. Right, the RNA levels are graphed as %control (LG-I) \pm SEM, n=16. * indicates a significant difference ($p < 0.05$) as compared to control.

IRS-1 Tyrosine Phosphorylation

3T3-L1 Cells

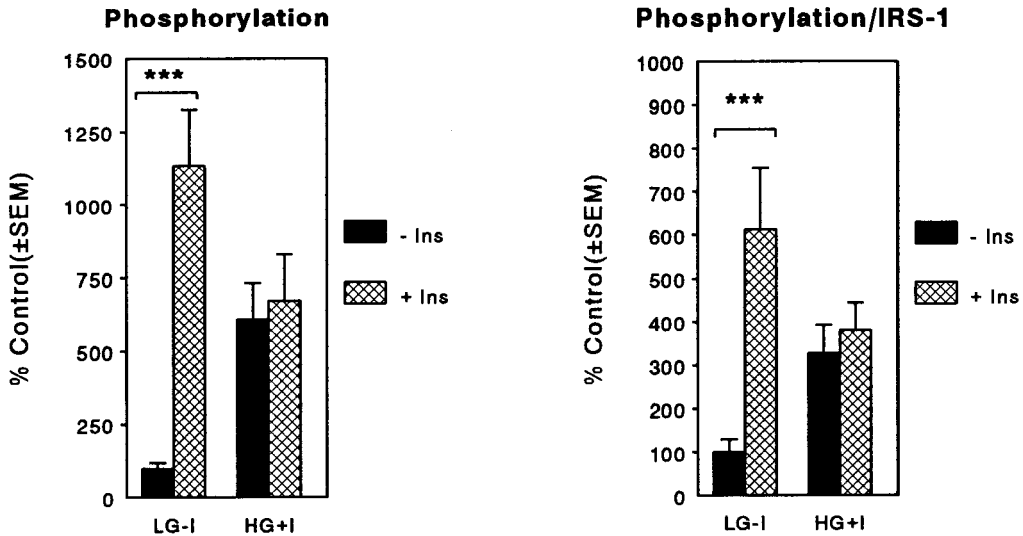


Fig. 18. Cumulative graphed results of acute insulin-stimulated phosphorylation of IRS-1 in 3T3-L1 cells are depicted as mean % unstimulated control (LG-I) \pm SEM, n=11. Left, total phosphorylation of IRS-1 as measured by western blotting of cell lysates with anti-phosphotyrosine antibodies. Right, phosphorylation per unit IRS-1. Solid bars represent unstimulated cells and hatched bars represent cells stimulated actually with 1×10^{-7} M insulin for 1 minute. *** represents a statistical difference (p < 0.001) between the bracketed groups.

PI3K p85 α Expression

3T3-L1 Cells

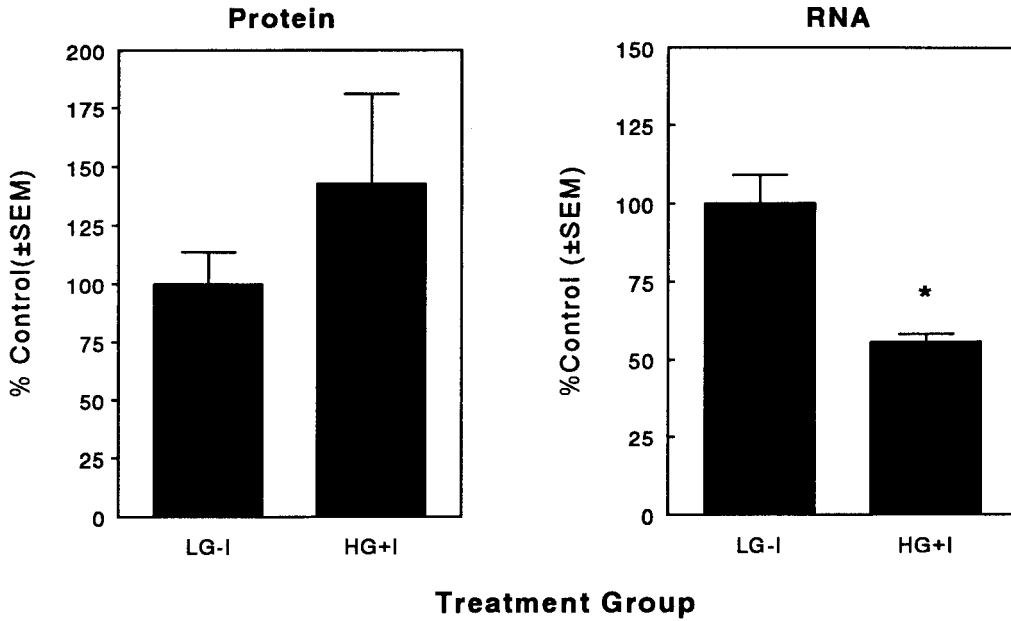


Fig. 19. Graphed results of the protein and RNA levels of PI3K p85 α in 3T3-L1 adipocytes. LG-I=3T3-L1 cells pre-fed overnight in low glucose (4.4 mM) DMEM; HG+I=3T3-L1 cells pre-fed overnight in high glucose (24.4 mM) DMEM with 2×10^{-6} M insulin. Left, protein levels are represented as % control (LG-I) \pm SEM, n=22. Right, the RNA levels are graphed as %control (LG-I) \pm SEM, n=16. * indicates a significant difference ($p < 0.05$) as compared to control.

increase in the variance of these cells which may have obscured a slight increase. This differs from the mouse experiment, where the expression of p85 α protein in KKA γ mice was 53% lower than the expression in C57 control mice. Also dissimilar from the mouse experiment was that the RNA levels of PI3K p85 α were lowered by 31 \pm 3.4% by high glucose and high insulin incubation of 3T3-L1 cells (fig. 19, right), whereas the RNA levels in KKA γ fat did not differ significantly from the RNA levels in the control mice (fig. 6, left), even though KKA γ mice are also hyperglycemic and hyperinsulinemic.

GRB2, Nck, and Syp. Incubation of 3T3-L1 cells in high insulin and high glucose resulted in a significant elevation of GRB2 and Nck protein levels, but did not change the expression of Syp protein (fig. 20). The elevation of these proteins in this model of insulin resistance is consistent with the higher expression of these proteins in KKA γ mice as compared to C57 mice (fig. 3); however, the magnitude of these increases were much smaller in this *in vitro* model than in the *in vivo* model. GRB2 and Nck levels in these insulin-resistant 3T3-L1 cells were 135.7 \pm 8.1% and 117 \pm 3.1% of control, respectively, while the levels of these proteins in KKA γ mice were 321 \pm 25.4% and 185.6 \pm 12.2% of the respective levels of GRB2 and Nck in control mice.

Expression of GRB2, Nck, and Syp 3T3-L1 Cells

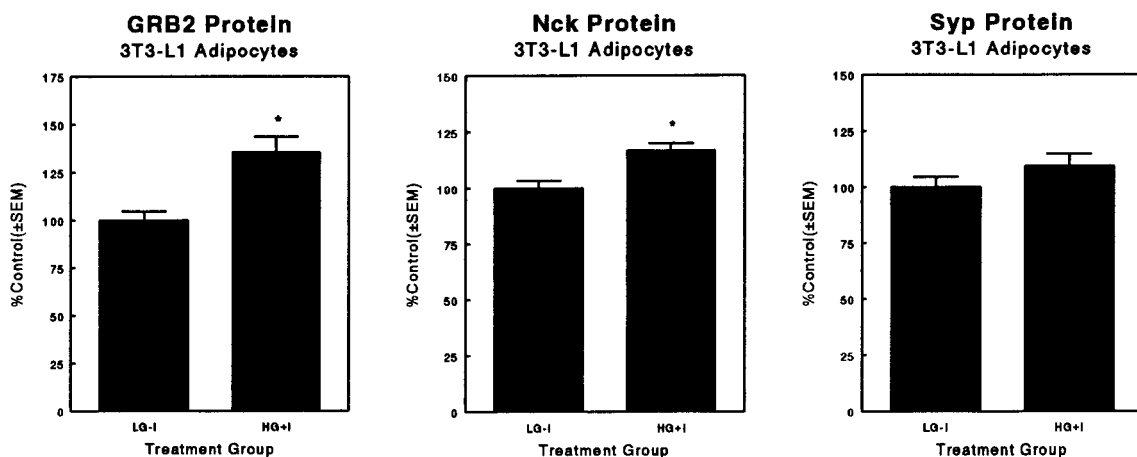


Fig. 20. The expression of GRB2, Nck, and Syp protein in 3T3-L1 adipocytes. LG-I=3T3-L1 cells pre-fed overnight in low glucose (4.4 mM) DMEM; HG+I=3T3-L1 cells pre-fed overnight in high glucose (24.4 mM) DMEM with 2×10^{-6} M insulin. Left, protein levels of GRB2; center, protein levels of Nck; and right, protein levels of Syp are graphed as % control (LG-I) \pm SEM, n=22. * indicates a significant difference (p<0.05) as compared to control.

Rat Streptozotocin-Induced IDDM

The expression of all six signaling components was studied in this *in vivo* model of IDDM to determine if high glucose levels in the absence of high insulin are associated with any alterations in the levels of these proteins.

Insulin receptor. The protein levels of the insulin receptor were altered somewhat differently in fat and liver of streptozotocin-treated rats as compared to control rats. In liver, the expression of the insulin receptor was significantly elevated to $183 \pm 25\%$ of control (fig. 21, left). In epididymal fat, the average receptor protein level was $130.6 \pm 11.4\%$ of control, although this difference was not significant (fig. 22, left). In both tissues, the mRNA levels were significantly elevated in the streptozotocin-treated rats compared to the control rats. The elevation in liver tissue was associated with an increase in the 9.5 kb transcript (fig. 21, center). The higher mRNA levels in epididymal fat were mainly associated with an increase in 7.5 kb transcripts, although the 9.5 kb receptor mRNA was also significantly higher than in the control animals (figure 22, center).

In addition to the differences in receptor protein expression between the two groups in both tissues, the ratio of the 9.5 to 7.5 kb transcripts was tissue-specific as well. In liver tissue, control rats had a significantly

Insulin Receptor Expression in Rat IDDM (Liver)

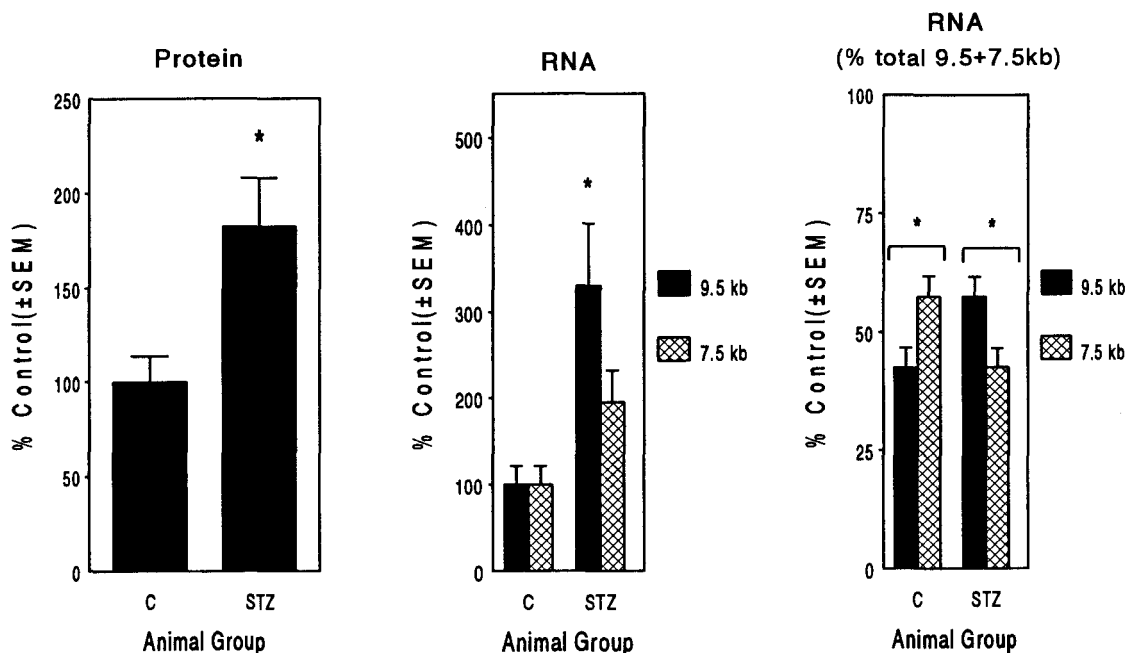


Fig. 21. Graphed results of the protein and RNA levels of the insulin receptor in rat liver. C=control rats; STZ=rats made insulin-deficient by streptozotocin treatment. Left, protein levels are represented as % control \pm SEM, n=9. Center, the RNA levels are graphed as %control \pm SEM for both the 9.5 and 7.5 kb species, n=7 control and 9 STZ. The solid bar represents the amount of 9.5 kb transcript, while the hatched bar represents the amount of 7.5 kb transcript. Right, the relative ratios of the 9.5 and 7.5 kb transcripts are shown as % of the total insulin receptor transcripts (9.5+7.5 kb) for both treatment groups. * indicates a significant difference ($p < 0.05$) as compared to control or between the bracketed groups.

higher ratio of 7.5 kb transcripts, and streptozotocin treatment reversed this ratio (fig. 21, right). In epididymal fat, the control animals had a significantly higher ratio of 9.5 kb transcripts, while the streptozotocin-treated animals had roughly an equal amount of each transcript (fig. 22, right).

IRS-1. The mRNA levels for IRS-1 were also increased in both fat (fig. 23, right) and liver tissue (fig. 24) of streptozotocin-diabetic rats as compared to control rats. This increase was to $198.6 \pm 28.5\%$ control and $217 \pm 18.4\%$ control in fat and liver, respectively. Unlike the expression of the insulin receptor, the elevated IRS-1 mRNA levels were not associated with a concomitant increase in the IRS-1 protein in fat tissue. In fact, IRS-1 protein levels in epididymal fat of streptozotocin-treated rats was significantly lowered to $62.2 \pm 4.7\%$ of control (fig. 23, left). The protein levels for IRS-1 in rat liver were not measurable on western blots due to a nonspecific band which was recognized by several anti-IRS-1 antibodies. This protein was very highly expressed in comparison to IRS-1, and the proximity of this protein to IRS-1 on SDS-PAGE gels was so close that its signal overshadowed IRS-1 expression. Substantial evidence suggests that this band represents a nonspecific protein interaction. First, the band migrated

Insulin Receptor Expression in Rat IDDM (Epididymal Fat)

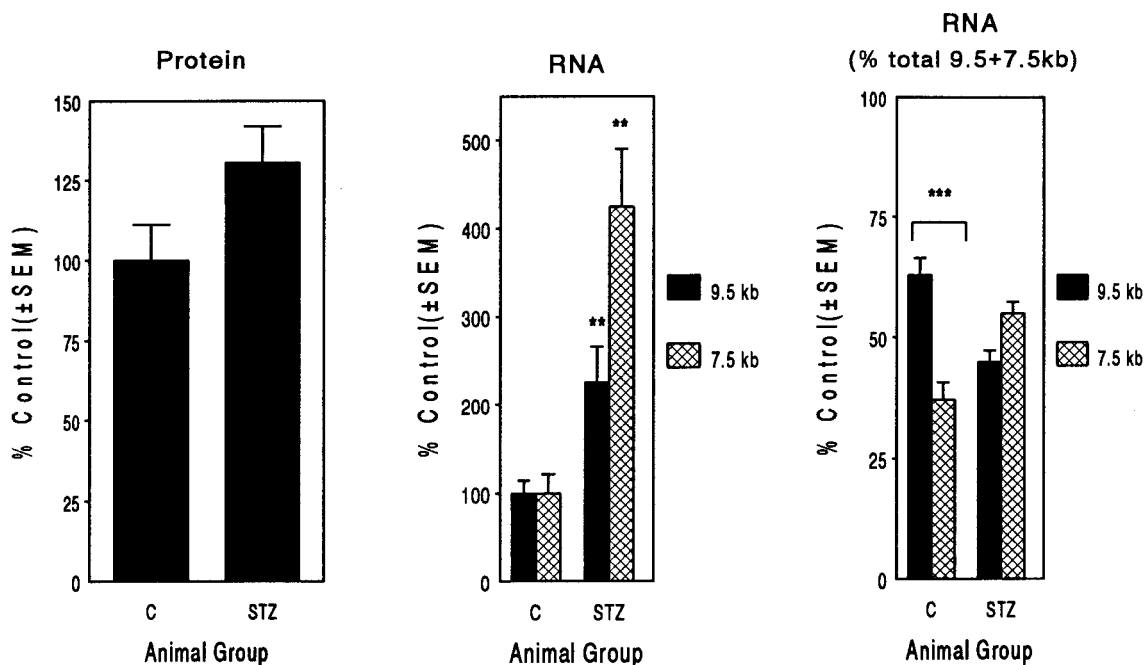


Fig. 22. Graphed results of the protein and RNA levels of the insulin receptor in rat epididymal fat. C=control rats; STZ=rats made insulin-deficient by streptozotocin treatment. Left, protein levels are represented as % control \pm SEM, n=9. Center, the RNA levels are graphed as %control \pm SEM for both the 9.5 and 7.5 kb species, n=9 control and 7 STZ. The solid bar represents the amount of 9.5 kb transcript, while the hatched bar represents the amount of 7.5 kb transcript. Right, the relative ratios of the 9.5 and 7.5 kb transcripts are shown as % of the total insulin receptor transcripts (9.5+7.5 kb) for both treatment groups. ** and *** indicate a significant difference ($p < 0.01$ and $p < 0.001$, respectively) as compared to control or between the bracketed groups.

IRS-1 Expression in Rat IDDM (Epididymal Fat)

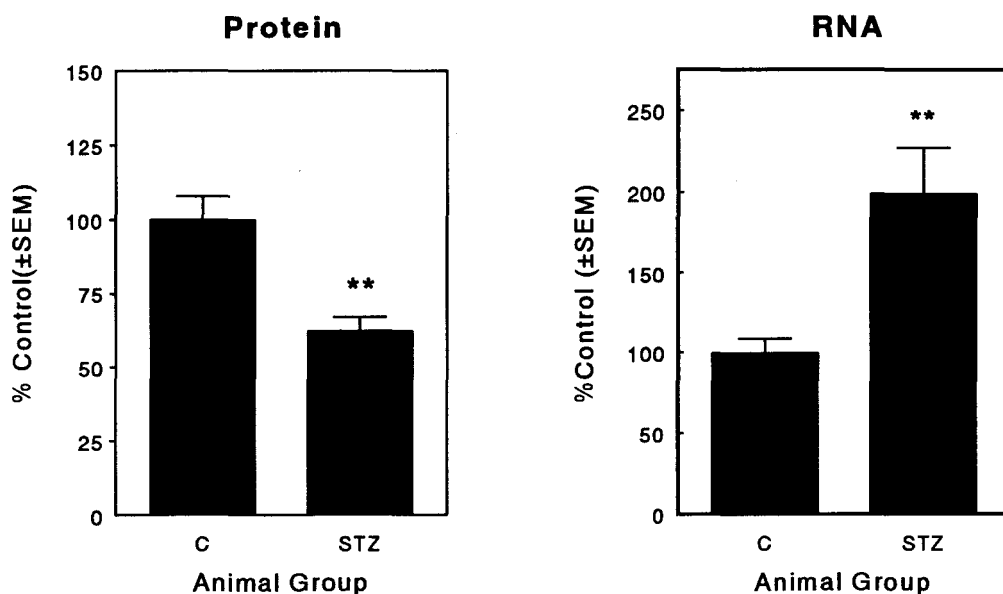


Fig. 23. Graphed results of the protein and RNA levels of IRS-1 in rat epididymal fat. C=control rats; STZ=streptozotocin-treated rats. Left, protein levels are represented as % control \pm SEM, n=9. Right, the RNA levels are graphed as %control \pm SEM, n=9 control and 7 STZ. ** indicates a significant difference (p<0.01) as compared to control.

IRS-1 RNA in Rat IDDM (Liver)

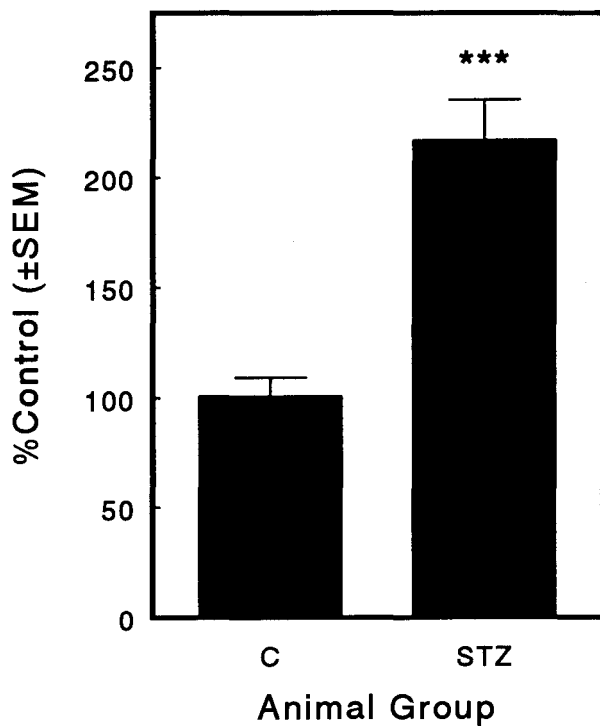


Fig. 24. Graphed results of the RNA levels of IRS-1 in rat liver. C=control rats; STZ=streptozotocin-treated rats. The RNA levels are graphed as %control \pm SEM, n=18 control and 17 STZ. *** indicates a significant difference ($p < 0.001$) as compared to control.

slightly ahead of the positive control, which normally lined up with IRS-1. Secondly, IRS-1 is expressed at very low levels in all tissues studied, and the expression of this band was much too high to have been IRS-1. Third, there was a faint band that lined up with the positive control which was not quantifiable due to the high expression of the nonspecific band (data not shown).

PI3K p85 α . In epididymal fat, streptozotocin treatment had no effect on the expression of p85 α at the protein or mRNA levels (fig. 25). In contrast, liver tissue of streptozotocin-treated rats showed a $68.9 \pm 12.7\%$ increase in the expression of p85 α protein over the expression in liver tissue from control rats (fig. 26, left). This increase in p85 α protein was not clearly reflected at the RNA level, as there was only a slight nonsignificant increase in p85 α mRNA between control and streptozotocin-treated animals in liver tissue (fig. 26, right).

GRB2, Nck, and Syp. Like the receptor, IRS-1, and p85 α , the expression of GRB2, Nck, and Syp tended to be regulated in the opposite manner in this model of IDDM (streptozotocin-treated rats) from the NIDDM model (KKA^y mice), as shown in figs. 27 and 28. In epididymal fat and liver tissue, there was no difference in the expression of GRB2 between control and streptozotocin-treated rats (figs.

PI3K p85 α Expression in Rat IDDM (Epididymal Fat)

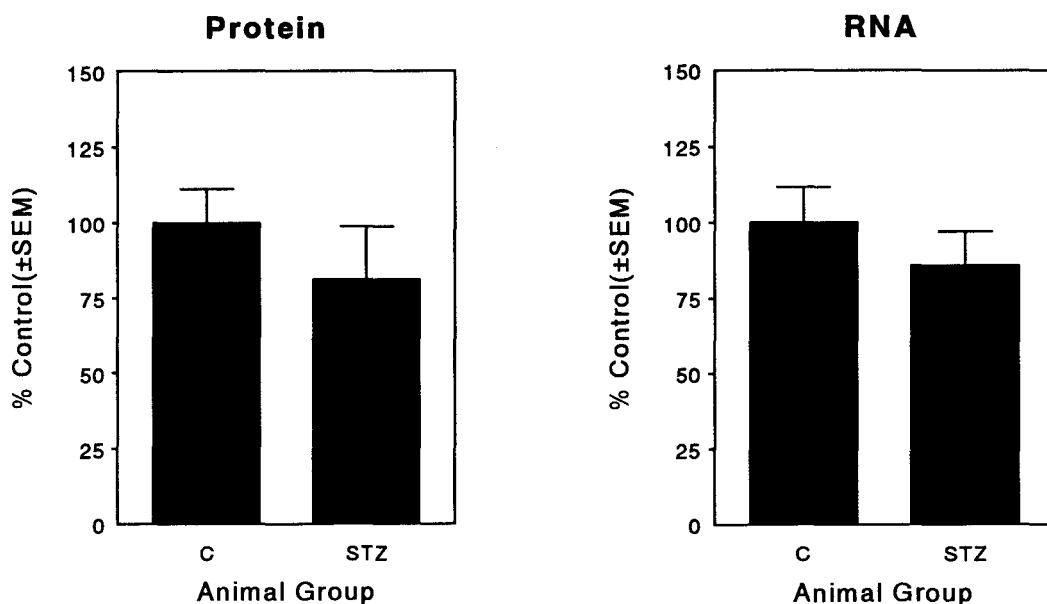


Fig. 25. Graphed results of the protein and RNA levels of PI3K p85 α in rat epididymal fat. C=control rats; STZ=streptozotocin-treated rats. Left, protein levels are represented as % control \pm SEM, n=9 control and 8 STZ. Right, the RNA levels are graphed as %control \pm SEM, n=6.

PI3K p85 α Expression in Rat IDDM (Liver)

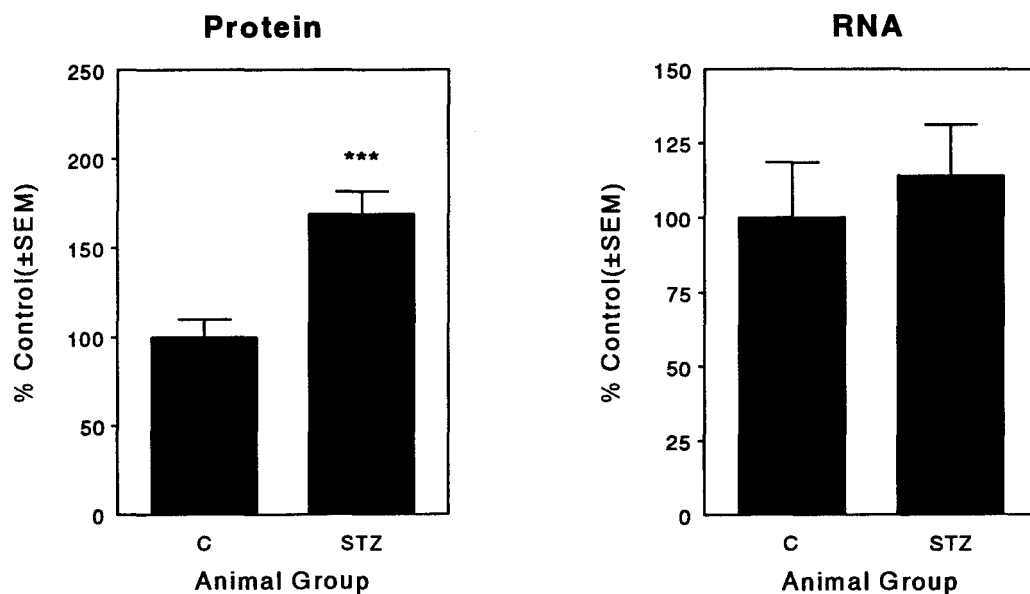


Fig. 26. Graphed results of the protein and RNA levels of PI3K p85 α in rat liver. C=control rats; STZ=streptozotocin-treated rats. Left, protein levels are represented as % control \pm SEM, n=9. Right, the RNA levels are graphed as %control \pm SEM, n=7. *** indicates a significant difference (p<0.001) between the two groups.

GRB2, Nck, and Syp Protein in Rat IDDM (Epididymal Fat)

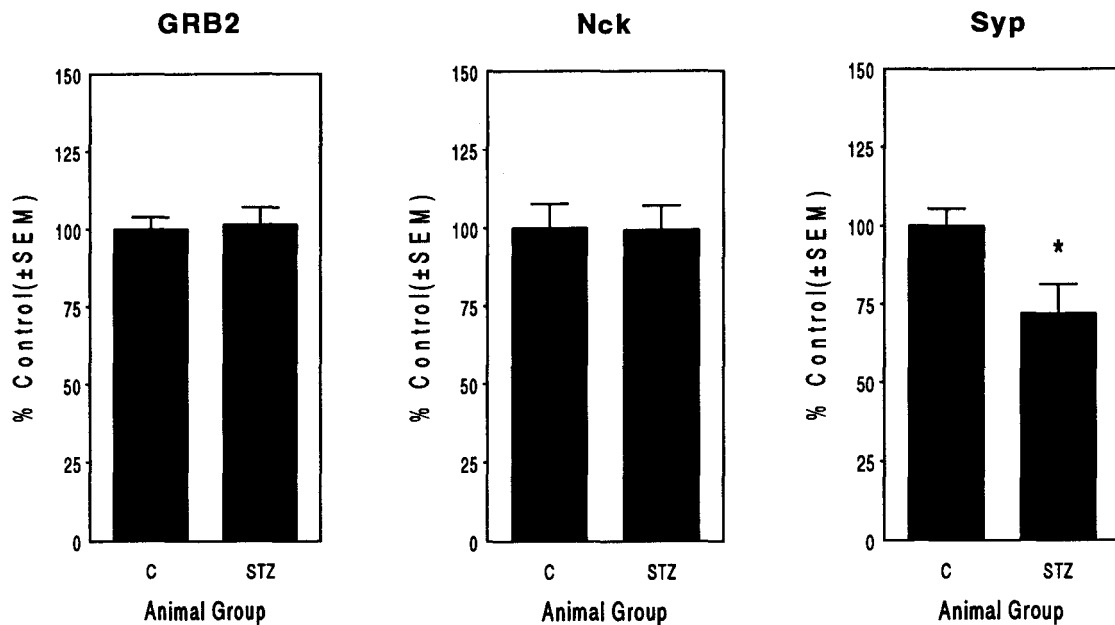


Fig. 27. The expression of GRB2, Nck, and Syp protein in rat epididymal fat. C=control rats; STZ=streptozotocin-treated rats. Left, protein levels of GRB2; center, protein levels of Nck; and right, protein levels of Syp are graphed as % control \pm SEM, n=9 control and 8 STZ. * indicates a significant difference (p<0.05) as compared to control.

GRB2, Nck, and Syp Protein in Rat IDDM (Liver)

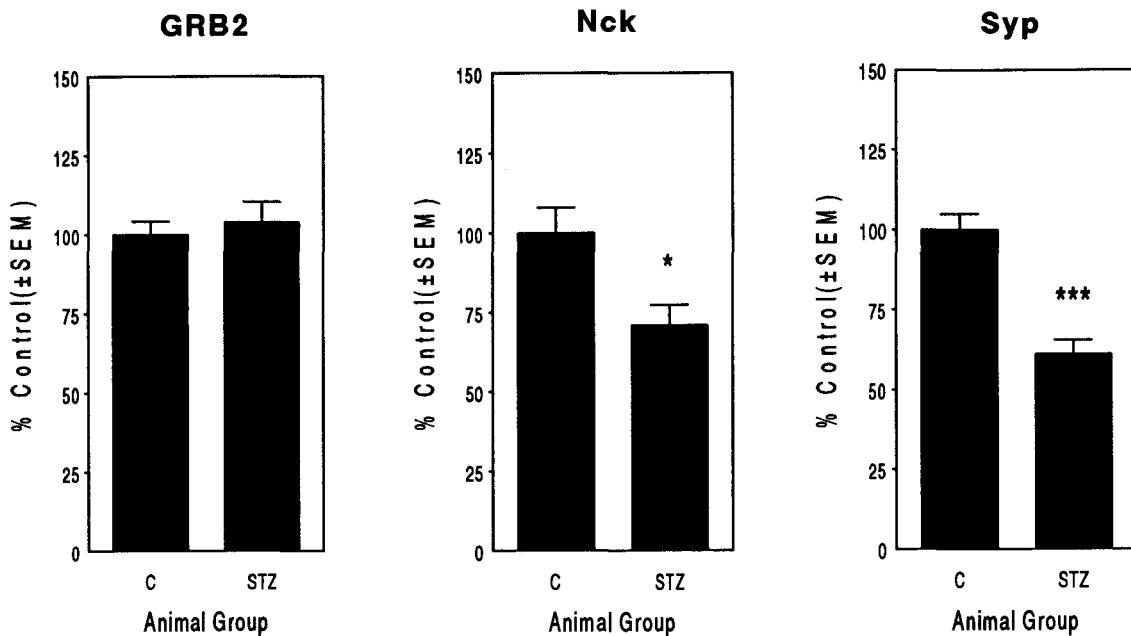


Fig. 28. The expression of GRB2, Nck, and Syp protein in rat liver. C=control rats; STZ=streptozotocin-treated rats. Left, protein levels of GRB2; center, protein levels of Nck; and right, protein levels of Syp are graphed as % control \pm SEM, n=9. * and *** indicate a significant difference of $p < 0.05$ or $p < 0.001$ as compared to control, respectively.

27 and 28, left). Nck protein levels were significantly reduced to $70.87 \pm 6.5\%$ of control in liver tissue of streptozotocin-treated animals, while Nck expression was unchanged in epididymal fat (figs. 27 and 28, center). Syp protein levels were significantly decreased to 71.8 ± 9.3 and $61.2 \pm 4.4\%$ of control in fat and liver tissues, respectively (figs. 27 and 28, right).

CHAPTER V
DISCUSSION

Because NIDDM is associated with a variety of metabolic derangements (2-5,120), and the cause of insulin resistance probably lies in a post-receptor defect in most cases, this project focused on studying early insulin signaling events as possible sites of defects. Earlier signal transduction defects would likely lead to multiple downstream derangements, particularly if alterations occurred before insulin's signal branched to elicit its many different cellular effects.

The current study indicates that there are multiple alterations in the expression and function of components involved in the first stages of insulin signal transduction in diabetic KKA^y mouse tissues as compared to control nondiabetic animals. The expression and function of the insulin receptor, IRS-1, and PI3K p85 α were found to be defective to varying degrees in KKA^y mice. Conversely, GRB2, Nck, and Syp levels were elevated in KKA^y mice as compared to nondiabetic controls.

However, results from the *in vitro* model of insulin resistance suggest that many of these alterations are likely

a result of hyperinsulinemia and hyperglycemia associated with the diabetic condition. Also, hyperglycemia with hypoinsulinemia tended to regulate the expression of these signaling components in the opposite direction from hyperglycemia with hyperinsulinemia relative to control animals. Therefore, the pathophysiology associated with the insulin-resistant diabetic condition of KKA^y mice, particularly hyperinsulinemia, may be responsible for the observed alterations. PI3K p85 α expression was the exception, as it was decreased in adipose from KKA^y mice relative to control, but not significantly altered in 3T3-L1 cells pre-fed with high levels of glucose and insulin.

Pioglitazone treatment of KKA^y mice had little effect on the expression or function of any of the proteins studied. While pioglitazone treatment increased PI3K p85 α levels in KKA^y fat to control levels, this increase in expression did not result in an increase in p85 α associated with IRS-1 on insulin stimulation of adipocytes from pioglitazone-treated KKA^y mice compared to untreated KKA^y mice. Therefore, pioglitazone probably elicits its insulin-sensitizing effect in this model of insulin-resistant diabetes by a mechanism other than the alteration of the expression or function of early signaling components.

Proteins with Altered Expression or Function in KKA^y Mice or
Streptozotocin-treated Rats

The Insulin Receptor

Expression

The protein levels of the insulin receptor in fat and liver from insulin-resistant KKA^y mice were lower than receptor levels in either tissue from nondiabetic C57 controls (fig. 2). However, high amounts of insulin have been shown to cause internalization and degradation of the insulin receptor (169,170), and the enzyme responsible for at least part of the degradation of the insulin receptor is a lysosomal thiol protease (170). In the 3T3-L1 cells pre-fed with high insulin and high glucose, a similar decrease in the amount of insulin receptor protein was seen (fig. 14), suggesting that the lower levels of receptor protein in the KKA^y mice may be due to the high circulating insulin levels in these animals.

Further evidence supporting this concept lies in the regulation of the RNA levels for the insulin receptor. In KKA^y mice, the RNA levels for the insulin receptor are not significantly lower than in C57 mice with the exception of the 7.5 kb transcript in liver (fig. 4). A significant difference in receptor RNA levels existed in the 3T3-L1 cells pre-fed with high glucose and high insulin as compared

to control cells, although this difference was only about 25% (fig. 14). This is about the same magnitude as the difference between the mean receptor RNA levels between KKA^y and C57 mice. The fact that this difference is significant in the cell culture experiment, but not the animal experiment, may be a result of the smaller variation in cell culture as opposed to animal studies. The differences in mRNA (about 25% control) are much smaller than the differences in protein in either study, suggesting a regulation of the receptor at the protein level, most likely due to insulin receptor internalization and degradation. Comparable results were found by Ludwig, *et al.* in livers of genetically obese and hyperinsulinemic mice, where receptor number was decreased even though mRNA levels were increased compared to controls (171).

Interestingly, insulin receptor mRNA levels were upregulated in fat and liver of the insulin-deficient streptozotocin-diabetic rats compared to control tissues, and liver tissue demonstrated a significant concordant rise in receptor protein (fig. 21 and fig. 22). Similar results were found by Tozzo, *et al.*, where both the 7.5 and 9.5 kb transcripts were increased 10-fold in liver tissue of streptozotocin-treated rats (172). This increase was due to an increase in transcription of the insulin receptor gene, and also resulted in increased insulin binding to liver plasma membranes by 40% (172). In this case, the RNA and

protein were upregulated in the absence of insulin. Such changes may represent cellular compensations to upregulate receptors when there is insufficient insulin to elicit normal effects.

If this were the case, there should have been a similar rise in insulin receptor mRNA in the insulin-resistant 3T3-L1 cells or tissues from KKA^y mice, as opposed to the observed decrease in both models (fig. 4 and fig. 14). Therefore, high insulin levels probably lower insulin receptor mRNA levels as well as receptor protein levels in KKA^y mice. To support the data shown in figs. 2, 4, 14, 21, and 22, the expression of the insulin receptor was regulated in a manner similar to KKA^y mice in liver and muscle of insulin-resistant ob/ob mice (173), while receptor levels were increased in tissues of streptozotocin-treated rats (173).

The physiological significance of insulin receptor regulation can be partially explained using the concept of spare receptors. Normal cells possess many more insulin receptors than are necessary to produce maximal cellular responses in the presence of physiological concentrations of insulin (174). Insulin-stimulated glucose oxidation is maximal in isolated fat cells when only 8-10% of the receptors are occupied (174). There are two major advantages to the presence of spare receptors in insulin-sensitive tissues. First, spare receptors protect cells

from hypoglycemia following the surge of insulin in response to a glucose challenge because the maximal effects are attained at an insulin concentration well below the concentration needed to bind all of the receptors.

Secondly, spare receptors help to prevent hyperglycemia when there is a sudden loss of receptors (174). However, spare receptors are not actually "spare," since decreasing receptor number causes a subsequent loss in sensitivity, requiring more insulin to elicit the maximal cellular effects (174). Therefore, the lower amount of insulin receptors in KKA^y mice probably contributes to the diabetic condition by making the cells less responsive to insulin, even though the receptor number was above the 8-10% of control involved in binding insulin in normal cells.

Pioglitazone treatment significantly increased receptor protein levels toward control levels in KKA^y epididymal fat ($p < 0.05$ between KKA^y and KKA^y + pioglitazone treatment), although there was not a statistically significant effect of pioglitazone on receptor levels in liver tissue (fig. 2). There was also no significant effect of pioglitazone on receptor mRNA levels. This seems to indicate that the effect of pioglitazone treatment on receptor expression, if any, is secondary to some other effect of pioglitazone. The effect of pioglitazone treatment on receptor number in fat is likely a result of the lowering of serum insulin levels and a subsequent partial alleviation of the insulin

downregulation of the receptor (20). This effect does not seem to change receptor binding, however, since pioglitazone was not found to significantly alter insulin binding (17,20,44). Therefore, while increased receptor number should increase insulin binding (174), the small increase in receptor number resulting from pioglitazone treatment of KKA^y mice may not be large enough to create a significant or detectable change in insulin binding.

Alternate Splicing of the Insulin Receptor

Although several transcript sizes of the insulin receptor have been reported (59), there are four main splicing products that result from alternate splicing of exon 11 in the α subunit (57,58,75-81,175,176) and alternate poly-A site selection (59). Agarose gel electrophoresis of total RNA can only distinguish between the 9.5 kb and 7.5 kb species, which differ by alternate poly-A-site selection (59). The poly-A site selection occurs independently of the splicing of exon 11, resulting in four possible products. The ratio of 9.5 to 7.5 kb transcripts did not differ between KKA^y and control mice (data not shown), nor did the ratio of exon 11+ to exon 11- between these groups (Susan Sell, phone conversation, March 1994) in muscle, fat, or liver tissue. In the 3T3-L1 adipocytes pre-treated with high glucose and high insulin, the ratio of 9.5 to 7.5 kb transcripts changed from a significantly higher percent of

9.5 than 7.5 kb transcripts in the control cells ($55.66 \pm 1.3\%$ 9.5 kb, $44.3 \pm 1.3\%$ 7.5 kb; $p < 0.001$, $n = 16$) to an even ratio ($50.5 \pm 1.3\%$ 9.5, $49.5 \pm 1.3\%$ 7.5; $p > 0.05$, $n = 16$), as is shown in fig. 14. Therefore, insulin and glucose may regulate the poly-A site selection of this transcript, though there is no known functional difference between the 9.5 and 7.5 kb transcripts (59).

In contrast to the insulin-resistant animals, the streptozotocin-treated rats showed opposite trends for insulin receptor transcript poly-A site selection compared to transcripts from control animal tissues (fig. 21 and fig. 22). There was also a tissue-specific difference in the ratio of these transcripts, even in the control animals. While control liver had a higher percentage of 7.5 kb transcripts, fat tissue possessed a higher percentage of 9.5 kb transcripts. Streptozotocin-treatment reversed this ratio in liver (fig. 21) and equalized it in fat (fig. 22), indicating that the streptozotocin-induced diabetic condition may alter RNA processing. It is interesting to note that treatment of 3T3-L1 adipocytes with high glucose and high insulin had the same effect on the ratio of these transcripts as did streptozotocin-induced diabetes on such transcripts in fat tissue. Due to the similarity of the tissue and cells (fat and adipocytes), it may be that poly-A site selection is altered by the elevated glucose present in both experimental models. However, the same effect was not

seen in hyperglycemic KKA^y mice as compared with C57 mice (data not shown), although there are many more factors influencing the tissues in this polygenic model (36,37).

Kinase Activity

Insulin-stimulated adipocytes isolated from C57 animals showed an 11-fold increase in the tyrosine-phosphorylation of the insulin receptor β subunit (fig. 7 and fig. 8), while control 3T3-L1 cells showed a 25-fold increase when acutely stimulated with insulin. This response was obliterated in insulin-resistant, hyperglycemic KKA^y mice as well as in 3T3-L1 cells pre-fed with high insulin and high glucose, suggesting that the high insulin and high glucose levels may contribute to the insulin resistance of these cells (fig. 7, fig. 8, and fig. 15). In both the animal and cell culture models of insulin resistance, the basal tyrosine phosphorylation of the receptor β subunit was increased well above the basal tyrosine phosphorylation of the receptor in control cells (fig. 8 and fig. 15), probably due to the high levels of circulating insulin. Another possibility is that the high glucose concentrations in both models could be inhibiting the insulin receptor kinase, since it has been shown that incubation of rat-1 fibroblasts with high glucose concentrations led to inhibition of the receptor kinase (42,43). The insulin dose-response curves in 3T3-L1 cells reflected an inhibition of insulin-stimulated glucose uptake

in the cells pre-fed with high glucose only (fig. 13), but it was also evident that treatment with high levels of insulin alone caused an even greater inhibition (fig. 13).

It is possible that hyperphosphorylation of the insulin receptor could lead to inhibition of its kinase activity. There is evidence that the C-terminal tyrosines 1316 and 1322 may play a role in negatively regulating the insulin receptor kinase (63,64). Mutation of these tyrosines to phenylalanine caused an increase in the phosphorylation of the receptor and IRS-1, along with an increase in p85 association with IRS-1, an increase in PI3K activity, and an increase in MAP kinase activity (64). Therefore, when these residues are phosphorylated, they may play a role in turning off receptor signaling in normal cells when the insulin levels are high enough to elicit the desired effects, or these residues could possibly inhibit the receptor in the hyperinsulinemic condition.

However, because of the nature of the methodology used to measure phosphotyrosine in this study, it is possible that acutely-stimulated receptor phosphorylation could not be measured due to the high amount of basal phosphorylation of the β subunit in the insulin-resistant condition. While there are many potential tyrosine phosphorylation sites per receptor, it is not known whether the binding of one or more antibody molecules to phosphotyrosines on the receptor could

block further antibody binding to additional phosphorylated tyrosines after insulin stimulation.

Another factor to be considered is that although the insulin resistant cells of both models have a higher degree of basal receptor tyrosine phosphorylation, they also have fewer receptors. To aid in interpreting this data, the phosphorylation per unit receptor was graphed in fig. 9 and fig. 15. Presentation of the data in this way accentuated the increased basal phosphorylation of the β subunit in the KKA^y mice and 3T3-L1 cells treated with high glucose and high insulin.

Similar results were found by Kanety, *et al.* in the sand rat model of insulin-resistant diabetes (177). In this model, the animals were induced to a state of hyperinsulinemia in the absence of hyperglycemia by altering their diet. This state of insulin resistance was associated with a decrease in the number of insulin receptors and an inhibition of the receptor kinase, while the basal receptor phosphorylation was increased (177). Upon restriction of the diet, these receptor defects were brought back to control levels. Comparable results were also found in adipocytes from NIDDM patients, where there was an observed decrease in the insulin-stimulated tyrosine phosphorylation of insulin receptors (53). Such patients did not have a decreased number of insulin receptors (53), presumably due to the tighter metabolic control maintained in human studies

compared to the extreme hyperglycemia and hyperinsulinemia in experimental KKA^y mice.

In the present study, pioglitazone had no effect on the insulin-stimulated insulin receptor kinase autophosphorylation in KKA^y mice (fig. 8 and fig. 9). This differs slightly from reports by Kellerer, *et al.* and Maegawa, *et al.* in which troglitazone or pioglitazone treatment reversed the inhibition of the insulin receptor kinase in rat-1 fibroblasts pre-fed with high glucose (42,43). Pioglitazone was also shown to correct receptor phosphorylation defects in Wistar fatty rats (16) and high-fat-fed rats (44). In another study, however, pioglitazone increased insulin stimulation of PI3K activity without increasing receptor phosphorylation in 3T3-L1 cells overexpressing insulin receptors and in L6 myotubes (48).

The difference between these studies and ours could represent a difference in the systems studied, or possibly a difference in methodology. In the present study, whole cell lysates were examined, so that the receptor number and phosphorylation is indicative of the total amount of receptor β subunits. The other studies purified the insulin receptors using wheat germ agglutinin (WGA). WGA binds carbohydrate moieties present on both α and β subunits, although the α subunits are glycosylated to a greater extent than the β subunits (74). Such methods would purify and evaluate mostly whole receptors. My study examined only the

receptor β subunit population, which may include phosphorylated β subunits separated from α subunits during degradation of the receptor. This possibility exists because phosphotyrosines in the juxtamembrane domain (67,169,178,179), kinase domain (169,178,180), and C-terminus (66,169) have all been shown to be involved in receptor internalization. Such measures may reflect elevated baseline phosphorylation of the β subunit, thus diminishing the observed proportion of insulin-stimulated phosphorylation of the receptor.

IRS-1

Expression

The protein levels of IRS-1 were not significantly different between control and KKA^y mice in fat or liver (fig. 2), even though the IRS-1 mRNA levels were significantly lower in KKA^y mice as compared to control in both tissues (fig. 5). These findings differ slightly from previous findings by Saad, *et al.* in another animal model of NIDDM, ob/ob mice. The protein levels for IRS-1 in ob/ob mice were found to be significantly lower in liver tissue as compared to nondiabetic ob/+ controls, while IRS-1 expression was unaltered in muscle tissue (173). Unfortunately, fat tissue was not a part of that study.

Saad, *et al.* also investigated the expression of IRS-1 protein in the streptozotocin-treated rat model of IDDM. IRS-1 protein expression was unaltered in either liver or muscle tissue from streptozotocin-treated rats as compared to control (173). In our study, IRS-1 mRNA abundance was increased in fat and liver tissues of streptozotocin-treated diabetic animals as compared to nondiabetic controls (fig. 23 and fig. 24, respectively). However, IRS-1 protein was not concomitantly increased but was in fact somewhat decreased in fat of these streptozotocin-treated animals (fig. 23).

IRS-1 protein was not detectable in rat liver tissue due to the presence of a nonspecific band of approximately the same size as IRS-1. This nonspecific protein was very highly expressed in comparison to IRS-1, and the proximity of this protein to IRS-1 on SDS-PAGE gels was so close that its signal masked IRS-1 expression. Substantial evidence suggests that this band represents a nonspecific protein interaction. First, the band migrated slightly ahead of the positive control, which normally lined up with IRS-1. Secondly, IRS-1 is expressed at very low levels in all tissues studied, and the expression of this band was much too high to have been IRS-1. Third, there was a faint band that lined up with the positive control which was not quantifiable due to the high expression of the nonspecific band (data not shown). Therefore, it is difficult to

determine whether our data is in full agreement with the work of Saad, *et al.* (173), since fat was not a part of their study, nor did they measure RNA levels in either model.

IRS-1 expression has also been shown to be affected by insulin levels at the level of protein stability (181-183). IRS-1 is degraded in 3T3-L1 adipocytes pre-treated with high insulin concentrations (1 μ M) by an extra-lysosomal calcium-dependent protease into two fragments of 79 and 90 kDa (181,182). Based on these studies, it would seem logical that the hyperinsulinemia of KKA^y mice would have an effect on protein levels of IRS-1. In contrast, there were no observed differences between KKA^y and C57 IRS-1 levels in fat or liver (fig. 2). One possible explanation for the lack of an observed decrease in IRS-1 protein levels in hyperinsulinemic KKA^y mice is that the insulin levels of these animals (500 μ U/ml) only corresponds to an insulin concentration of 3 nM, which may not be high enough to elicit insulin-induced proteolysis of IRS-1. One dissimilarity between the present study and the prior studies (181,182) is that we failed to achieve statistically significant effects of insulin to lower IRS-1 protein levels in 3T3-L1 cells pre-fed overnight with 2 μ M insulin (fig. 17), although the mean values for IRS-1 protein in the insulin-treated cells tended to be lower than control cells.

Phosphorylation

As is shown in fig. 7 and fig. 10, the basal phosphorylation of IRS-1 is not elevated in KKA^y mice as compared to control C57 mice. This is different from the high basal phosphorylation of the insulin receptor in these animals (fig. 7 and fig. 8). However, like the insulin receptor, acute insulin treatment did not stimulate tyrosine phosphorylation of IRS-1 in adipocytes from KKA^y mice or KKA^y mice treated with pioglitazone. This was not surprising, since specific increases in insulin receptor tyrosine autophosphorylation are required for subsequent IRS-1 phosphorylation (67,94,184-186).

The hyperglycemic and hyperinsulinemic condition probably plays a role in the lack of IRS-1 phosphorylation in insulin-stimulated KKA^y adipocytes, since the 3T3-L1 cells pre-fed with high insulin and high glucose were likewise unresponsive (fig. 18). Another study likewise showed a decrease in the responsiveness of 3T3-L1 cells to insulin-stimulated phosphorylation of IRS-1 after a 24 hr incubation of the cells in 100 nM insulin (183). Insulin pre-treatment of the 3T3-L1 cells in both cases also led to an increase in the basal tyrosine phosphorylation of IRS-1 (fig. 18).

Pioglitazone treatment of KKA^y mice did not restore the insulin-stimulated tyrosine phosphorylation of IRS-1 (fig. 7 and fig. 10). As mentioned above, pioglitazone and

troglitazone have both been shown to increase receptor tyrosine kinase activity for autophosphorylation and phosphorylation of synthetic substrates (16,42-44), although there is one study by Zhang, *et al.* in which no effect of pioglitazone treatment was seen on insulin-stimulated phosphorylation of the insulin receptor or IRS-1 (48). The study by Zhang, *et al.* and another by Sizer, *et al.* (47), although done in nonphysiologic cell culture models, both suggested a more direct effect of pioglitazone on PI3K activity. Therefore, it is possible that the increased insulin sensitivity (20) and insulin-stimulated glucose transport (18) in KKA^y mice treated with pioglitazone may be due to a more direct effect of pioglitazone further downstream in the insulin-signaling pathway than IRS-1.

Significance of IRS-1 Function

It should be noted that expression of a nonfunctional IRS-1 molecule in transgenic IRS-1 knockout mice resulted in a decrease in both pre-and post-natal growth as well as insulin resistance (109,110). However, the viability of these animals homozygous for disrupted IRS-1 suggests that there are IRS-1-independent pathways in insulin signaling to both mitogenic and metabolic effects. In fact, in one of these studies, Araki, *et al.* found that another IRS-like molecule immunologically distinct from IRS-1 and slightly larger was discovered to be tyrosine-phosphorylated by

insulin stimulation (110). It is therefore likely that alterations observed in IRS-1 expression or phosphorylation, while they may contribute to insulin resistance or lack of insulin signaling to growth effects, may not be entirely disruptive to cellular processes due to the existence of alternate pathways of signaling from the insulin receptor (110).

On the other hand, IRS-1 is a multisite docking protein, binding to at least four different proteins on insulin stimulation of the insulin receptor and consequent tyrosine phosphorylation of IRS-1 (10,91,116-120). These four proteins, PI3K p85 α , GRB2, Nck, and Syp, are thought to branch insulin's signal to various cellular processes (10,91). Therefore, IRS-1 is probably a very important molecule in insulin signaling even though there are likely other substrates of the receptor as well. One such substrate, Shc, may actually be more important than IRS-1 in insulin signaling through GRB2 (105,116,141-143,145) and will be discussed in more detail below.

PI3K p85 α

Expression

The expression of PI3K p85 α was measured using a monoclonal antibody directed against the SH2 domains of p85 α . As seen in fig. 2, two major bands of approximately

the same size are recognized by this antibody in fat tissue. This may be due to cross-reactivity with another protein, p87 β , which has high homology to p85 α (128). While both proteins may associate with the p110 subunit (128), we have found that only the lower band (p85 α) associates with IRS-1 on insulin stimulation of isolated adipocytes (fig. 11). In addition, the lower band was aligned with the baculovirus-expressed p85 α positive control, while the upper band did not. Also, a recently available antibody specific for the SH3 domains of p85 α detected only the lower of the two bands in fat tissue (data not shown). For these reasons, the lower band observed in fat tissue was quantitated as p85 α .

PI3K p85 α protein levels in liver of diabetic KKA γ mice were not significantly different from the levels in liver tissue of nondiabetic control animals (fig. 2), and there was no effect of pioglitazone treatment. In contrast, p85 α protein levels were significantly decreased in epididymal fat tissue of KKA γ mice by 53% relative to the C57 p85 α levels (fig. 2). The correction of p85 α levels in KKA γ fat by pioglitazone treatment occurred in the absence of a concordant increase in p85 α mRNA, indicating that pioglitazone treatment may increase p85 α levels in adipose by augmenting p85 α translation or protein stability. Such findings support two conclusions. First, the expression of p85 α in KKA γ mice is regulated differently in fat than in liver tissue. Secondly, the action of pioglitazone on p85 α

expression appeared to be tissue-specific and post-transcriptional.

The decreased expression of p85 α in KKA γ fat does not seem to be caused by the diabetic condition. First, if the decreased expression was due to the high circulating insulin and glucose levels of the KKA γ mice, one would expect to see the same decreased expression in liver tissue as in the case of the insulin receptor; however, this difference could be explained by tissue-specific regulation. Secondly, the results from the 3T3-L1 cells indicated that high insulin and glucose actually caused a near-significant increase ($p=0.052$) in PI3K protein levels over the expression in control cells (fig. 19). Likewise, another group found a slight increase in PI3K protein levels with a 24 hr pretreatment of 3T3-L1 cells with high insulin alone (181).

Hyperglycemia in the absence of hyperinsulinemia showed a tissue-specific effect in the opposite direction from that observed in KKA γ mice. In epididymal fat from streptozotocin-treated insulin-deficient rats, there was no significant difference in p85 α protein or RNA levels relative to control (fig. 25). In liver tissue, PI3K p85 α protein levels were $68.9 \pm 12.7\%$ higher than control ($n=9$, $p=0.0006$). Once again, there was not a similar increase in p85 α mRNA (fig. 26). Although the tissue-specific increase cannot be explained, one possibility is that p85 α is regulated in a tissue-specific manner by the hyperglycemic

hypoinsulinemic condition itself. This is quite plausible owing to the differing glucose uptake properties of fat versus liver. Liver is more freely permeable to glucose due to the higher K_m of the GLUT2 glucose transporter compared to fat tissue, which expresses the low K_m GLUT4 (187). As a result, liver may be more susceptible to the effects of hyperglycemia than fat.

Insulin-Stimulated Association with IRS-1

There is considerable evidence to suggest that PI3K p85 α associates with IRS-1 on insulin stimulation (10,91,100-102,106,111-113,115,119,126,134-139). As shown in fig. 11, p85 α was found in anti-IRS-1 immunoprecipitates in the insulin-stimulated adipocytes from nondiabetic control animals, but very little was found in the non-stimulated control cells. However, the association of p85 α with IRS-1 was not stimulated by insulin in adipocytes isolated from KKA^y mice or KKA^y mice treated with pioglitazone (fig. 11, fig 12). This finding is consistent with the lack of insulin-stimulated tyrosine phosphorylation of the insulin receptor and IRS-1 in adipocytes from these groups (figs. 7, 8, and 10), since IRS-1 must be tyrosine-phosphorylated to associate with the SH2 domains of PI3K p85 α (100,101,112,113).

The failure of KKA^y adipocytes to show insulin-stimulated phosphorylation of IRS-1 and recruitment of p85 α

to IRS-1 complexes has implications regarding sensitivity of these cells to insulin. The association of p85 α to phosphorylated IRS-1 activates the catalytic activity of the p110 subunit of PI3K, an action related to insulin stimulation of GLUT4 glucose transporter recruitment to the plasma membrane and insulin-stimulated glucose uptake (95,96,98,99,102,111). In epididymal fat from KKA^y mice, the expression of GLUT4 was reported to be decreased relative to control C57 mice (18). In the present study, the expression of p85 α , the insulin-stimulated phosphorylation of the receptor and IRS-1, and the association of p85 α with IRS-1 were all found to be lower than normal. These combined alterations in adipose tissue likely contribute to the insulin resistance of these animals, since glucose uptake through GLUT4 is the primary mechanism by which insulin stimulates glucose transport into these cells (188). Other studies would suggest that a defect in recruitment of GLUT4 to the plasma membrane is more likely than a defect in expression of GLUT4 in NIDDM (187), although the present data and past results from this laboratory (18) suggest that both defects may exist in KKA^y mice.

One point that becomes apparent from the data in figs. 11 and 12 is that pioglitazone treatment did not increase the amount of p85 α in anti-IRS-1 immunoprecipitates of insulin-stimulated isolated adipocytes, even though

pioglitazone treatment corrected the levels of p85 α in the treated animals (fig. 2). This result may indicate that the correction of p85 α levels by pioglitazone treatment as shown in fig. 2 is unrelated to the correction of blood glucose levels by pioglitazone. However, Dailey, et al. found that insulin-stimulated isolated abdominal adipocytes from pioglitazone-treated KKA^y mice showed an increased amount of PI3K activity in anti-phosphotyrosine immunoprecipitates as compared to non-treated KKA^y adipocytes (189).

While these results seem contradictory to my findings, there are several possible explanations for this difference. First, Dailey et al. used anti-phosphotyrosine immunoprecipitates, which are not necessarily the same as anti-IRS-1 immunoprecipitates. While IRS-1 needs to be phosphorylated for the association with p85 α to occur, the anti-phosphotyrosine antibodies immunoprecipitate a plethora of tyrosine-phosphorylated proteins. It is possible, then, that an anti-phosphotyrosine immunoprecipitation could precipitate unidentified phosphotyrosine-containing proteins other than IRS-1, which may also associate with p85 α . The presence of an IRS-2 in IRS-1 knockout mice is an example of a possible alternate substrate for the receptor (110). There are several reports of p85 α association with the insulin receptor alone (190-192), although this is controversial (115). Also, there are reports documenting

insulin-stimulated tyrosine phosphorylation of p85 α (125,133).

Another difference is that Dailey *et al.* measured PI3K activity, while fig. 11 demonstrates the amount of p85 α protein in the IRS-1 immunoprecipitates. This difference may mean that the activity measurement is more sensitive than the measurement of the amount of protein in immunoprecipitates, or possibly that pioglitazone acted to increase the activity of the enzyme in the absence of an association with IRS-1.

Finally, the PI3K activity data generated by Dailey, *et al.* were obtained from abdominal rather than epididymal fat (189). The same study showed a higher responsiveness of abdominal fat to insulin and pioglitazone as compared to epididymal fat (189). Therefore, the effect of pioglitazone on insulin-stimulated PI3K association with IRS-1 may not be detectable in epididymal fat to the same extent as pioglitazone's effect on PI3K activity in abdominal fat.

One other study by Zhang, *et al.* showed results corresponding to the data shown in fig. 6, as well as the results of Dailey, *et al.* Pioglitazone-treated Chinese hamster ovary cells overexpressing the insulin receptor showed an increase in the insulin-stimulated PI3K activity in anti-phosphotyrosine immunoprecipitates as compared to such activity in untreated cells. At the same time, there was not an increase in the tyrosine phosphorylation of the

insulin receptor or IRS-1 (48). There was also an increase in the amount of PI3K p85 α protein in anti-phosphotyrosine immunoprecipitates in the pioglitazone-treated cells over the control cells (48). Therefore, although the present studies failed to detect an effect of pioglitazone treatment on PI3K association with IRS-1 (fig. 11 and fig. 12), pioglitazone may actually be acting at this level to increase insulin sensitivity and insulin-stimulated glucose uptake through GLUT4.

There is one additional report suggesting another possible mechanism of pioglitazone action. Sizer, *et al.* showed that pioglitazone treatment of 3T3-L1 cells prevented isoproterenol-induced inhibition of insulin-stimulated PI3K activity (47). Such results indicated that pioglitazone inhibited a cAMP-dependent negative control mechanism, since the drug also prevented the inhibition of PI3K activity by cell-penetrating analogs of cAMP (47). Therefore, it is possible that pioglitazone may act at points other than insulin receptor phosphorylation and association of IRS-1 with PI3K.

Proteins Elevated in KKA^y Mice

While the levels of the insulin receptor and p85 α were found to be decreased in KKA^y mice, the levels of GRB2, Nck, and Syp were found to be elevated, as is shown in fig. 2. Each of these proteins has been implicated in insulin

signaling to growth-related effects (116,141,148,155,157, 161), as opposed to PI3K, which appears to have primarily a metabolic role (95,96,99,102). The difference in the levels of these proteins as compared to control levels were all more pronounced in epididymal fat tissue than liver, although all three were found to be significantly higher in KKA^y liver than control. Pioglitazone had little or no effect on the expression of any of these proteins.

GRB2

Expression

As shown in fig. 3, the expression of GRB2 was more than 3 times higher in KKA^y fat than in the control animals, and pioglitazone treatment did not alter these levels. This increased expression may be partially due to the hyperinsulinemia and hyperglycemia of the animals because overnight incubation of 3T3-L1 cells with high insulin and high glucose caused a significant $35.7 \pm 8.1\%$ increase ($p < 0.05$, $n = 22$) in expression. Although the change in cultured cells was much smaller than the difference observed in the animal model, such findings may imply that there is an effect of these agents on the expression of this protein. It is possible that the overnight incubation in high glucose and high insulin is not long enough to replicate the chronic condition of the diabetic animals, or that there are other

factors involved *in vivo* that are absent in an *in vitro* model. Also, the streptozotocin-treated rats showed no alteration in the expression of GRB2 in either fat or liver (fig. 27 and fig. 28), suggesting that hyperglycemia alone is probably not a factor leading to increased GRB2 expression.

Association with IRS-1 or Shc

The association of GRB2 with IRS-1 was not measurable with the methodology used in the present study. The studies that have shown association of IRS-1 with GRB2 have been done in cell systems constructed to overexpress the insulin receptor, IRS-1, or GRB2 (91,105,116,120,148). The physical association of GRB2 with IRS-1 may not be as strong or as abundant as the association of IRS-1 with p85 α *in vivo*. Another possible explanation for our ability to detect p85 α but not GRB2 in the anti-IRS-1 immunoprecipitates is the time course used. The time point used for insulin stimulation of the isolated adipocytes (2 minutes) was chosen because it was the time point at which maximal insulin-stimulated phosphorylation of IRS-1 was achieved in control cells (data not shown). This time course also seemed appropriate for measuring p85 α association, since the association with IRS-1 was measurable in the stimulated control cells (fig. 11). The stimulation of glucose transport (18) appears to occur more rapidly than the

stimulation of growth-related effects (104,145) by insulin, and therefore a longer time point may be required for detection of GRB2 in anti-IRS-1 immunoprecipitates.

Another reason that GRB2 may not be detectable in anti-IRS-1 immunoprecipitates in this study is that GRB2 is found to associate with another protein, Shc, to a much greater extent than with IRS-1 (142). Future studies should be directed at measuring the regulation of Shc and its association with GRB2 in this model, since the higher expression of GRB2 in KKA^y mouse fat was the largest difference compared to C57 control mice observed in this study.

Possible Downstream Effects of Increased GRB2 Expression

The elevated expression of GRB2 in KKA^y mice has several possible implications in cell signaling, presuming that higher levels of this protein increased insulin signaling through this pathway. One possible explanation for the increased GRB2 expression in these animals is that this elevated expression is a compensatory mechanism brought about by the diabetic condition. First, evidence exists for the association of dynamin with GRB2, and the subsequent activation of the GTPase activity of dynamin by insulin stimulation (140,154). Dynamin function may be involved in the pinching off of coated vesicles from the plasma membrane for endocytosis, and it could thus be involved in receptor

internalization (154). If the high insulin levels in KKA^y mice do indeed cause an increase in insulin receptor internalization and degradation, then more GRB2 may be needed to meet the increased demands for receptor internalization in these animals. This theory is consistent with the findings in 3T3-L1 adipocytes where high insulin and high glucose caused an increase in GRB2 expression (fig. 20). It is also consistent with the absence of a difference in GRB2 levels between control and streptozotocin-treated rats, since the insulin levels in streptozotocin-treated rats are lowered (fig.27 and fig. 28). One might even expect a decrease in the expression of GRB2 in IDDM if this were actually the case, unless a basal level is maintained even in the absence of high insulin levels.

Another mechanism by which an increased GRB2 expression may compensate for the diabetic condition involves the expression of glucose transporters. Adipose tissue contains both GLUT1 and GLUT4 glucose transporters, although GLUT4 is the predominant species (21,187,188). GLUT1 is present in many tissues, and is believed to be responsible for basal glucose uptake (21,188), while GLUT4 is known to be the transporter responsible for the majority of insulin-stimulated glucose uptake in fat and muscle tissue (21,95,187,188). In prior studies, the expression of GLUT4 was shown to be significantly lower in epididymal fat from KKA^y mice as compared to control C57 mice, and KKA^y mice were

also nearly unresponsive to insulin stimulation of glucose uptake (18). Therefore, the lower levels of GLUT4 and PI3K p85 α (fig. 1) in adipose tissue could contribute to the insulin resistance of KKA y mice, since both have been implicated in insulin-stimulated glucose uptake (21,95,99, 102,187,188). In contrast to this insulin-stimulated pathway, the levels of GRB2 (fig. 2) and GLUT1 (Bonini, Dailey, Colca, White, and Hofmann, submitted for publication, September 1994) in adipose tissue from this model of insulin resistance were much higher than control levels. GRB2 binding to phosphorylated IRS-1 or Shc causes it to bind to and activate the guanine nucleotide exchange factor Sos, leading to activation of ras (116,141,144,148). Activated ras binds to and activates raf-1, which then phosphorylates MAP kinase kinase. Overexpression of constitutively active forms of either ras or raf-1 in 3T3-L1 adipocytes has been shown to increase the expression and activity of GLUT1, resulting in increased basal glucose uptake (149-151). Such findings were consistent with the concordantly higher expression of GRB2 and GLUT1 in KKA y mice, as well as the higher basal glucose uptake measured in adipocytes from these animals compared to those from nondiabetic controls (18).

Further evidence for a role of GLUT1 upregulation as a compensatory response comes from studies in which 3T3-L1 adipocytes were deprived of glucose for 24 hr. This

resulted in an increase in GLUT1 expression and a decrease in GLUT4 (193,194). During glucose deprivation, GLUT1 was found primarily in the plasma membrane, and the increase in GLUT1 was attributed to an increase in the rate of synthesis and stability of the protein. One potential role for GLUT1 is to act as a stress response protein, and it is thought that the upregulation of GLUT1 in this condition was a compensatory response to meet the glucose requirement of the cells (188,194,195). In the case of the KKA^y mice, it is thus possible that the elevated levels of GRB2 and GLUT1 are a compensatory response to the insulin resistance and the lower levels of IR, PI3K p85 α , and GLUT4 in these animals. Although pioglitazone treatment did not significantly alter the levels of GRB2 in KKA^y epididymal fat, it increased IR, p85 α , and GLUT4 expression toward control levels, while GLUT1 protein levels were decreased to control levels by pioglitazone treatment.

Finally, GRB2 signaling has also been related to the growth and mitogenic effects of insulin (105,142,146). An increase in GRB2 may therefore route more of insulin's signal in this direction, since GRB2 was found to be rate-limiting in insulin signal transduction to AP-1 and fos when IRS-1 was overexpressed in CHO cells (142). Therefore, a disruption of the proper stoichiometries in insulin signaling could alter the expression of other genes as well (142).

Nck

Expression

The expression of Nck, like GRB2, was higher in KKA^y mice as compared to control mice (fig. 3), although this difference was not as large as that of GRB2. The higher expression was much more pronounced in adipose than in liver tissue. Also similar to the expression of GRB2 was the effect of high glucose and high insulin in raising the levels of Nck protein (fig. 20). This observation may indicate that these factors contribute to the higher expression of Nck protein in KKA^y mice. Interestingly, Nck protein levels were decreased significantly by $29.1 \pm 6.5\%$ ($p=0.0123$, $n=9$) in streptozotocin-treated rat liver, but not in fat tissue (fig. 27 and fig. 28). This result would suggest that insulin may somehow regulate Nck expression, or that other factors associated with hyperinsulinemia serve to upregulate this protein in KKA^y mouse liver as compared to control animals.

Because the nature of this protein is not entirely known, it is difficult to speculate on the possible downstream effects of Nck overexpression in KKA^y mice. Nck has been shown to be a transforming oncogene when overexpressed (157,196), and it may have a serine/threonine kinase activity (156). There is no data indicating that KKA^y mice have an increased incidence of tumor formation;

however, there is some evidence suggesting that serine phosphorylation of IRS-1 inhibits its insulin-stimulated tyrosine phosphorylation (197), although there is no evidence indicating that IRS-1 is a substrate for Nck. It remains possible that Nck could act as a negative regulator of insulin-stimulated phosphorylation of IRS-1.

Association with IRS-1

As in the experiments with GRB2, Nck was not found in IRS-1 immunoprecipitates at the time point used for the detection of p85 α .

Syp

Expression

The protein levels of Syp were also increased in insulin-resistant KKA^y fat and liver as compared to nondiabetic control tissues (fig. 3). Unlike GRB2 and Nck, Syp expression was not significantly altered in 3T3-L1 adipocytes pre-fed with high insulin and high glucose (fig. 20). As demonstrated with GRB2 and Nck, however, the changes in expression observed with high insulin and high glucose treatment of 3T3-L1 cells were not as great as those seen in the animals, but it is possible that a longer incubation in this medium might result in an increase similar to that seen in the KKA^y mice.

By contrast, Syp expression was significantly decreased in the insulin-deficient streptozotocin-treated diabetic rats as compared to the control rats in both tissues studied. This result suggests that under some conditions insulin levels may regulate the expression of Syp. This conclusion would be consistent with a catalytic role of Syp as a protein tyrosine phosphatase with the insulin receptor as a potential substrate (159). The increased basal phosphorylation of the insulin receptor in KKA^y mice may require a higher level of tyrosine phosphatases to dephosphorylate the β subunit, which is required for receptor recycling (198). In the hypoinsulinemic state of IDDM, the receptor is not phosphorylated and the demand for Syp to dephosphorylate it would be decreased.

In addition to a potential role for facilitating receptor recycling, other actions for Syp have also been suggested. First, Syp has been shown to be a positive mediator of insulin signaling to mitogenesis (161). In rat-1 fibroblasts stably expressing the insulin receptor, insulin-stimulated DNA synthesis was inhibited by microinjection of anti-Syp antibodies, phosphonopeptides containing the IRS-1 phosphotyrosine binding sites for Syp SH2 domains, or Syp SH2-GST fusion proteins by 60-90%, 50-60%, and 90%, respectively (161). Secondly, the insulin receptor reportedly phosphorylated Syp in its SH2 domains, thus inactivating it (159). This suggests that in a

condition where the insulin receptor is activated, Syp would be inactivated. Therefore, the high basal phosphorylation of the insulin receptor in KKA^y mice could be altering Syp function.

Association with IRS-1

As in the case of GRB2 and Nck, Syp was not detectable in IRS-1 immunoprecipitates from the isolated adipocytes at the time point studied. As mentioned above, the association of all three of these proteins with IRS-1 had been discovered using systems where one or more of the components (the receptor, IRS-1, GRB2, Nck, or Syp) were overexpressed, or using systems with peptide sequences corresponding to pYXXX sequences of IRS-1 or SH2 domains of the other proteins. Most, if not all of the work done concerning these factors has been done in such systems. Therefore, although these associations are most likely real, they may not be measurable when present at normal physiologic levels in the *in vivo* system used in this study.

To complicate the matter, the immunoprecipitation methodology results in including the immunoprecipitating antibody in the final pellet. When this pellet is disrupted by adding Laemmli buffer and boiling, the IgG heavy and light chains of the immunoprecipitating antibody become part of the sample to be run on the gel. The IgG heavy chain migrates as 50 kDa (fig. 11), while the IgG light chain

migrates as 25 kDa (data not shown). Both chains cross-react with the anti-mouse secondary antibody used for the detection of the co-precipitating proteins. Nck and GRB2 migrate as 44.2 and 25.7 kDa, respectively, and thus their signals may be obscured by this cross reactivity of the heavy and light IgG chains of the immunoprecipitating antibody with the secondary immunoblotting antibody.

Significance of Alterations in Signaling Components

Alterations as Contributing Factors to the Development of NIDDM

Because the pathophysiology of KKA^y mice closely resembles the symptoms of NIDDM in humans, several of the alterations observed in KKA^y mice may contribute to the onset of NIDDM. While the lower insulin receptor levels in KKA^y mice are most likely secondary to the hyperinsulinemia of these animals, this certainly would contribute to insulin resistance. Insulin resistance of peripheral tissues would result in elevated blood glucose levels, thus leading to further increased insulin release. High circulating insulin would in turn decrease the number of receptors by internalization and degradation. Such a decrease in receptor number would thus exacerbate the diabetic condition.

The receptor kinase defect measured in KKA^y epididymal adipocytes would similarly contribute to the development of diabetes. Increased glucose and insulin levels inhibit the insulin receptor kinase (42,43,177,199-201). Accordingly, diminished receptor kinase activity would contribute to insulin resistance, thus leading to further elevation of blood glucose and circulating insulin levels (1).

Likewise, the inability of insulin to acutely stimulate phosphorylation of IRS-1 and the subsequent association with and activation of PI3K in these receptor-defective cells would also decrease the sensitivity of the cells to insulin due to the connection between PI3K activity and GLUT4 translocation and activation (95,96,99,102). The decreased amounts of PI3K p85 α (fig. 2) and GLUT4 (18) in KKA^y mice would also exacerbate this condition. The lowered expression of p85 α in KKA^y mouse fat did not appear to be due to the diabetic condition, and may thus be a contributing factor to the initial resistance of adipose tissue to insulin.

The increased expression of the other three proteins could all potentially play a role in contributing to the insulin resistant condition, especially if proper stoichiometries of signaling components are required for proper signaling (142). In the case of KKA^y mice, where the stoichiometry of these early signaling components is much different than in the normal C57 mice, proper signaling

could be disrupted. This could result in routing the signals that enter the cell in inappropriate directions.

Alterations as Compensation for Insulin Resistance

The higher expression of GRB2 in adipose tissue of KKA^y mice over control levels was the most dramatic change seen in this study. As an early insulin signaling component upstream of ras and MAP kinase, GRB2 has been implicated in regulation of cell growth (105,142), mitogenesis (105,142), gene expression (142), protein synthesis (44,116,144,202), and glucose transport (116,144,149,151). Therefore, an alteration at this upstream level could have a profound effect on many cellular processes. As discussed above, it is possible that GRB2 overexpression is a cellular compensation for the insulin resistance of the cells in two respects. First, GRB2 overexpression could lead to activation of ras, which could then result in increased GLUT1 expression and activation (149,151). This could bring glucose into the insulin resistant cells without GLUT4 recruitment, thus accommodating the elevated blood glucose levels. Secondly, the association of GRB2 with dynamin and the role dynamin may play in receptor-mediated endocytosis suggests that increased GRB2 expression could be an attempt by the cell to turn off the insulin signal by increasing endocytosis. Alternatively, GRB2 may be upregulated as a response to the increased demand for internalization. It

would be interesting to measure the levels of GRB2 and dynamin in tissues of diabetic patients.

Pioglitazone as an Antihyperglycemic Agent

Pioglitazone treatment had very little effect on the proteins studied, with the exception of raising the levels of p85 α in KKA^y fat to control levels and partially correcting the receptor number. Each of these corrections were lessened in importance by studying the function of these proteins. The insulin receptor tyrosine kinase was not significantly corrected, nor was the association of p85 α with IRS-1. Therefore, it seems likely that pioglitazone elicits its effects at points other than these early signaling components. However, there is evidence to suggest that it may act on PI3K directly (47,48), in which case a correction of p85 α protein by pioglitazone may still be functionally significant. The inability to measure many effects of pioglitazone at this level does not decrease its clinical importance in any way, since the fact still remains that pioglitazone is a potent antihyperglycemic agent which also acts to lower blood insulin levels, triglycerides, and hepatic glucose production (20). The exact mechanism of pioglitazone action remains to be elucidated. However, as mentioned in the above discussion, there are reports of thiazolidinediones affecting receptor tyrosine kinase activity (16,42-44), mRNA stability (40), PI3K activity

(47,48), and expression of genes encoding GLUT4, (18,41,203), lipoprotein lipase (203), glucose-6-phosphate dehydrogenase (203), GLUT1 (19,41,203), adipsin (41), ap2 (41), and phosphoenolpyruvate carboxykinase (19). It is quite possible that one or more of these effects could bring about some of the others.

The clinical trials of another compound of this class, troglitazone, have been very favorable. Troglitazone increased insulin sensitivity and glucose tolerance in obese patients with either normal or impaired glucose tolerance prior to the study (46). Therefore, this class of insulin sensitizers, the thiazolidinediones, could be used to treat type II diabetes in the future (46).

Caveats of this Study

As in any study of this kind, it is important to remember that an animal model of diabetes is not exactly the same as the actual disease in humans. Therefore, although KKA^y mice display quite a few of the same symptoms as type II diabetics (36,37), they are not diabetic humans. Also, NIDDM is most likely a polygenic disorder with different defects in different populations of affected individuals, so one model would not suffice to demonstrate the actions of a drug or the sites of defects. In addition, due to the nature of the breeding required to produce KKA^y mice, that is, the crossing of an obese mouse with a glucose-intolerant

one, there is no genetically related normal control with which to compare them. C57Bl/6J mice were used as control mice because they have blood insulin and glucose levels analogous to normal humans, and they respond well to insulin (18,37). However, these are two different strains of mice, so even though insulin signaling components may be altered in their expression in KKA^y mice relative to C57 mice, they may not necessarily be involved in the onset of the diabetic condition.

The other two models used have their own limitations as well. While 3T3-L1 adipocytes pre-fed with high insulin and high glucose may help to isolate the effects of these factors on fat cells, this model is limited in that the other factors involved in type II diabetes such as high triglyceride levels (20,36,37) or TNF α (204) are not present. Streptozotocin-induced IDDM is also not a perfect model due to the possible effects of streptozotocin on other cell types expressing GLUT2. If this compound were indeed cytotoxic to liver or kidney cells (205), then streptozotocin treatment could result in alterations in the physiology of the animals which may not occur in IDDM.

Lastly, although this study has identified alterations in the expression of some early signaling components in this model of insulin resistant diabetes, many of these alterations were found to be associated with the diabetic condition itself. It is quite possible that the alterations

observed in this study are a result of one or more other defects in downstream signaling or glucose metabolism. Such defects could cause insulin resistance, resulting in hyperglycemia and hyperinsulinemia, which may in turn alter the expression or function of the insulin receptor, IRS-1, PI3K, GRB2, Nck, or Syp. Therefore, although the above results help to increase our understanding of type II diabetes and insulin resistance, they must be interpreted with the understanding that these are just pieces of a much larger puzzle.

Summary and Conclusions

The purpose of this study was to determine if the expression or function of early insulin signaling components were altered in an animal model of NIDDM compared to nondiabetic animals, and also to determine if the antidiabetic agent pioglitazone corrected or compensated for any of these defects. The results of this study show that the expression of the insulin receptor, PI3K p85 α , GRB2, Nck, and Syp was indeed altered in obese diabetic KKA^y mice compared to control nondiabetic C57Bl/6J mice. In addition, the tyrosine kinase activity of the insulin receptor was found to be defective in insulin-stimulated autophosphorylation of the receptor β -subunit and phosphorylation of IRS-1 in adipocytes isolated from KKA^y mice compared to control adipocytes. As a consequence, PI3K

p85 α association with IRS-1 following acute insulin stimulation was also impaired in KKA γ adipocytes. While the altered expression of the insulin receptor, GRB2, and Nck was most likely due to the hyperglycemic and hyperinsulinemic condition of KKA γ compared to nondiabetic mice, the lower levels of p85 α in fat tissue of KKA γ mice may not have been due to the high glucose and high insulin levels in these animals. Therefore, the lower expression of PI3K p85 α in KKA γ fat may contribute to the onset of diabetes in this model, while altered expression of the insulin receptor, GRB2, Nck, and Syp may have resulted from the diabetic condition. Pioglitazone treatment of KKA γ mice had limited effects on the signaling components studied, although administration of the drug fully corrected the altered p85 α levels in KKA γ fat to control levels. However, the amount of p85 α associated with IRS-1 in acutely-stimulated adipocytes isolated from pioglitazone-treated KKA γ mice was not increased over that observed in adipocytes from untreated KKA γ mice.

The observed alterations in insulin signaling are likely to be a result of the insulin resistant condition as well as contributing factors to the development of overt NIDDM. Because there are many different pathways involved in insulin signaling, insulin-sensitive cells in pre-diabetic animals may upregulate certain factors to compensate for a defect elsewhere in signaling or

metabolism, and this may explain the increased GRB2, Nck, and Syp expression in cells with decreased insulin receptors or PI3K p85 α . Such compensatory measures may delay the onset of severe NIDDM until the altered stoichiometry of signaling molecules can no longer make up for the deficit or until the stoichiometry is altered in such a way as to inhibit appropriate signaling. While further work is needed to determine if such compensatory mechanisms exist, this study has identified several alterations associated with insulin resistant diabetes in this animal model of NIDDM. Hopefully, these results will contribute to our understanding of diabetes mellitus and the development of a more efficient treatment for such a prevalent disease.

REFERENCES

1. Kahn, C. R. 1994. Insulin action, diabetogenes, and the cause of type II diabetes. *Diabetes* 43:1066-1084.
2. Unger, R.H. and Foster, D.W. Diabetes Mellitus. In: *Williams Textbook of Endocrinology*, edited by Wilson, J.D. and Foster, D.W. Philadelphia, PA: W.B. Saunders Company, 1981, p. 1018-1080.
3. DeFronzo, R. A., R. C. Bonadonna and E. Ferrannini. 1992. Pathogenesis of NIDDM. *Diabetes Care* 15:318-368.
4. Moller, D. E. and J. S. Flier. 1991. Insulin resistance - mechanisms, syndromes, and implications. *N. Engl. J. Med.* 325:938-948.
5. Taylor, R. 1989. Aetiology of non-insulin dependent diabetes. *Br. Med. Bull.* 45:73-91.
6. Taylor, S. I., D. Accili and Y. Imai. 1994. Insulin resistance or insulin deficiency: Which is the primary cause of insulin resistance? *Diabetes* 43:735-740.
7. Roth, R. A., F. Liu and J. E. Chin. 1994. Biochemical mechanisms of insulin resistance. *Horm. Res.* 41:51-55.
8. Muller-Wieland, D., R. Streicher, G. Siemeister and W. Krone. 1993. Molecular biology of insulin resistance. *Exp. Clin. Endocrinol.* 101:17-29.
9. Felber, J. P., E. Haesler and E. Jequier. 1993. Metabolic origin of insulin resistance in obesity with and without type 2 (non-insulin-dependent) diabetes mellitus. *Diabetologia* 36:1221-1229.
10. White, M. F. and C. R. Kahn. 1994. The insulin signaling system. *J. Biol. Chem.* 269:1-4.
11. Gerich, J. E. 1989. Oral hypoglycemic agents. *N. Engl. J. Med.* 321:1231-1245.
12. Taylor, S. I., T. Kadowaki, H. Kadowaki, D. Accili, A. Cama and C. McKeon. 1990. Mutations in the insulin

receptor gene in insulin-resistant patients. *Diabetes Care* 13:257-279.

13. Sugiyama, Y., S. Taketomi, Y. Shimura, H. Ikeda and T. Fujita. 1990. Effects of pioglitazone on glucose and lipid metabolism in wistar fatty rats. *Arzneim. -Forsch. /Drug Res.* 40:263-267.
14. Sugiyama, Y., Y. Shimura and H. Ikeda. 1990. Effects of pioglitazone on hepatic and peripheral insulin resistance in wistar fatty rats. *Arzneim. -Forsch. /Drug Res.* 40:436-440.
15. Ikeda, H., S. Taketomi, Y. Sugiyama, Y. Shimura, T. Sohda, K. Meguro and T. Fujita. 1990. Effects of pioglitazone on glucose and lipid metabolism in normal and insulin resistant animals. *Arzneim. -Forsch. /Drug Res.* 40:156-162.
16. Kobayashi, M., M. Iwanishi, K. Egawa and Y. Shigeta. 1992. Pioglitazone increases insulin sensitivity by activating insulin receptor kinase. *Diabetes* 41:476-483.
17. Hofmann, C. A. and J. R. Colca. 1992. New oral thiazolidinedione antidiabetic agents act as insulin sensitizers. *Diabetes Care* 15:1075-1078.
18. Hofmann, C., K. Lorenz and J. R. Colca. 1991. Glucose transport deficiency in diabetic animals is corrected by treatment with the oral anti-hyperglycemic agent pioglitazone. *Endocrinology* 129:1915-1925.
19. Hofmann, C. A., C. W. Edwards, R. M. Hillman and J. R. Colca. 1992. Treatment of insulin-resistant mice with the oral antidiabetic agent pioglitazone: Evaluation of liver glut 2 and phosphoenolpyruvate carboxykinase expression. *Endocrinology* 130:735-740.
20. Colca, J.R. and Morton, D.R. Antihyperglycaemic thiazolidinediones: ciglitazone and its analogues. In: *New Antidiabetic Drugs*, edited by Bailey, C.J. and Flatt, P.R. London: Smith-Gordon, 1990, p. 255-261.
21. James, D. E. and R. C. Piper. 1994. Insulin resistance, diabetes, and the insulin-regulated trafficking of GLUT-4. *J. Cell Biol.* 126:1123-1126.
22. Deschamps, I., J. P. Beressi, I. Khalil, J. J. Robert and J. Hors. 1991. The role of genetic predisposition to type I (insulin dependent) diabetes mellitus. *Ann. Med.* 23:427-435.

23. Sumbureru, D. 1991. Insulin dependent diabetes mellitus: An etiologic model. *Medical Hypotheses* 35:363-368.
24. Kostraba, J. N. 1994. What can epidemiology tell us about the role of infant diet in the etiology of IDDM? *Diabetes Care* 17:87-91.
25. Bottazzo, G. F., S. Genovese, E. Bosi, B. M. Dean, M. R. Christie and E. Bonifacio. 1991. Novel considerations on the antibody/autoantigen system in type I (insulin-dependent) diabetes mellitus. *Ann. Med.* 23:453-461.
26. Michelson, B. K., J. S. Petersen, E. Boel, A. Moldrup, T. Dyrberg and O. D. Madsen. 1991. Cloning, characterization, and autoimmune recognition of rat islet glutamic acid decarboxylase in insulin-dependent diabetes mellitus. *Biochemistry* 88:8754-8758.
27. Kawasaki, E., R. Moriuchi, M. Watanabe, K. Saitoh, F. C. Brunicardi, P. C. Watt, T. Yamaguchi, Y. Mullen, S. Akazawa, T. Miyamoto and S. Nagataki. 1993. Cloning and expression of large isoform of glutamic acid decarboxylase from human pancreatic islet. *Biochem. Biophys. Res. Commun.* 192:1353-1359.
28. Drash, A. L., R. B. Lipton, J. S. Dorman, D. J. Becker, R. E. LaPorte, T. J. Orchard, W. J. Riley, M. Trucco and L. H. Kuller. 1991. The interface between epidemiology and molecular biology in the search for the causes of insulin dependent diabetes mellitus. *Ann. Med.* 23:463-471.
29. Yoon, J. -W. 1991. Role of viruses in the pathogenesis of IDDM. *Ann. Med.* 23:437-445.
30. Martin, J. M., B. Trink, D. Daneman, H. -M. Dosch and B. Robinson. 1991. Milk proteins in the etiology of insulin-dependent diabetes mellitus (IDDM). *Ann. Med.* 23:447-452.
31. Haring, H. U. 1991. The insulin receptor: Signaling mechanism and contribution to the pathogenesis of insulin resistance. *Diabetologia* 34:848-861.
32. Clauser, E., I. Leconte and C. Auzan. 1992. Molecular basis of insulin resistance. *Horm. Res.* 38:5-12.
33. Vague, P. and D. Raccah. 1992. The syndrome of insulin resistance. *Horm. Res.* 38:28-32.

34. Scheen, A. J. and P. J. Lefebvre. 1992. Assessment of insulin resistance in vivo: Application to the study of type II diabetes. *Horm. Res.* 38:19-27.
35. Warram, J. H., B. C. Martin, A. S. Krolewski, J. S. Soeldner and C. R. Kahn. 1990. Slow glucose removal rate and hyperinsulinemia precede the development of type II diabetes in the offspring of diabetic parents. *Ann. Intern. Med.* 113:909-915.
36. Iwatsuka, H., A. Shino and Z. Suzuoki. 1970. General survey of diabetic features of yellow KK mice. *endocrinol. japon.* 17:23-35.
37. Chang, A.Y., Wyse, B.M., Copeland, E.J., Peterson, T. and Ledbetter, S.R. The Upjohn colony of KKAY mice: A model for obese type II diabetes. In: *Diabetes 1985*, edited by Serrano-Rios, M. and Lefebvre, P.J. New York: Elsevier Science Publishers B.V., 1986, p. 466-470.
38. Stevenson, R. W., R. K. McPherson, P. E. Genereaux, B. H. Danbury and D. K. Kreutter. 1991. Antidiabetic agent englitazone enhances insulin action in nondiabetic rats without producing hypoglycemia. *Metabolism* 40:1268-1274.
39. Weinstein, S. P., A. Holand, E. O'Boyle and R. S. Haber. 1993. Effects of thiazolidinediones on glucocorticoid-induced insulin resistance and glut4 glucose transporter expression in rat skeletal muscle. *Metabolism* 42:1365-1369.
40. Sandouk, T., D. Reda and C. Hofmann. 1993. The antidiabetic agent pioglitazone increases expression of glucose transporters in 3T3-F442A cells by increasing messenger ribonucleic acid transcript stability. *Endocrinology* 133:352-359.
41. Sandouk, T., D. Reda and C. Hofmann. 1993. Antidiabetic agent pioglitazone enhances adipocyte differentiation of 3T3-F442A cells. *Am. J. Physiol.* 264:C1600-C1608.
42. Kellerer, M., G. Kroder, S. Tippmer, L. Berti, R. Kiehn, L. Mosthaf and H. Haring. 1994. Troglitazone prevents glucose-induced insulin resistance of insulin receptor in rat-1 fibroblasts. *Diabetes* 43:447-453.
43. Maegawa, H., R. Tachikawa-Ide, S. Ugi, M. Iwanishi, K. Egawa, R. Kikkawa, Y. Shigeta and A. Kashiwagi. 1993. Pioglitazone ameliorates high glucose induced desensitization of insulin receptor kinase in Rat 1

- fibroblasts in culture. *Biochem. Biophys. Res. Commun.* 197:1078-1082.
44. Iwanishi, M. and M. Kobayashi. 1993. Effect of pioglitazone on insulin receptors of skeletal muscles from high-fat-fed rats. *Metabolism* 42:1017-1021.
 45. Fujita, T., Y. Sugiyama, S. Taketomi, T. Shoda, Y. Kawamatsu, H. Iwatsuka and Z. Suzuki. 1983. Reduction of insulin resistance in obese and/or diabetic animals by 5-[4-(1-methyl-cyclohexylmethoxy)benzyl]-thiazolidine-2,4-dione (ADD-3878, U-63,287, ciglitazone) a new antidiabetic agent. *Diabetes* 32:804-810.
 46. Nolan, J. J., B. Ludvik, P. Beerdsen, M. Joyce and J. Olefsky. 1994. Improvement in glucose tolerance and insulin resistance in obese subjects treated with troglitazone. *N. Engl. J. Med.* 331:1188-1193.
 47. Sizer, K. M., C. L. Smith, C. S. Jacob, M. L. Swanson and J. E. Bleasdale. 1994. Pioglitazone promotes insulin-induced activation of phosphoinositide 3-kinase in 3T3-L1 adipocytes by inhibiting a negative control mechanism. *Mol. Cell. Endocrinol.* 102:119-129.
 48. Zhang, B., D. Szalkowski, E. Diaz, N. Hayes, R. Smith and J. Berger. 1994. Potentiation of insulin stimulation of phosphatidylinositol 3-kinase by thiazolidinedione-derived antidiabetic agents in chinese hamster ovary cells expressing human insulin receptors and L6 myotubes. *J. Biol. Chem.* 269:25735-25741.
 49. Wilden, P. A., K. Siddle, E. Haring, J. M. Backer, M. F. White and C. R. Kahn. 1992. The role of insulin receptor kinase domain autophosphorylation in receptor-mediated activities. *J. Biol. Chem.* 267:13719-13727.
 50. White, M. F., J. N. Livingston, J. M. Backer, V. Lauris, T. Dull, A. Ullrich and C. R. Kahn. 1988. Mutation of the insulin receptor at tyrosine 960 inhibits signal transduction but does not effect its tyrosine kinase activity. *Cell* 54:641-649.
 51. White, M. F. and C. R. Kahn. 1989. Cascade of autophosphorylation in the B subunit of the insulin receptor. *J. Cell. Biochem.* 39:429-441.
 52. Kapeller, R., K. S. Chen, M. Yoakim, B. S. Schaffhausen, J. Backer, M. F. White, L. C. Cantley and N. B.

- Ruderman. 1991. Mutations in the juxtamembrane region of the insulin receptor impair activation of phosphatidylinositol 3-kinase by insulin. *Mol. Endocrinol.* 5:769-777.
53. Thies, R. S., J. M. Molina, T. P. Ciaraldi, G. R. Freidenberg and J. M. Olefsky. 1990. Insulin-receptor autophosphorylation and endogenous substrate phosphorylation in human adipocytes from control, obese, and NIDDM subjects. *Diabetes* 39:250-259.
54. Rosen, O. M. 1989. Structure and function of insulin receptors. *Diabetes* 38:1508-1511.
55. Okamoto, M., A. Karasik, M. F. White and C. R. Kahn. 1991. Coordinate phosphorylation of insulin-receptor kinase and its 175,000-Mr endogenous substrate in rat hepatocytes. *Diabetes* 40:66-72.
56. Olefsky, J. M. 1990. The insulin receptor - a multifunctional protein. *Diabetes* 39:1009-1016.
57. Mosthaf, L., B. Vogt, H. Haring and A. Ullrich. 1991. Altered expression of insulin receptor types A and B in the skeletal muscle of non-insulin dependent diabetes mellitus patients. *Proc. Natl. Acad. Sci. USA* 88:4728-4730.
58. Kellerer, M., R. Lammers, B. Ermel, S. Tippmer, B. Vogt, B. Obermaier-Kusser, A. Ullrich and H. Haring. 1992. Distinct α -subunit structures of human insulin receptor A and B variants determine differences in tyrosine kinase activities. *Biochemistry* 31:4588-4596.
59. Levy, J. R. and V. Hug. 1992. Regulation of insulin receptor gene expression: Cell cycle-mediated effects on insulin receptor mRNA stability. *J. Biol. Chem.* 267:25289-25295.
60. Chou, C. K., T. J. Dull, D. S. Russell, R. Gherzi, D. Lebowitz, A. Ullrich and O. R. Rosen. 1987. Human insulin receptors mutated at the ATP-binding site lack protein kinase activity and fail to mediate postreceptor effects of insulin. *J. Biol. Chem.* 262:1842-1847.
61. Goren, H. J., M. F. White and C. R. Kahn. 1987. Separate domains of the insulin receptor contain sites of autophosphorylation and tyrosine kinase activity. *Biochemistry* 26:2374-2381.

62. Baron, V., N. Gautier, P. Kaliman, J. Dolais-Kitabgi and E. Van Obberghen. 1991. The carboxyl-terminal domain of the insulin receptor: Its potential role in growth-promoting effects. *Biochemistry* 30:9365-9370.
63. Kaliman, P., V. Baron, F. Alengrin, Y. Takata, N. J. G. Webster, J. M. Olefsky and E. Van Obberghen. 1993. The insulin receptor C-terminus is involved in regulation of the receptor kinase activity. *Biochemistry* 32:9539-9544.
64. Pang, L., K. L. Milarski, M. Ohmichi, Y. Takata, J. M. Olefsky and A. R. Saltiel. 1994. Mutation of the two carboxyl-terminal tyrosines in the insulin receptor results in enhanced activation of mitogen-activated protein kinase. *J. Biol. Chem.* 269:10604-10608.
65. Yamamoto-Honda, R., T. Kadowaki, K. Momomura, K. Tobe, Y. Tamori, Y. Shibasaki, Y. Mori, Y. Kaburagi, O. Koshio, Y. Akanuma, Y. Yazaki and M. Kasuga. 1993. Normal insulin receptor substrate-1 phosphorylation in autophosphorylation-defective truncated insulin receptor. *J. Biol. Chem.* 268:16859-16865.
66. Smith, R. M., T. Sasaoka, N. Shah, Y. Takata, J. Kusari, J. M. Olefsky and L. Jarret. 1993. A truncated human insulin receptor missing the COOH-terminal 365 amino acid residues does not undergo insulin-mediated receptor migration or aggregation. *Endocrinology* 132:1453-1462.
67. Kaburagi, Y., K. Momomura, R. Yamamoto-Honda, K. Tobe, Y. Tamori, H. Sakura, Y. Akanuma, Y. Yazaki and T. Kadowaki. 1993. Site-directed mutagenesis of the juxtamembrane domain of the human insulin receptor. *J. Biol. Chem.* 268:16610-16622.
68. Longo, N., R. C. Shuster, L. D. Griffin, S. D. Langley and L. J. Elsas. 1992. Activation of insulin receptor signaling by a single amino acid substitution in the transmembrane domain. *J. Biol. Chem.* 267:12416-12419.
69. Kasuga, M., Y. Zick, D. L. Blithe, F. A. Karlsson, H. U. Haring and C. R. Kahn. 1982. Insulin stimulation of phosphorylation of the β subunit of the insulin receptor: formation of both phosphoserine and phosphotyrosine. *J. Biol. Chem.* 257:9891-9894.
70. Takayama, S., M. F. White and C. R. Kahn. 1988. Phorbol ester induced serine phosphorylation of the insulin receptor decreases its tyrosine kinase activity. *J. Biol. Chem.* 263:3440-3447.

71. Feener, E. P., J. M. Backer, G. L. King, P. A. Wilden, X. J. Sun, C. R. Kahn and M. F. White. 1993. Insulin stimulates serine and tyrosine phosphorylation in the juxtamembrane region of the insulin receptor. *J. Biol. Chem.* 268:11256-11264.
72. Ahn, J., O. M. Rosen and D. B. Donner. 1993. Human Insulin receptor mutated at threonine 1336 functions normally in Chinese hamster ovary cells. *J. Biol. Chem.* 268:16839-16844.
73. Liu, F. and R. A. Roth. 1994. Identification of serines-967/968 in the juxtamembrane region of the insulin receptor as insulin-stimulated phosphorylation sites. *Biochem. J.* 298:471-477.
74. Collier, E., J. Carpentier, L. Beitz, L. Caro, S. Taylor and P. Gorden. 1993. Specific glycosylation site mutations of the insulin receptor α subunit impair intracellular transport. *Biochemistry* 32:7818-7823.
75. Sesti, G., M. A. Marini, A. N. Tullio, A. Montemurro, P. Borboni, A. Fusco, D. Accili and R. Lauro. 1991. Altered expression of the two naturally occurring human insulin receptor variants in isolated adipocytes of non-insulin-dependent diabetes mellitus patients. *Biochem. Biophys. Res. Commun.* 181:1419-1424.
76. Kellerer, M., G. Sesti, E. Seffer, B. Obermaier-Kusser, D. E. Pongratz, L. Mosthaf and H. U. Haring. 1993. Altered pattern of insulin receptor isotypes in skeletal muscle membranes of type 2 (non-insulin-dependent) diabetic subjects. *Diabetologia* 36:628-632.
77. Mosthaf, L., J. Eriksson, H. U. Haring, L. Groop, E. Widen and A. Ullrich. 1993. Insulin receptor isotype expression correlates with risk of non-insulin-dependent diabetes. *Proc. Natl. Acad. Sci. USA* 90:2633-2635.
78. Benecke, H., J. S. Flier and D. E. Moller. 1992. Alternatively spliced variants of the insulin receptor protein: Expression in normal and diabetic human tissues. *J. Clin. Invest.* 89:2066-2070.
79. Anderson, C. M., R. R. Henry, P. E. Knudson, J. M. Olefsky and N. J. G. Webster. 1993. Relative expression of insulin receptor isoforms does not differ in lean, obese, and noninsulin-dependent diabetes mellitus subjects. *J. Clin. Endocrinol. Metab.* 76:1380-1382.

80. Norgren, S., J. Zierath, D. Galuska, H. Wallberg-Henriksson and H. Luthman. 1993. Differences in the ratio of RNA encoding two isoforms of the insulin receptor between control and NIDDM patients. *Diabetes* 42:675-681.
81. Norgren, S., J. Zierath, A. Wedell, H. Wallberg-Henriksson and H. Luthman. 1994. Regulation of human insulin receptor RNA splicing in vivo. *Proc. Natl. Acad. Sci. USA* 91:1465-1469.
82. Bell, G. I. 1991. Molecular defects in diabetes mellitus. *Diabetes* 40:413-422.
83. Krook, A., S. Kumar, I. Laing, A. J. M. Boulton, J. A. H. Wass and S. O'Rahilly. 1994. Molecular scanning of the insulin receptor gene in syndromes of insulin resistance. *Diabetes* 43:357-368.
84. Rice, K. M., G. E. Lienhard and C. W. Garner. 1992. Regulation of the expression of pp160, a putative insulin receptor signal protein, by insulin, dexamethasone, and 1-methyl-3-isobutylxanthine in 3T3-L1 adipocytes. *J. Biol. Chem.* 267:10163-10167.
85. Sun, X. J., P. Rothenberg, C. R. Kahn, J. M. Backer, E. Araki, P. A. Wilden, D. A. Cahill, B. J. Goldstein and M. F. White. 1991. Structure of the insulin receptor substrate IRS-1 defines a unique signal transduction protein. *Nature* 352:73-77.
86. White, M. F., E. W. Stegmann, T. J. Dull, A. Ullrich and C. R. Kahn. 1987. Characterization of an endogenous substrate of the insulin receptor in cultured cells. *J. Biol. Chem.* 262:9769-9777.
87. Kellerer, S. R., L. Lamphere, B. E. Lavan, M. R. Kuhne and G. E. Lienhard. 1993. Insulin and IGF-I signaling through the insulin receptor substrate 1. *Molecular Reproduction and Development* 35:346-352.
88. Araki, E., B. L. Haag, III. and C. R. Kahn. 1994. Cloning of the mouse insulin receptor substrate-1 (IRS-1) gene and complete sequence of mouse IRS-1. *Biochimica et Biophysica Acta* 1221:353-356.
89. Sun, X. J., M. Miralpeix, M. G. Myers, Jr., E. M. Glasheen, J. M. Backer, C. R. Kahn and M. F. White. 1992. Expression and function of IRS-1 in insulin signal transmission. *J. Biol. Chem.* 267:22662-22672.

90. Myers, M. G., Jr., X. J. Sun and M. F. White. 1994. The IRS-1 signaling system. *TIBS* July:289-293.
91. Sun, X. J., D. L. Crimmons, M. G. Myers, Jr., M. Miralpeix and M. F. White. 1993. Pleiotropic insulin signals are engaged by multisite phosphorylation of IRS-1. *Mol. Cell. Biol.* 13:7418-7428.
92. White, M. F., R. Maron and C. R. Kahn. 1985. Insulin rapidly stimulates tyrosine phosphorylation of a Mr-185,000 protein in intact cells. *Nature* 318:183-186.
93. Keller, S. R., K. Kitagawa, R. Aebersold, G. E. Lienhard and C. W. Garner. 1991. Isolation and characterization of the 160,000-Da phosphotyrosyl protein, a putative participant in insulin signaling. *J. Biol. Chem.* 266:12817-12820.
94. Backer, J. M., G. G. Schroeder, C. R. Kahn, M. G. Myers, Jr., P. A. Wilden, D. A. Cahill and M. F. White. 1992. Insulin stimulation of phosphatidylinositol 3-kinase activity maps to insulin receptor regions required for endogenous substrate phosphorylation. *J. Biol. Chem.* 267:1367-1374.
95. Clarke, J. F., P. W. Young, K. Yonezawa, M. Kasuga and G. D. Holman. 1994. Inhibition of the translocation of GLUT1 and GLUT4 in 3T3-L1 cells by the phosphatidylinositol 3-kinase inhibitor, wortmannin. *Biochem. J.* 300:631-635.
96. Shimizu, Y. and T. Shimazu. 1994. Effects of wortmannin on increased glucose transport by insulin and norepinephrine in primary culture of brown adipocytes. *Biochem. Biophys. Res. Commun.* 202:660-665.
97. Cheatham, B., C. J. Vlahos, L. Cheatham, L. Wang, J. Blenis and C. R. Kahn. 1994. Phosphatidylinositol 3-kinase activation is required for insulin stimulation of pp70 S6 Kinase, DNA synthesis and glucose transporter translocation. *Diabetes* 43:81A. (Abstract)
98. Rice, K. M. and C. W. Garner. 1994. Correlation of the insulin receptor substrate-1 with insulin responsive deoxyglucose transport in 3T3-L1 adipocytes. *Biochem. Biophys. Res. Commun.* 198:523-530.
99. Okada, T., Y. Kawano, T. Sakakibara, O. Hazeki and M. Ui. 1994. Essential role of phosphatidylinositol 3-kinase in insulin-induced glucose transport and antilipolysis in rat adipocytes. *J. Biol. Chem.* 269:3566-3573.

100. Backer, J. M., M. G. Myers, Jr., S. E. Shoelson, D. J. Chin, X. J. Sun, M. Miralpeix, P. Hu, B. Margolis, E. Y. Skolnik, J. Schlessinger and M. F. White. 1992. Phosphatidylinositol 3-kinase is activated by association with IRS-1 during insulin stimulation. *EMBO J.* 11:3469-3479.
101. Folli, F., M. J. A. Saad, J. Backer and C. R. Kahn. 1992. Insulin stimulation of phosphatidylinositol 3-kinase activity and association with insulin receptor substrate 1 in liver and muscle of the intact rat. *J. Biol. Chem.* 267:22171-22177.
102. Kanai, F., K. Ito, M. Todaka, H. Hayashi, S. Kamohara, K. Ishii, T. Okada, O. Hazeki, M. Ui and Y. Ebina. 1993. Insulin-Stimulated Glut4 Translocation is Relevant to the Phosphorylation of IRS-1 and the Activity of PI3-Kinase. *Biochem. Biophys. Res. Commun.* 195:762-768.
103. Wang, L. -M., M. G. Myers, Jr., X. J. Sun, S. A. Aaronson, M. White and J. H. Pierce. 1993. IRS-1: Essential for insulin- and IL-4-stimulated mitogenesis in hematopoietic cells. *Science* 261:1591-1593.
104. Rose, D. W., A. R. Saltiel, M. Majumdar, S. J. Decker and J. M. Olefsky. 1994. Insulin receptor substrate 1 is required for insulin-mediated mitogenic signal transduction. *Proc. Natl. Acad. Sci. USA* 91:797-801.
105. Myers, M. G., Jr., L. -M. Wang, X. J. Sun, Y. Zhang, L. Yenush, J. Schlessinger, J. H. Pierce and M. F. White. 1994. Role of IRS-1-GRB2 complexes in insulin signaling. *Mol. Cell. Biol.* 14:3577-3587.
106. Chuang, L. -M., M. G. Myers, Jr., J. M. Backer, S. E. Shoelson, M. F. White, M. J. Birnbaum and C. R. Kahn. 1993. Insulin-stimulated oocyte maturation requires insulin receptor substrate 1 and interaction with the SH2 domains of phosphatidylinositol 3-kinase. *Mol. Cell. Biol.* 13:6653-6660.
107. Rose, D. W., B. Jhun, S. Xiao, L. Cantley and S. Shoelson. 1994. phosphatidylinositol 3-kinase (PI3-K) is a required component of the insulin (I) mitogenic signaling pathway. *Diabetes* 43:82A. (Abstract)
108. Waters, S. B., K. Yamauchi and J. E. Pessin. 1993. Functional expression of insulin receptor substrate-1 is required for insulin-stimulated mitogenic signalling. *J. Biol. Chem.* 268:22231-22234.

109. Tamemoto, H., T. Kadowaki, K. Tobe, T. Yagi, H. Sakura, T. Hayakawa, Y. Terauchi, K. Ueki, Y. Kaburagi, S. Satoh, H. Sekihara, S. Yoshioka, H. Horikoshi, Y. Furuta, Y. Ikawa, M. Kasuga, Y. Yazaki and S. Alzawa. 1994. Insulin resistance and growth retardation in mice lacking insulin receptor substrate-1. *Nature* 372:182-186.
110. Araki, E., M. Lipes, M. -E. Patti, J. C. Bruning, B. Haag, III, R. S. Johnson and C. R. Kahn. 1994. Alternative pathway of insulin signalling in mice with targeted disruption of the IRS-1 gene. *Nature* 372:186-190.
111. Kelly, K. L. and N. B. Ruderman. 1993. Insulin-stimulated phosphatidylinositol 3-kinase: association with a 185-kDa tyrosine-phosphorylated protein (IRS-1) and localization in a low density membrane vesicle. *J. Biol. Chem.* 268:4391-4398.
112. Herbst, J. J., G. Andrews, L. Contillo, L. Lamphere, J. Gardner, G. E. Lienhard and E. M. Gibbs. 1994. Potent activation of phosphatidylinositol 3'-kinase by simple phosphotyrosine peptides derived from insulin receptor substrate 1 containing two YMXM motifs for binding SH2 domains. *Biochemistry* 33:9376-9381.
113. Lamphere, L., C. L. Carpenter, Z. -F. Sheng, R. G. Kallen and G. E. Lienhard. 1994. Activation of PI 3-kinase in 3T3-L1 adipocytes by association with insulin receptor substrate-1. *Am. J. Physiol.* 266:E486-E494.
114. Zhang, W., J. D. Johnson and W. J. Rutter. 1993. Association and phosphorylation-dependent dissociation of proteins in the insulin receptor complex. *Proc. Natl. Acad. Sci. USA* 90:11317-11321.
115. Liu, R. and J. N. Livingston. 1994. Association of the insulin receptor and phosphatidylinositol 3-kinase requires a third component. *Biochem. J.* 297:335-342.
116. Skolnik, E. Y., A. Batzer, N. Li, C. Lee, E. Lowenstein, M. Mohammadi, B. Margolis and J. Schlessinger. 1993. The function of GRB2 in linking the insulin receptor to ras signaling pathways. *Science* 260:1953-1955.
117. Kuhne, M. R., T. Pawson, G. E. Lienhard and G. Feng. 1993. The insulin receptor substrate 1 associates with the SH2-containing phosphotyrosine phosphatase Syp. *J. Biol. Chem.* 268:11479-11489.

118. Lee, C., W. Li, R. Nishimura, M. Zhou, A. G. Batzer, M. G. Myers, Jr., M. F. White, J. Schlessinger and E. Y. Skolnik. 1993. Nck associates with the SH2 domain-docking protein IRS-1 in insulin-stimulated cells. *Proc. Natl. Acad. Sci. USA* 90:11713-11717.
119. Myers, M. G., Jr., J. M. Backer, X. J. Sun, S. Shoelson, P. Hu, J. Schlessinger, M. Yoakim, B. Schaffhausen and M. F. White. 1992. IRS-1 activates phosphatidylinositol 3'-kinase by associating with src homology 2 domains of p85. *Proc. Natl. Acad. Sci. USA* 89:10350-10354.
120. Tobe, K., H. Matuoka, H. Tamemoto, K. Ueki, Y. Kaburagi, S. Asai, T. Noguchi, M. Matsuda, S. Tanaka, S. Hattori, Y. Fukui, Y. Akanuma, Y. Yazaki, T. Takenawa and T. Kadowaki. 1993. Insulin stimulates the association of insulin receptor substrate-1 with the protein abundant src homology/growth factor receptor-bound protein 2. *J. Biol. Chem.* 268:11167-11171.
121. Sugimoto, S., T. J. Wandless, S. E. Shoelson, B. G. Neel and C. T. Walsh. 1994. Activation of the SH2-containing protein tyrosine phosphatase, SH-PTP2, by phosphotyrosine-containing peptides derived from insulin receptor substrate-1. *J. Biol. Chem.* 269:13614-13622.
122. Almind, K., C. Bjorbaek, H. Vestergaard, T. Hansen, S. Echwald and O. Pedersen. 1993. Aminoacid polymorphisms of insulin receptor substrate-1 in non-insulin-dependent diabetes mellitus. *Lancet* 342:828-832.
123. Hager, J., H. Zouali, G. Velho and P. Froguel. 1993. Insulin receptor substrate (IRS-1) gene polymorphisms in French NIDDM families. *Lancet* 342:1430.
124. Shimokawa, K., H. Kadowaki, H. Sakura, S. Otabe, R. Hagura, K. Kosaka, Y. Yazaki, Y. Akanuma and T. Kadowaki. 1994. Molecular scanning of the glycogen synthase and insulin receptor substrate-1 genes in Japanese subjects with non-insulin dependent diabetes mellitus. *Biochem. Biophys. Res. Commun.* 202:463-469.
125. Hayashi, H., N. Miyake, F. Kanai, F. Shibasaki, T. Takenawa and Y. Ebina. 1991. Phosphorylation in vitro of the 85 kDa subunit of phosphatidylinositol 3-kinase and its possible activation by insulin receptor tyrosine kinase. *Biochem. J.* 280:769-775.

126. Ruderman, N. B., R. Kapeller, M. F. White and L. C. Cantley. 1990. Activation of phosphatidylinositol 3-kinase by insulin. *Proc. Natl. Acad. Sci. USA* 87:1411-1415.
127. Hiles, I. D., M. Otsu, S. Volinia, M. J. Fry, I. Gout, R. Dhand, G. Panayotou, F. Ruiz-Larrea, A. Thompson, N. F. Totty, J. J. Hsuan, S. A. Courtneidge, P. J. Parker and M. D. Waterfield. 1992. Phosphatidylinositol 3-kinase: Structure and expression of the 110 kd catalytic subunit. *Cell* 70:419-429.
128. Otsu, M., I. Hiles, I. Gout, M. J. Fry, F. Ruiz-Larrea, G. Panayotou, A. Thompson, R. Dhand, J. Hsuan, N. Totty, A. D. Smith, S. J. Morgan, S. A. Courtneidge, P. J. Parker and M. D. Waterfield. 1991. Characterization of two 85 kd proteins that associate with receptor tyrosine kinases, middle-T/pp60c-src complexes, and PI3-kinase. *Cell* 65:91-104.
129. Thomason, P. A., S. R. James, P. J. Casey and C. P. Downes. 1994. A G-protein $\beta\gamma$ -subunit-reponsive phosphoinositide 3-kinase activity in human platelet cytosol. *J. Biol. Chem.* 269:16525-16528.
130. Nakanishi, H., K. A. Brewer and J. H. Exton. 1993. Activation of the ζ isozyme of protein kinase C by phosphatidylinositol 3,4,5 - trisphosphate. *J. Biol. Chem.* 268:13-16.
131. Toker, A., M. Meyer, K. K. Reddy, J. R. Falck, R. Aneja, S. Aneja, A. Parra, D. J. Burns, L. M. Ballas and L. C. Cantley. 1994. Activation of protein kinase C family members by the novel polyphosphoinositides PtdIns-3,4-P2 and PtdIns-3,4,5-P3. *J. Biol. Chem.* 269:32358-32367.
132. Yonezawa, K., K. Yokono, K. Shii, W. Ogawa, A. Ando, K. Hara, S. Baba, Y. Kaburagi, R. Yamamoto-Honda, K. Momomura, T. Kadawaki and M. Kasuga. 1992. In vitro association of phosphatidylinositol 3-kinase activity with the activated insulin receptor tyrosine kinase. *J. Biol. Chem.* 267:440-446.
133. Hayashi, H., Y. Nishioka, S. Kamohara, F. Kanai, K. Ishii, Y. Fukui, F. Shibasaki, T. Takenawa, H. Kido, N. Katsunuma and Y. Ebina. 1993. The α -type 85-kDa subunit of phosphatidylinositol 3-kinase is phosphorylated at tyrosines 368, 580, and 607 by the insulin receptor. *J. Biol. Chem.* 268:7107-7117.

134. Backer, J. M., M. G. Myers, Jr., X. J. Sun, D. J. Chin, S. E. Shoelson, M. Miralpeix and M. F. White. 1993. Association of IRS-1 with the insulin receptor and the phosphatidylinositol 3'-kinase: Formation of binary and ternary complexes in intact cells. *J. Biol. Chem.* 268:8204-8212.
135. Yonezawa, K., H. Ueda, K. Hara, K. Nishida, A. Ando, A. Chavanieu, H. Matsuba, K. Shii, K. Yokono, Y. Fukui, B. Calas, F. Grigorescu, R. Dhand, I. Gout, M. Otsu, M. D. Waterfield and M. Kasuga. 1992. Insulin-dependent formation of a complex containing an 85-kDa subunit of phosphatidylinositol 3-kinase and tyrosine-phosphorylated insulin receptor substrate 1. *J. Biol. Chem.* 267:25958-25966.
136. Hadari, Y. R., E. Tzahar, O. Nadiv, P. Rothenberg, C. T. Roberts, D. LeRoith, Y. Yarden and Y. Zick. 1992. Insulin and insulinomimetic agents induce activation of phosphatidylinositol 3'-kinase upon its association with pp185 (IRS-1) in intact rat livers. *J. Biol. Chem.* 267:17483-17486.
137. Myers, M. G., Jr., X. J. Sun, B. Cheatham, B. R. Jachna, E. M. Glasheen, J. M. Backer and M. F. White. 1993. IRS-1 is a common element in insulin and insulin-like growth factor-I signalling to the phosphatidylinositol 3'-kinase. *Endocrinology* 132:1421-1430.
138. Giorgetti, S., R. Ballotti, A. Kowalski-Chauvel, M. Cormont and E. Van Obberghen. 1992. Insulin stimulates phosphatidylinositol-3-kinase activity in rat adipocytes. *Eur. J. Biochem.* 207:599-606.
139. Heydrick, S. J., D. Jullien, N. Gautier, J. Tanti, S. Giorgetti, E. Van Obberghen and Y. Le Marchand-Brustel. 1993. Defect in skeletal muscle phosphatidylinositol -3-kinase in obese insulin-resistant mice. *J. Clin. Invest.* 91:1358-1366.
140. Downward, J. 1994. The GRB2/Sem-5 adaptor protein. *FEBS. Lett.* 338:113-117.
141. Skolnik, E. Y., C. Lee, A. Batzer, L. M. Vicentini, M. Zhou, R. Daly, M. G. Myers, Jr., J. M. Backer, A. Ullrich, M. F. White and J. Schlessinger. 1993. The SH2/SH3 domain-containing protein GRB2 interacts with tyrosine-phosphorylated IRS1 and Shc: implications for insulin control of ras signalling. *EMBO J.* 12:1929-1936.

142. Yamauchi, K. and J. E. Pessin. 1994. Enhancement of insulin signaling by insulin receptor substrate 1 is cell context dependent. *Mol. Cell. Biol.* 14:4427-4434.
143. Kovacina, K. S. and R. A. Roth. 1993. Identification of SHC as a substrate of the insulin receptor kinase distinct from the GAP-associated 62 kDa tyrosine phosphoprotein. *Biochem. Biophys. Res. Commun.* 192:1303-1311.
144. Egan, S. E., B. W. Giddings, M. W. Brooks, L. Buday, A. M. Sizeland and R. A. Weinberg. 1993. Association of Sos Ras exchange protein with GRB2 is implicated in tyrosine kinase signal transduction and transformation. *Nature* 363:45-51.
145. Giorgetti, S., P. G. Pelicci, G. Pelicci and E. Van Obberghen. 1994. Involvement of Src-homology/collagen (SHC) proteins in signaling through the insulin receptor and the insulin-like-growth-factor-I-receptor. *Eur. J. Biochem.* 223:195-202.
146. Buday, L. and J. Downward. 1993. Epidermal growth factor regulates p21ras through the formation of a complex of receptor, GRB2 adapter protein, and Sos nucleotide exchange factor. *Cell* 73:611-620.
147. Howe, L. R., S. J. Leever, N. Gomez, S. Nakielny, P. Cohen and C. J. Marshall. 1992. Activation of the MAP kinase pathway by the protein kinase raf. *Cell* 71:335-342.
148. Lowenstein, E. J., R. J. Daly, A. G. Batzer, W. Li, B. Margolis, R. Lammers, A. Ullrich, E. Skolnik, D. Bar-Sagi and J. Schlessinger. 1992. The SH2 and SH3 domain-containing protein GRB2 links receptor tyrosine kinases to ras signaling. *Cell* 70:431-442.
149. Hausdorff, S. F., J. V. Frangioni and M. J. Birnbaum. 1994. Role of p21ras in insulin-stimulated glucose transport in 3T3-L1 adipocytes. *J. Biol. Chem.* 269:21391-21394.
150. Kozma, L., K. Baltensperger, J. Klarlund, A. Porras, E. Santos and M. P. Czech. 1993. The Ras signaling pathway mimics insulin action on glucose transporter translocation. *Proc. Natl. Acad. Sci. USA* 90:4460-4464.
151. Fingar, D. C. and M. J. Birnbaum. 1994. A role for Raf-1 in the divergent signaling pathways mediating insulin-stimulated glucose transport. *J. Biol. Chem.* 269:10127-10132.

152. Bar-Sagi, D., D. Rotin, A. Batzer, V. Mandiyan and J. Schlessinger. 1993. SH3 domains direct cellular localization of signaling molecules. *Cell* 74:83-91.
153. Lin, T. -A., X. Kong, T. A. J. Haystead, A. Pause, G. Belsham, N. Sonenberg and J. C. Lawrence, Jr.. 1994. PHAS-1 as a link between mitogen-activated protein kinase and translation initiation. *Science* 266:653-656.
154. Ando, A., K. Yonezawa, I. Gout, T. Nakata, H. Ueda, K. Hara, Y. Kitamura, Y. Noda, T. Takenawa, N. Hirokawa, M. D. Waterfield and M. Kasuga. 1994. A complex of GRB2-dynamin binds to tyrosine-phosphorylated insulin receptor substrate-1 after insulin treatment. *EMBO J.* 13:3033-3038.
155. Park, D. and S. G. Rhee. 1992. Phosphorylation of Nck in response to a variety of receptors, phorbol myristate Acetate, and cyclic AMP. *Mol. Cell. Biol.* 12:5816-5823.
156. Birge, R. B. and H. Hanafusa. 1993. Closing in on SH2 specificity. *Science* 262:1522-1524.
157. Li, W., P. Hu, E. Y. Skolnik, A. Ullrich and J. Schlessinger. 1992. The SH2 and SH3 domain-containing Nck protein is oncogenic and a common target for phosphorylation by different surface receptors. *Mol. Cell. Biol.* 12:5824-5833.
158. Ugi, S., H. Maegawa, J. M. Olefsky, Y. Shigeta and A. Kashiwagi. 1994. Src homology 2 domains of protein tyrosine phosphatase are associated in vitro with both the insulin receptor and insulin receptor substrate-1 via different phosphotyrosine motifs. *FEBS. Lett.* 340:216-220.
159. Maegawa, H., S. Ugi, M. Adachi, Y. Hinoda, R. Kikkawa, A. Yachi, Y. Shigeta and A. Kashiwagi. 1994. Insulin receptor kinase phosphorylates protein tyrosine phosphatase containing src homology 2 regions and modulates its PTPase activity in vitro. *Biochem. Biophys. Res. Commun.* 199:780-785.
160. Maegawa, H., S. Ugi, O. Ishibashi, R. Tachikawa-Ide, N. Takahara, Y. Tanaka, Y. Takagi, R. Kikkawa, Y. Shigeta and A. Kashiwagi. 1993. Src homology 2 domains of protein tyrosine phosphatase are phosphorylated by insulin receptor kinase and bind to the COOH-terminus of insulin receptors in vitro. *Biochem. Biophys. Res. Commun.* 194:208-214.

161. Xiao, S., D. W. Rose, T. Sasaoka, S. E. Shoelson and J. M. Olefsky. 1994. Syp is a positive mediator of mitogenic signaling and is necessary for insulin, IGF-1, and EGF stimulation of DNA synthesis. *Diabetes* 43:1A. (Abstract)
162. Zaharto, D. S. and L. V. Beck. 1968. Studies of a simplified plasma insulin immunoassay using cellulose powder. *Diabetes* 17:444-457.
163. Kosmakos, F. C. and J. Roth. 1980. Insulin-induced loss of the insulin receptor in IM-9 lymphocytes. *J. Biol. Chem.* 255:9860-9869.
164. Chomczynski, P. and N. Sacchi. 1987. Single-step method of RNA isolation by acid guanidinium thiocyanate-phenol-chloroform extraction. *Anal. Biochem.* 162:156-159.
165. Fourney, R. M., J. Miyashi, R. S. Day and M. C. Paterson. 1988. Northern blotting: Efficient RNA staining and transfer. *FOCUS* 10:5-7.
166. Bonini, J. and C. Hofmann. 1991. A rapid, accurate, nonradioactive method for quantitating RNA on agarose gels. *Biotech.* 11:708-709.
167. Lowry, O. H., N. J. Rosebrough, A. L. Farr and R. J. Randall. 1951. Protein measurement with the folin phenol reagent. *J. Biol. Chem.* 193:265-275.
168. Laemmli, U. K. 1970. Cleavage of structural proteins during the assembly of the head of bacteriophage T4. *Nature* 227:680-685.
169. Carpentier, J. -L. 1992. Insulin-induced and constitutive internalization of the insulin receptor. *Horm. Res.* 38:13-18.
170. Knutson, V. 1991. Proteolytic processing of the insulin receptor β subunit is associated with insulin-induced receptor down-regulation. *J. Biol. Chem.* 266:15656-15662.
171. Ludwig, S., D. Muller-Wieland, B. J. Goldstein and C. R. Kahn. 1988. The insulin receptor gene and its expression in insulin resistant mice. *Endocrinology* 123:594-600.
172. Tozzo, E. and B. Desbuquois. 1992. Effects of STZ-Induced Diabetes and Fasting on Insulin Receptor

mRNA Expression and Insulin Receptor Gene Transcription in Rat Liver. *Diabetes* 41:1609-1616.

173. Saad, M. J. A., E. Araki, M. Miralpeix, P. L. Rothenberg, M. F. White and C. R. Kahn. 1992. Regulation of insulin receptor substrate-1 in liver and muscle of animal models of insulin resistance. *J. Clin. Invest.* 90:1839-1849.
174. Blecher, M. and Bar, R.S. *Receptors and Human Disease*, Baltimore: Williams and Wilkins, 1981. pp. 43-44.
175. Kosaki, A. and N. J. G. Webster. 1993. Effect of dexamethasone on the alternative splicing of the insulin receptor mRNA and insulin action in HepG2 hepatoma cells. *J. Biol. Chem.* 268:21990-21996.
176. Norgren, S., P. Arner and H. Luthman. 1994. Insulin receptor ribonucleic acid levels and alternative splicing in human liver, muscle, and adipose tissue: tissue specificity and relation to insulin action. *J. Clin. Endocrinol. Metab.* 78:757-762.
177. Kanety, H., S. Moshe, E. Shafir, B. Lununfeld and A. Karasik. 1994. Hyperinsulinemia induces a reversible impairment in insulin receptor function leading to diabetes in the sand rat model of non-insulin-dependent diabetes mellitus. *Proc. Natl. Acad. Sci. USA* 91:1853-1857.
178. Carpentier, J., J. Paccaud, J. Baecker, A. Gilbert, L. Orci and C. R. Kahn. 1993. Two steps of insulin receptor internalization depend on different domains of the β -subunit. *J. Cell. Biol.* 122:1243-1252.
179. Tavaré, J. M. and K. Sidde. 1993. mutational analysis of insulin receptor function: Consensus and controversy. *Biochimica et Biophysica Acta* 1178:21-39.
180. Reynet, C., M. Caron, J. Magre, J. Picard, G. Cherqui and J. Capeau. 1994. Insulin receptor autophosphorylation sites tyrosines 1162 and 1163 control both insulin-dependent and insulin-independent receptor internalization pathways. *Cellular Signalling* 6:35.
181. Rice, K. M., M. A. Turnbow and C. W. Garner. 1993. Insulin stimulates the degradation of IRS-1 in 3T3-L1 adipocytes. *Biochem. Biophys. Res. Commun.* 190:961-967.
182. Smith, K. L., M. Bradshaw, D. E. Croall and C. W. Garner. 1993. The insulin receptor substrate (IRS-1) is

- a PEST protein that is susceptible to calpain degradation *in vitro*. *Biochem. Biophys. Res. Commun.* 196:767-772.
183. Saad, M. J. A., F. Folli, E. Araki, N. Hashimoto, P. Csermely and C. R. Kahn. 1994. Regulation of insulin receptor, insulin receptor substrate-1 and phosphatidylinositol 3-kinase in 3T3-F442 adipocytes. Effects of differentiation, insulin, and dexamethasone. *Mol. Endocrinol.* 8:545-557.
184. Rolband, G. C., J. F. Williams, N. J. G. Webster, D. Hsu and J. M. Olefsky. 1993. Deletion of exon 21 of the insulin receptor eliminates tyrosine kinase activity but preserves mitogenic signaling. *Biochemistry* 32:13545-13550.
185. Murakami, M. S. and O. M. Rosen. 1991. The role of insulin receptor autophosphorylation in signal transduction. *J. Biol. Chem.* 266:22653-22660.
186. Wilden, P. A., C. R. Kahn, K. Siddle and M. F. White. 1992. Insulin receptor kinase domain autophosphorylation regulates receptor enzymatic function. *J. Biol. Chem.* 267:16660-16668.
187. Kahn, B. B. 1992. Facilitative glucose transporters: regulatory mechanisms and dysregulation in diabetes. *J. Clin. Invest.* 89:1367-1374.
188. Klip, A., T. Tsakiridis, A. Marette and P. A. Ortiz. 1994. Regulation of expression of glucose transporters by glucose: a review of studies *in vivo* and in cell cultures. *FASEB J.* 8:43-53.
189. Dailey, C., B. Paluzuk, C. Jacob, J. Bleasdale and J. Colca. 1993. Pioglitazone (Pio) augments early steps in the insulin transduction system. *Diabetes* 42:116A. (Abstract)
190. Van Horn, D. J., M. G. Myers, Jr. and J. M. Backer. 1994. Direct activation of the phosphatidylinositol 3'-kinase by the insulin receptor. *J. Biol. Chem.* 269:29-32.
191. Staubs, P. A., D. R. Reichart, A. R. Saltiel, K. L. Milarski, H. Maegawa, P. Berhanu, J. M. Olefsky and B. L. Seely. 1994. Localization of the insulin receptor binding sites for the SH2 domain proteins p85, Syp, and GAP. *J. Biol. Chem.* 269:27186-27192.

192. Levy-Toledano, R., M. Taouis, D. H. Blaettler, P. Gorden and S. I. Taylor. 1994. Insulin-induced activation of phosphatidylinositol 3-kinase: Demonstration that the p85 subunit binds directly to the COOH terminus of the insulin receptor in intact cells. *J. Biol. Chem.* 269:31178-31182.
193. Kitzman, H. H., R. J. McMahon, M. G. Williams and S. C. Frost. 1993. Effect of glucose deprivation on GLUT1 expression in 3T3-L1 adipocytes. *J. Biol. Chem.* 268:1320-1325.
194. Tordjman, K. M., K. A. Leingang and M. Mueckler. 1990. Differential regulation of the HepG2 and adipocyte/muscle glucose transporters in 3T3L1 adipocytes: Effect of chronic glucose deprivation. *Biochem. J.* 271:201-207.
195. Pasternak, C. A., J. E. J. Aiyathurai, V. Makinde, A. Davies, S. A. Baldwin, E. M. Konieczko and C. C. Widnell. 1991. Regulation of glucose uptake by stressed cells. *J. Cell. Physiol.* 149:324-331.
196. Chou, M. M., J. E. Fajardo and H. Hanafusa. 1992. The SH2- and SH3-containing Nck protein transforms mammalian fibroblasts in the absence of elevated phosphotyrosine levels. *Mol. Cell. Biol.* 12:5834-5842.
197. Tanti, J. -F., T. Gremeaux, E. Van Obberghen and Y. Le Marchand-Brustel. 1994. Serine/threonine phosphorylation of insulin receptor substrate 1 modulates insulin receptor signaling. *J. Biol. Chem.* 269:6051-6057.
198. Knutson, V. P. 1991. Cellular trafficking and processing of the insulin receptor. *FASEB J.* 5:2130-2138.
199. Bryer-Ash, M. 1991. Regulation of rat insulin-receptor kinase by glucose *in vivo*. *Diabetes* 40:633-640.
200. Giorgino, F., J. Chen and R. Smith. 1992. Changes in tyrosine phosphorylation of insulin receptors and a 170,000 molecular weight nonreceptor protein *in vivo* in skeletal muscle of streptozotocin-induced diabetic rats: Effects of insulin and glucose. *Endocrinology* 130:1433-1444.
201. Berti, L., L. Mosthaf, G. Kroder, M. Kellerer, S. Tippmer, J. Mushak, E. Seffer, K. Seedorf and H. Haring. 1994. Glucose-induced translocation of protein kinase C isoforms in rat-1 fibroblasts is paralleled by

inhibition of the insulin receptor tyrosine kinase. *J. Biol. Chem.* 269:3381-3386.

202. Pause, A., G. J. Belsham, A. -C. Gingras, O. Donze, T. -A. Lin, J. C. Lawrence, Jr. and N. Sonenberg. 1994. Insulin-dependent stimulation of protein synthesis by phosphorylation of a regulator of 5'-cap function. *Nature* 371:762-767.
203. Kletzien, R. F., S. D. Clarke and R. G. Ulrich. 1992. Enhancement of adipocyte differentiation by an insulin-sensitizing agent. *Molec. Pharmacol.* 41:393-398.
204. Hotamisigil, G. S. and B. M. Spiegelman. 1994. Tumor necrosis factor α : A key component of the obesity-diabetes link. *Diabetes* 43:1271-1278.
205. Schnedl, W., S. Ferber, J. Johnson and C. Newgard. 1994. STZ-transport and cytotoxicity: Specific enhancement in GLUT2-expressing cells. *Diabetes* 43:1326-1333.

VITA

The author, James Anthony Bonini, was born in Milwaukee, Wisconsin.

In August, 1986, Mr. Bonini entered Marquette University, receiving the degree of Bachelor of Science in biochemistry in May, 1990.

In July, 1990, Mr. Bonini entered the Department of Molecular and Cellular Biochemistry at Loyola University of Chicago, enabling him to complete the Doctorate of Philosophy in May, 1995.

APPROVAL SHEET

The dissertation submitted by James A. Bonini has been read and approved by the following committee:

Dr. Cecilia Hofmann, Director
Professor, Surgery
Loyola University Chicago

Dr. Allen Frankfater
Associate Professor, Molecular and Cellular
Biochemistry
Loyola University Chicago

Dr. William Simmons
Professor, Molecular and Cellular Biochemistry
Loyola University Chicago

Dr. Leon Platanias
Assistant Professor, Medicine and Section of
Hematology/Oncology
Loyola University Chicago

Dr. James Filkins
Professor, Physiology
Loyola University Chicago

The final copies have been examined by the director of the dissertation and the signature which appears below verifies the fact that any necessary changes have been incorporated and that the dissertation is now given final approval by the Committee with reference to content and form.

The dissertation is therefore accepted in partial fulfillment of the requirements for the degree of Ph.D.

2/3/95
Date

Cecilia Hofmann
Director's Signature